Polysilane High Polymers

ROBERT D. MILLER*

IBM Research Division, Almaden Research Center, 650 Harry Road, San Jose, California 95120-6099

JOSEF MICHL

Center for Structure and Reactivity, Department of Chemistry, The University of Texas at Austin, Austin, Texas 78712-1167

Contents

Overview

Although the first substituted silane polymers were probably prepared in the 1920s, these and related materials were poorly characterized, were intractable, and elicited little scientific interest for almost 50 years. The synthesis of the first soluble, high molecular weight materials in the late 1970s has caused an explosive rebirth of interest in polysilanes that continues today. This review deals mainly with developments that have occurred during the modern era of polysilane studies beginning around 1975. It attempts to treat in a comprehensive fashion the synthesis of homo- and copolymers, including mechanistic studies, modern theoretical treatments describing conformational predictions, studies of the electronic structure of ground and excited states, UV–visible and emission spectroscopic studies, various aspects of polymer structure both in solution and in the solid state, the photochemistry of substituted silane polymers, including theoretical descriptions, and finally potential applications. The relevant literature is surveyed through 1988.

I. Introduction

It has been recognized for some time that the properties of cyclic and acyclic silicon catenates differed significantly from those of their carbon analogues. This was manifested most dramatically by their curious electronic spectra, which suggested significant interaction and electronic delocalization within the σ-bonded framework. In this regard, Gilman et al. reported in 1964 that permethylated silane oligomers, unlike the corresponding carbon systems, absorbed strongly in the UV spectral region and their spectra showed unusual substituent effects.[1,2] For example, silane oligomers terminated with phenyl substituents showed significant

Robert D. Miller was born in Philadelphia, PA, in 1941. He received a B.Sc. in Chemistry from Lafayette College in 1963 and a Ph.D. in Organic Chemistry from Cornell University in 1968 working with Professor A. T. Blomquist. After postdoctoral work at Union Carbide Research Institute in Tarrytown, NY, where he worked on the generation and characterization of reactive intermediates by flash vacuum pyrolysis, he joined the Research Division of IBM in 1969. His current interests include basic photochemical processes, radiation-sensitive polymers, the spectroscopy and chemistry of reactive intermediates, reactions and rearrangements of strained ring compounds, and new synthetic methods.

Josef Michl was born in 1939 in Prague, Czechoslovakia. He received his M.S. in Chemistry in 1961 under V. Horak and P. Zuman at Charles University, Prague, and his Ph.D. in 1965 under R. Zahradnik at the Czechoslovak Academy of Sciences, also in Prague. He left Czechoslovakia in 1968. Postdoctoral positions include work with R. S. Becker at the University of Houston; with M. J. S. Dewar at The University of Texas at Austin; with J. Linderberg at Aarhus University, Denmark; and with F. E. Harris at the University of Utah, where he stayed and became a full professor in 1975. Since 1986, he has held the M. K. Collie-Welch Regents Chair in Chemistry at The University of Texas at Austin. He is a member of the National Academy of Sciences and of the International Academy of Quantum Molecular Science. Dr. Michl's main research interest has recently become the development of a molecular-size "Tinkertoy" construction set for the assembly of supramolecular structures and new solids. His other research interests include preparation of reactive organic and main-group organometallic molecules by conventional methods and by low-temperature photochemical techniques (matrix isolation) and the study of their properties, development of new matrix-isolation spectroscopic methods, investigation of the sputtering of frozen gases and properties of gaseous cluster ions, and the use of quantum chemical and experimental methods for better understanding of the mechanisms of organic photochemical reactions and of electronic excited states of organic and main-group inorganic molecules (linear dichroism, magnetic circular dichroism). He has been the editor of Chemical Reviews since July 1, 1984.

red shifts in absorption similar to those reported for α,ω-diphenylpolyenes. This generated considerable theoretical interest in the nature of bonding in the silicon chain. An excellent review of the early molecular orbital treatments and predictions for short silicon catenates is given in ref 3.

From their early beginnings, studies of the chemistry and spectroscopy of acyclic and cyclic silanes expanded rapidly. Since it is beyond the scope of this review to discuss this work in detail, the reader is directed to several useful review articles in the field for background information.[4-9] A number of reviews dealing with more specific aspects of the chemistry of oligosilanes are also available. For example, the photochemistry of organosilane derivatives has been heavily investigated and two useful summaries are available.[10,11] Likewise, a comprehensive review of multiply bonded silicon species has recently appeared.[9] All of these contributions contain background material useful for understanding the properties and characteristics of higher molecular weight silicon catenates. It is the intent in this review to focus on high molecular weight substituted silane polymers, an interesting class of radiation-sensitive materials whose curious spectral and chemical properties have resulted in a host of new potential applications.

Substituted silane polymers 1 contain only silicon atoms catenated together to form a linear backbone.

$$\left(\begin{array}{c} R^2 \\ | \\ Si \\ | \\ R^1 \end{array}\right)_n$$

1
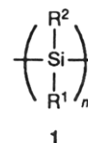
Silicon, among the elements, is almost unique in its ability to homocatenate and form stable long linear chains in a manner similar to carbon, which forms an almost limitless variety of carbon backbone polymers. Stable silicon backbone polymers have been generated that contain up to 40 000 monomer units in a single chain! Recently, a number of soluble high molecular weight polygermane derivatives have also been reported,[12,13] suggesting that germanium, like silicon, can also form stable polymeric linear catenates with interesting spectroscopic properties.

With respect to nomenclature for substituted silane polymers, two variations appear in the literature. The materials may be named as polymeric derivatives of the parent substituted silylene or alternatively as a substituted silane derivative (e.g., poly(dimethylsilylene) or poly(dimethylsilane) for 1, $R^1 = R^2 = Me$). Although both systems appear frequently in the literature, we have arbitrarily adopted the latter for this review. Furthermore, we will use the term polysilane here to refer specifically to high molecular weight polymers as distinguished from lower molecular weight materials (cyclic and acyclic), which will be designated as oligosilanes.

II. Historical

The first polysilane derivatives were probably prepared by Kipping in the early 1920s by the condensation of diphenyldichlorosilane with sodium metal.[14,15] This highly crystalline material, however, attracted little scientific interest because it was infusible and intractable. After these initial efforts, the field remained dormant for over 25 years until Burkhard described the

preparation of the simplest dialkyl derivative, poly-(dimethylsilane), by a similar synthetic route.[16,17] This material also suffered from the same problems as poly(diphenylsilane) and as a consequence was poorly characterized and little investigated. Because of the difficulty with characterization, the description of substituted polysilanes was relegated to the patent literature until around 1975. In this regard, Clark[18,19] described the preparation of a number of poorly characterized polysilane homopolymers by sodium-mediated condensation without the need for an autoclave. Beginning around 1975, Yajima and co-workers revived the interest in silane polymers with a series of publications and patents describing the pyrolytic preparation of β-silicon carbide (see section X.A).[20-27] Soon afterward, Wesson and Williams described the preparation of poly(dimethylsilane) from highly purified monomer. This polymer was slightly soluble in a number of organic solvents at elevated temperatures.[28]

The modern era in the study of substituted polysilanes began about 10 years ago with the synthesis of a number of soluble homo- and copolymers. In 1980 Wesson and Williams[29] reported the synthesis of soluble random copolymers containing the dimethylsilylene subunit in combination with either ethylmethylsilylene or methyl-n-propylsilylene. These materials, while more soluble in common organic solvents, were reported to have poor film-forming properties and were not extensively investigated. The same authors[30] reported that a number of soluble block copolymers with acceptable film-forming properties could be prepared by the coupling of various α,ω-dichlorosilane oligomers with 1,5-dilithiodecaphenylpentasilane in yields of 30–35%. The molecular weights of these block copolymers were respectable, with number-average molecular weights ranging from 5000 to 10 000. In 1981 West and co-workers[31-33] described the preparation of a soluble copolymer from methylphenyldichlorosilane and dimethyldichlorosilane which they called polysilastyrene based on its structural similarity to the carbon-based polymer polystyrene. Depending on the monomer ratio, this material was soluble in common organic solvents and molecular weights in excess of 1 000 000 were obtained. At about the same time, Trujillo[34] reported the preparation of a soluble homopolymer from methylphenyldichlorosilane by condensation with sodium in refluxing dodecane in crude yields approaching 60%. This material had a broad bimodal molecular weight distribution, and considerable quantities of insoluble and presumably cross-linked material were simultaneously generated. These pioneering studies suggested that high molecular weight polysilane polymers were not necessarily insoluble, intractable materials and triggered the explosive interest in the synthesis and characterization of polysilane materials that continues today.

Since the first reports of soluble materials, the syntheses and characterization of a large number of soluble homo- and copolymers have been reported, and studies on these materials have resulted both in a better understanding of the polymer properties and characteristics and in the discovery of a number of potential applications. It is our intention to review in a comprehensive fashion primarily work that has transpired during the modern era of polysilane study through 1988

and to complement and expand the existing reviews[6,35-40] on the topic.

III. Synthesis

A. Wurtz-Type Coupling of Dichlorosilanes

As mentioned, Kipping[14,15] probably prepared the first substituted polysilane in the 1920s by the condensation of dichlorodiphenylsilane with sodium metal. It is interesting to note that in spite of considerable efforts invested in a search for alternatives, the modified Wurtz coupling of dichlorosilanes remains currently the most viable general procedure for the preparation of high molecular weight, linear polysilane derivatives. The reaction, which is shown in eq 1, is usually run at

$$R^1R^2SiCl_2 + 2Na \rightarrow (R^1R^2Si)_n + 2NaCl \qquad (1)$$
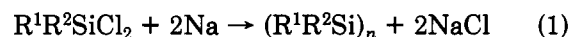
elevated temperatures in an inert solvent using an appropriate alkali metal in dispersion. Sodium is usually favored over lithium since the latter often results in cyclooligomerization.[4-6] Potassium metal and sodium-potassium alloys of varying composition have been used extensively for the formation of SiSi bonds[4-8] but these reagents often lead to the degradation of high molecular weight linear polymers and the formation of cyclic oligomers at elevated temperatures, particularly in more polar solvents such as THF.[41,42] This, coupled with the increased hazards associated with the use and disposal of potassium metal or sodium–potassium alloy, has led to the almost exclusive use of sodium for the condensation reaction. Recently, however, NaK used at room temperature in conjunction with ultrasonic agitation has been employed for the condensation of a variety of alkyl-substituted trichlorosilanes to form soluble, branched, substituted silane polymers.[43]

The sodium is normally employed as a dispersion in an inert aromatic solvent such as toluene or xylene. Alternatively, high-boiling alkane solvents can be used, although the success of the polymerization reaction often depends critically on the nature of the solvent (vide infra). The polymerization is usually terminated and the polymer subsequently precipitated by the addition of a variety of alcohols. Alternatively, when the polymer is soluble in the cooled reaction medium, the reaction mixture can be filtered without quenching to remove any excess sodium prior to precipitation. The preformed sodium dispersion itself can be added to the dichlorosilane dissolved in the reaction solvent at elevated temperatures or vice versa. The latter procedure constitutes the normal addition mode (N), while the former technique is termed inverse addition (I). The inverse addition mode generally results in lower yields of higher molecular weight polymer,[44] although the procedure is experimentally more difficult and hazardous than normal addition. The onset of the polymerization is usually strongly and often violently exothermic depending on the monomer structure, and the reaction mixture usually darkens to a blue or purple color. If the stirring is stopped at this point, most of the color eventually settles, leaving only a slightly colored solution. The origin of the dark color that settles is uncertain but it is suspected to be "defect" sodium chloride, i.e., color centers produced by the incorporation of sodium in the precipitating sodium chloride.[41,45]

TABLE 1. Polysilane Homopolymers

$$R^1R^2SiCl_2 + 2Na \rightarrow (R^1R^2Si)_n + 2NaCl$$
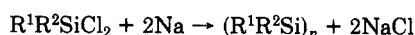
entry	polymer	yield,[a] %	$\bar{M}_w \times 10^{-3}$ [b]	R [c]	ref
1	$(n\text{-PrSiMe})_n$	32	64.4, 13.3	0.4	44
2	$(PhC_2H_4SiMe)_n$	35	286, 4.4	3.5	44
3	$(i\text{-PrSiMe})_n$	12	1.6		59
4	$(n\text{-BuSiMe})_n$	34	110, 5.9	1.5	44
5	$(n\text{-HexSiMe})_n$	11	524, 20.5	2.4	44
6	$(n\text{-dodecylSiMe})_n$	8	1345, 9.4	2.7	44
7	$(c\text{-HexSiMe})_n$	20	1192, 18.8	0.8	44
8	$(n\text{-Pr}_2Si)_n$	39	1159, 26.9	1.3	60
9	$(n\text{-Bu}_2Si)_n$	34	110, 5.9	1.5	47
10	$(n\text{-pentyl}_2Si)_n$	39[d]	1129, 26.9	1.3	59
11	$(n\text{-Hex}_2Si)_n$	6	1982, 1.2	3.1	47, 50, 178
12	$(n\text{-Hept}_2Si)_n$	30[d]	3528, 42.5	1.9	178
13	$(n\text{-octyl}_2Si)_n$	35[d]	3071, 27.8	3.2	178
14	$(n\text{-decyl}_2Si)_n$	3	1693, 14.1	5.1	48
15	$(n\text{-dodecyl}_2Si)_n$	20[d]	996.8, 15.1	1.5	59
16	$(n\text{-tetradecyl}_2Si)_n$	60[d]	3071, 27.8	1.9	59
17	$(PhSiMe)_n$	55	193, 5.6	0.7	44, 51, 58b
18	$(p\text{-tolylSiMe})_n$	25	213, 5.9	0.6	44
19	$(p\text{-}t\text{-BuC}_6H_4SiMe)_n$	14	153		59
20	$(2,4,5\text{-Me}_3C_6H_2SiMe)_n$	20	109.8, 31.4	1.9	59
21	$(PhSiCH_2Ph)_n$	30			55
22	$(p\text{-MeOC}_6H_4SiMe)_n$	12	13.0		59, 49
23	$(p\text{-}n\text{-C}_8H_{17}OC_6H_4SiMe)_n$	19	61.7, 15.2	0.13	59
24	$(3\text{-OHC}_6H_4CHMeCH_2SiMe)_n$	9	110.0		55
25	$(p\text{-MeOC}_6H_4(CH_2)_3SiMe)_n$	16	333, 10.4	0.9	59
26	$(p\text{-Me}_2NC_6H_4SiMe)_n$	13	3.3		51
27	$[(TMS)SiMe]_n$	e	359		57
28	$(PhSiMe_2SiMe)_n$	9	13.2		58a
29	$[p\text{-}(TMS)C_6H_4SiMe]_n$	30	476.4, 8.1	0.2	59
30	$[p\text{-}(TMS)CH_2C_6H_4SiMe]_n$	27	516.7		59
31	$[(2\text{-}(3\text{-cyclohexenyl})ethyl)SiMe]_n$	10	105, 13.0	0.3	54
32	$(\beta\text{-naphthylSiMe})_n$	20	30		49
33	$(p\text{-biphenylSiMe})_n$	40	80.0		35
34	$(SiPhH)_n$	e	1.0		35

[a] Reaction solvent was toluene unless otherwise noted. [b] Molecular weights were determined by GPC analyses and are relative to polystyrene calibration standards. [c] Ratio of high to low molecular weight products. [d] Solvent was 70/30 by volume toluene/diglyme. [e] No polymer yields reported.

1. Polysilane Homopolymers

As expected, the major drawbacks in the Wurtz coupling polymerization are the limited substituent tolerance to the vigorous reaction conditions and the sensitivity of the polymerization to the steric size of the substituents. Regarding the former, suitable substituents are limited to a number of robust alkyl- and aryl-substituted derivatives. The examples shown in Tables 1 and 2 are intended to be illustrative and the reader is referred to the original literature for a complete list of polysilane homopolymers.[34-37,39-41,43,44,46-58] Only materials for which some polymer characterization data are available are included in the tables.

The homopolymer structures have been verified by standard spectroscopic techniques. High-resolution NMR in solution is particularly valuable both for identification of gross overall structural features and for the elucidation of polymer microstructure[61] in unsymmetrically substituted derivatives. In addition to the wealth of information provided by ^{1}H and ^{13}C NMR, the use of high-resolution [29]Si techniques has particularly been illuminating, especially for the analysis of polymer chain microstructure. Schilling et al.[62] have analyzed the ^{29}Si NMR spectra of a variety of symmetrically and unsymmetrically substituted poly(dialkylsilanes) and have concluded that the polymer structures of the latter are predominantly random atactic. Analysis of the multiplet structures suggests that the

polymerization conforms to Bernoullian statistics with $P_m = 0.5$. In short, in the growing polymer chain each monomer unit appears to be added without a significant configurational preference. West and co-workers[39,63] have also studied a variety of unsymmetrical dialkyl derivatives and reached similar conclusions regarding the polymer microstructure. In addition, these authors report an approximately linear correlation between the observed [29]Si chemical shifts and the UV absorption maxima of the polymers in solution for alkyl-substituted derivatives in a manner predicted from Ramsey's shielding formula. Although random atactic sequences predominate in the alkyl polymer series, analysis of a number of aryl-substituted polymers where the aryl group is directly bonded to the polymer backbone provides some evidence for a stereochemically nonrandom polymerization process.[39,64]

The crude polymer yields range from a few percent to approximately 50%. It should be noted that the crude polymer yield depends to some extent on the conditions of the workup. For example, precipitation with methanol often leads to the isolation of more solid than comparable treatment with acetone or 2-propanol. In the former case, however, the bulk of the increased material is oligomer and low molecular weight polymer. In a typical polymerization solvent such as toluene, both the polymer yields and the molecular weights are very sensitive to the steric bulk of the substituents. For example, while cyclohexylmethyldichlorosilane produces

TABLE 2. Peraryl Polysilane Homopolymers

entry	polymer	yield, %	$\bar{M}_w \times 10^{-3}$ [a]
1	[(n-Bu—⬡)₂Si]ₙ	6.2	231.6 / 2.1
2	[(n-Hex—⬡)₂Si]ₙ	7.5	244.7 / 3.0
3	[(i-Bu—⬡)₂Si]ₙ	4.0	104.1 / 1.8
4	[(⬡)₂Si]ₙ (n-Hex)	6.0	3576 / 110.0
5	[n-Bu—⬡ / n-BuO—⬡ Si]ₙ	7.5	800 / 18.4 / 2.6
6	[(n-BuO—⬡)₂Si]ₙ	8.5	1248 / 2.6
7	[(⬡)₂Si]ₙ (n-BuO)	7.0	823 / 1.7
8	[n-BuO—⬡ / ⬡ Si]ₙ (n-BuO)	5.0	618 / 25.7 / 3.2

[a] Molecular weights were determined by GPC analyses and are relative to polystyrene calibration standards.

a high polymer in yields up to 20% in toluene solvent, no high polymer is isolated from dicyclohexyldichlorosilane under comparable conditions. Solvent effects on the polymerization can be significant and are discussed in more detail in section A.3.

Certain heteroatom substituents survive the polymerization conditions and these are generally introduced as substituents on an aromatic ring. For example, the polymer derived from (p-(dimethylamino)phenyl)-methyldichlorosilane has been prepared[51] (Table 1, entry 26) as have a number of polymers containing m- and p-alkoxyphenyl substituents[49,51,52,59] (Table 1, entries 22–25; Table 2, entries 5–8). The polymerization of monomers containing olefinic substitution appears to be very structure sensitive. For example, the polymerization of methylvinyldichlorosilane and allylmethyldichlorosilane yields very little (<2%) soluble polymer and a large quantity of insoluble and presumably cross-linked material under the usual reaction conditions.[60] Similar results have been described for the polymerization of (6-hexenyl)methyldichlorosilane, a fact that has been used to justify the suggestion that silyl radicals are involved in the polymerization. In these cases, the vinyl moieties clearly react under the reaction conditions, although cross-linking might be suppressed by operating at lower temperatures. However, it has been recently demonstrated that soluble polymers can be prepared from (2-(3-cyclohexenylmethyl)ethyl)methyldichlorosilane (Table 1, entry 31) under normal polymerization conditions.[54] The unsaturation in the polymer may be used for subsequent cross-linking in the presence of radical initiators, and the elements of HX (X = Cl, Br) can be added to the double bond without degradation of the polymer.

Recently, a base-soluble, hydrophilic phenolic polysilane homopolymer prepared by the condensation of [2-(m-(trimethylsiloxy)phenyl)propyl]methyldichlorosilane has been described (Table 1, entry 24).[55] The monomer was easily prepared from 3-isopropenylphenol, protected as the trimethylsilyl ether, by hydrosilylation with methyldichlorosilane. The trimethylsilyl protecting group was subsequently removed after polymerization by treatment with methanol. Polymerization reactions of dichlorosilanes containing trimethylsilyl-protected phenolic moieties are quite structure specific and depend critically on the nature and position of the substituents on the aromatic ring. Polysilane derivatives containing phenolic substituents potentially offer the possibility of further functionalization through electrophilic aromatic ring substitution or functionalization of the phenolic hydroxyl group.

Recently, a number of low molecular weight ($\bar{M}_w$ = 1000–1500) homo- and copolymers containing SiH bonds in the backbone have been prepared[35] by the condensation of phenyldichlorosilane. The molecular weight of the isolated homopolymer (Table 1, entry 34) is low but increases slightly in the copolymers (vide infra). These materials are interesting because they can be subsequently cross-linked by oxidation or functionalized by hydrosilylation with unsaturated reagents. Cross-linking of these materials can also be effected by using trivinylphenylsilane and chloroplatinic acid to produce room-temperature vulcanizing polysilanes. The SiH linkages in the polymers are labile and care must be taken in the workup and polymer processing to avoid basic hydrolysis. In addition, these polymers were end-capped with diphenylmethylchlorosilane prior to workup.[35]

Recently, polysilane high polymers containing pendant silyl substituents have been prepared by the Wurtz coupling technique. For example, Nagai et al.[56] have discussed the preparation of a number of bis(silyl)-substituted polysilane derivatives. Harrah and Zeigler have described the preparation and characterization of the homopolymer poly[(trimethylsilyl)methylsilane] (Table 1, entry 27).[57] Watanabe et al. have described a similar synthesis of poly[(phenyldimethylsilyl)-methylsilane] from the corresponding dichlorosilane (Table 1, entry 28).[58a] Homopolymers containing trimethylsilyl substituents separated from the backbone by an aryl or benzyl substituent (e.g., poly[(p- and m-(trimethylsilyl)phenyl)methylsilane] and poly[(p- and m-((trimethylsilyl)methyl)phenyl)methylsilane] have also been prepared (Table 1, entries 29 and 30).[59]

Cyclodichlorosilanes may also be utilized in the Wurtz-type polymerization, and a number of homo- and copolymers derived from penta- and tetramethylenedichlorosilane have been reported.[35] The polymers incorporating the latter monomer have unusual spectral properties and are reported to undergo facile oxidative cross-linking when heated in air to 80 °C, suggesting that ring strain may facilitate carbon–silicon bond cleavage.

Although a large number of phenyl-substituted polysilanes have been described, there is limited information on the incorporation of polynuclear aromatic

substituents. These materials are of interest because of the anticipated long-wavelength absorption of the polysilanes caused by the substituents. The preparation and spectroscopic characterization of poly(methyl-β-naphthylsilane)[49] have been reported, but its polymer properties have not been described in detail (Table 1, entry 32). Interestingly, attempts to prepare high molecular weight homopolymers from methyl-α-naphthyldichlorosilane[60] and methyl-α-phenanthryldichlorosilane[60] have been unsuccessful. Apparently, the steric congestion in the respective homopolymers is too great, although it is also possible that high polymers derived from these monomers are rapidly degraded under the reaction conditions. In this regard, it is interesting that high molecular weight copolymers have been prepared from methyl-α-naphthyldichlorosilane and dimethyldichlorosilane.[65,66] The steric congestion is apparently relieved for biphenyl derivatives, and a high polymer has been isolated from the condensation of p-biphenylmethyldichlorosilane.[35]

In general, the polymer yields from the condensation of substituted dichlorosilanes in a solvent such as toluene are strongly affected by the steric bulk of the substituents. For n-alkyl substituents, the substituent bulk is approximately cylindrically symmetric and steric interactions cannot be alleviated by rotation around the carbon–silicon substituent bond. Simple aryl substituents, however, offer the possibility for relief of steric interactions in the polymers, since the groups are sterically unsymmetrical; i.e., steric effects are much larger in the plane of the substituent carbon atoms than perpendicular to this plane. For this reason, the aryl substituents in peraryl polysilane derivatives can minimize substituent interactions by rotation around the carbon–silicon single bond connecting the substituent to the polymer backbone. The degree to which substituent interactions can be minimized by rotation of the substituent group will depend to some extent on the backbone conformation of the polymer. As described by Kipping,[14,15] the simplest diaryldichlorosilane, diphenyldichlorosilane, reacts vigorously with sodium to yield an insoluble, intractable highly crystalline polymer. However, ring substitution with n-alkyl[53] or n-alkyloxy substituents[52] yields soluble and characterizable polymeric materials. Some representative soluble poly(diarylsilanes) that have been prepared by sodium condensation are shown in Table 2. For the alkyl-phenyl-substituted derivatives the nature of the alkyl substituent itself appears to be rather critical. Methyl or ethyl substitution results in low molecular weight polymers ($\bar{M}_w$ = 1000–4000) with limited solubility in common organic solvents. Similar results were obtained when the alkyl substituent was branched (e.g., 3-methylbutyl, tert-butyl). On the other hand, incorporation of longer n-alkyl side chains resulted in soluble high molecular weight products. The yields for all of the poly[bis(alkyl(alkyloxy)phenyl)silanes] were low (5–10%), which is consistent with the steric bulk of the substituents. The electronic properties of these polymers are, however, very interesting and will be discussed in some detail later.
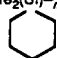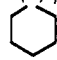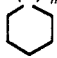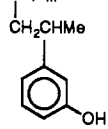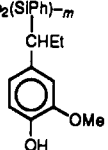
2. Copolymers

Finally, it should be mentioned that considerable synthetic effort has been devoted to the preparation of polysilane copolymers.[29,31-33,35-39,50,51,54,55,58,65-76] The number of possible copolymers is staggering if one considers not only changes in comonomer type but also compositional variations within a given structural class. For this reason, the long list of copolymers shown in Table 3 should be considered as representative, and the reader is referred to the cited literature for a more complete description of the known compositional variants.

The preparation of copolymers often offers a number of advantages relative to the respective homopolymers. First, the physical, mechanical, and electronic properties of the copolymers can be altered and adjusted in accordance with the properties of the monomeric components. For example, while the homopolymers poly(dimethylsilane) and poly(diphenylsilane) are highly intractable and insoluble, copolymers containing these monomeric units are often quite soluble and characterizable. In this fashion, many of the valuable properties of the respective homopolymers, such as thermal and oxidative stability, high glass transition temperatures, etc., can be imparted to the copolymer without sacrificing polymer solubility. Since the copolymer composition can be varied not only according to the structural type of monomer components but also with regard to the respective monomer composition, there exists an almost limitless potential for variation. Second, certain dichlorosilane monomers either produce no polymer or yield materials of such low molecular weights that the polymers are unsuitable for subsequent applications. Copolymerization may allow the incorporation of monomers whose respective substituents impart useful electronic or physical properties when the respective homopolymers themselves are not accessible. For example, dicyclohexyldichlorosilane, which produces only low molecular weight materials when homopolymerized, readily yields a variety of soluble copolymers with other dichlorosilane monomers.[59] Similarly, monomers such as methyl-α-naphthyldichlorosilane,[65,66] ferrocenylmethyldichlorosilane,[72] and tert-butylmethyldichlorosilane,[57] which do not yield high molecular weight homopolymers, readily yield copolymers (see Table 3). For these reasons, a large number of copolymers have been prepared and characterized.

Characterization of substituted silane copolymers can be quite difficult relative to similar studies on homopolymers. The characterization of copolymers in the literature is often incomplete. In addition to the usual spectroscopic data, DSC studies are often necessary to determine whether the material is a true copolymer rather than a homopolymer mixture. For copolymers derived from unsymmetrically substituted monomers there is the question of tacticity within the polymer chain. Even if the monomer units are symmetrically substituted to reduce the complexity, there is the additional problem of monomer sequence (i.e., random, blocky, etc.).[61] For problems of this type, ^{1}H and ^{13}C NMR have proved particularly useful for carbon-based polymers. As mentioned, ^{29}Si NMR is a powerful tool for the polysilanes and is finding increasing usage. A number of polysilane copolymers have been examined by high-resolution solution ^{29}Si NMR. West and co-workers have analyzed the data obtained for two different compositions of poly(methylphenylsilane-co-di-

TABLE 3. Polysilane Copolymers

entry	copolymer structure	yield,[a] %	m[b]	$\bar{M}_w \times 10^{-3c}$	ref
1	-SiMe$_2$(SiMe,n-Hex)$_m$-	57	0.66	170, 10	67, 71, 58b
2	-SiMe$_2$(SiMe,c-Hex)$_m$-	63	0.66	900, 70, 9.0	50, 67, 71, 58b
3	-SiMe$_2$(Si)-$_m$ ⬡	45	1.04	70, 13, 5	67
4	-SiMe$_2$[Si(TMS),Me]$_m$-	d	1.0	33	57
5	-SiMe$_2$(SiMe,Ph)$_m$-	10	1.51	900	31, 58b
6	-SiMe$_2$(SiPh$_2$)$_m$-	70	0.89	350, 2	67, 58b
7	-SiMe$_2$(SiMe,α-naphthyl)$_m$-	60	1.7	40, 10.5, 2.3	65
8	-SiMe$_2$(SiMe,p-tolyl)$_m$-	51	0.91	170, 8.0	67
9	-SiMe$_2$(SiMe,C$_2$H$_4$PhH$_2$)$_m$-	59	0.65	330, 7.0	67
10	-SiMe,Ph(SiMe,n-Pr)$_m$-	d	1.0^e	910, 3.0	71
11	-SiMe,Ph(SiMe,i-Pr)$_m$-	d	1.0^e	980, 4.0	50, 71
12	-SiMe,Ph(SiMe,c-Hex)$_m$-	d	1.0^e	150, 8.0	71
13	-SiPh$_2$(SiMe,C$_2$H$_4$Ph)$_m$-	41	1.7	300, 2.5	69
14	-SiPh$_2$(SiMe,c-Hex)$_m$-	48	1.9	310, 2.5	69
15	-SiPh$_2$(SiMe,n-Hex)$_m$-	51	0.83	360, 3.0	69, 58b
16	-SiPh$_2$(Si-n-Hex$_2$)$_m$-	43	0.50	530, 2.5	69, 58b
17	-SiMe,n-Pr(Si-i-Pr,Me)$_m$-	d	1.0^e	1700, 14	50, 71, 58b
18	-Si-c-Hex,Me(SiMe,n-Pr)$_m$-	d	1.0^e	600	71
19	-Si-c-Hex,Me(Si-i-Pr,Me)$_m$-	d	1.0^e	1000, 5	71
20	-Si-c-Hex,Me(SiC$_2$H$_4$Ph,Me)$_m$-	80	0.67	150, 2.5	68
21	-Si-c-Hex,Me(SiMe,p-tolyl)$_m$-	58	0.56	92, 2.6	68
22	-Si-c-Hex, Me(Si)-$_m$ ⬡	71	0.57	130, 4.0	68
23	-SiC$_2$H$_4$Ph,Me(SiMe,Ph)$_m$-	18	1.0^e	170, 3	68
24	-SiC$_2$H$_4$Ph,Me(SiMe,p-tolyl)$_m$-	58	0.48	390, 2	68
25	-SiC$_2$H$_4$Ph, Me(Si)-$_m$ ⬡	50	0.56	400, 84	68
26	-Si(2-(3-cyclohexenyl)ethyl),Me(SiMe,Ph)$_m$-	20	1.0	300, 9	54
27	-Si(2-(3-cyclohexenyl)ethyl),Me(SiMe,n-Pr)$_m$-	20	1.0	180, 20	54
28	-SiPh,H(SiMe$_2$)$_m$-	d	0.63	1.2	35
29	-SiPh,H(SiMe,Ph)$_m$-	d	4.5	1.0	35
30	-SiPh,H(SiC$_2$H$_4$Ph,Me)$_m$-	d	5.4	1.2	35
31	-SiPh,H(Si-c-Hex,Me)$_m$-	d	5.3	1.3	35
32	-SiPh,H(Si-n-Hex,Me)$_m$-	d	4.8	1500	35
33	-Si-c-Hex,Me(Si-t-Bu,Me)$_m$-	d	1.0^e	119	57
34	-Si(TMS),Me(SiMe,n-Pr)$_m$-	d	1.0^e	43	57
35	-Si(TMS),Me(Si-c-Hex,Me)$_m$-	d	1.0^e	164	57
36	-Si(TMS),Me(SiMe,Ph)$_m$-	d	1.0	169	57
37	-SiMe$_2$(SiPh)-$_m$ | CH$_2$CHMe ⬡—OH	15	1.6	7.5	55
38	-SiMe$_2$(SiPh)-$_m$ | CHEt ⬡—OMe OH	9	1.3	7.5	55
39	-SiMe,Ph(SiFc,Me)$_m$-^{f}	5	0.16	80, 2.5	72
40	-[(SiMe$_2$)$_2$Si(n-Bu)$_2$]$_n$-	20		2000, 200, 3.0	75
41	-(SiHMeSiMe$_2$)$_n$-	36		3.6	58
42	-SiPhMe(Si-n-Hex)$_m$-	12	0.67	290.5	84
43	-SiPhMe(SnPh$_2$)$_m$-	75	1.0^e	3.7	84

[a] Reaction solvent was toluene unless otherwise noted. [b] Monomer ratio in polymer as determined by ^{1}H NMR unless otherwise noted. [c] Molecular weights were determined by GPC analyses and are relative to polystyrene calibration standards. [d] No yields reported. [e] Monomer feed ratios were 1:1. [f] Fc = (η^5-C$_5$H$_4$)Fe(η^5-C$_5$H$_5$).

methylsilane) containing different monomer ratios and concluded that the structure of the polymer was blocky, containing runs of the respective monomer units.[64] They reached a similar conclusion regarding the structure of another copolymer, poly(methylphenyl-silane-co-n-hexylmethylsilane).[64] The results are in accord with the prediction of Worsfold,[41] who found in a rate study of the copolymerization of methyl-phenyldichlorosilane and dimethyldichlorosilane that the initial rate of disappearance of the former was approximately 4 times that of the latter. Interestingly, NMR studies on a number of copolymers derived from the dialkyl-substituted monomers suggested that the copolymer sequences were predominantly random.[63]

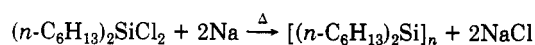TABLE 4. Effect of Diglyme Additive on the Polymerization of Some Representative Dichlorosilane Monomers

entry	polymer	solvent (vol % toluene)a	yield %	$\bar{M}_w \times 10^{-3\,b}$	R^c
1a	(c-HexSiMe)n	100	20	804	8.7
				4.5	
1b		90	35	1477	0.12
				24.8	
1c		75	32	23.1	
1d		25	33	16.5	
2a	(n-dodecylSiMe)n	100	8	1345	2.73
				9.4	
2b		70	33	476	0.74
				40.7	
3a	(n-Hex2Si)n	100	5.9	1982	3.12
				1.2	
3b		70	37	2091	1.27
				24.4	
4a	(n-dodecyl2Si)n	100	3	521	5.2
				14.1	
4b		70	34	570	2.3
				27.4	
5a	(p-t-BuC6H4SiMe)n	100	14	153	
5b		70	8.1	55.9	9.1
				0.64	
6a	(p-MeOC6H4SiMe)n	100	12	12.8	
6b		70	25	14.4	
7a	(p-MeOC6H4(CH2)3SiMe)n	100	16	333	0.90
				10.4	
7b		70	44	164	0.91
				12.0	

a Solvent was toluene/diglyme, reaction temperature 110–115 °C, normal addition mode. b Molecular weights were determined by GPC analyses and are relative to polystyrene calibration samples. c Ratio of high to low molecular weight polymer.

TABLE 5. Effect of Solvent Additives in the Polymerization of Dichloro-di-n-hexylsilane

$$(n\text{-}C_6H_{13})_2SiCl_2 + 2Na \xrightarrow{\Delta} [(n\text{-}C_6H_{13})_2Si]_n + 2NaCl$$

| entry	additivea in toluene	yield %	$\bar{M}_w \times 10^{-3\,b}$	$\bar{M}_n \times 10^{-3}$	R^c
1	toluene	6	1982	1120	3.1
			1.2	1.1	
2	30% diglyme	37	1073	561	1.42
			31.7	13.5	
3	10% diglyme	36	1358	712	2.61
			26.6	13.0	
4	5% diglyme	34	1008	539	3.41
			22.3	12.6	
5	xylene (75%)d diglyme (25%), ultrasound	22	37.6	14.0	
6	15-crown-5, 0.5 mmol/ mmol of Na	18	6.4	4.5	
7	15-crown-5, 1.1 mmol/ mmol of Na	13	6.4	4.6	
8	16% heptane	27	1386	679	9.61
			1.1	1.1	

a Reaction run at reflux unless otherwise noted; normal addition mode. b Molecular weights were determined by GPC analyses and are relative to polystyrene calibration standards. c Ratio of high to low molecular weight polymer. d Ultrasonic agitation with reaction temperature maintained below 60 °C.

Almost all of the copolymers shown in Table 3 were prepared by allowing the mixture of comonomers to couple in the presence of sodium in the usual manner. However, the polymer listed as entry 40 (Table 3)[75] is unique in that it is a perfectly alternating copolymer that was prepared not by condensation of dimethyldichlorosilane with dibutyldichlorosilane but instead by the polymerization of 1,3-dichloro-1,1,3,3-tetramethyl-2,2-dibutyltrisilane. It appears that coupling of appropriately substituted 1,3-dichlorotrisilanes represents a method of preparing sequence-regular copolymers. High molecular weight copolymers have also been reported from the coupling of substituted 1,2-dichlorodisilanes (see Table 3, entry 41).[58a,64]

3. Mechanistic Studies of Wurtz-Type Polymerization

(a) Solvent Effects. Two features of the heterogeneous polymerization become obvious upon examination of the experimental data: (i) the polymer yields in a solvent such as toluene, which are never spectacular, decrease markedly with increasing steric bulk of the substituents and (ii) the molecular weight distributions in the crude polymer mixture are often strongly polymodal. A trimodal distribution is often produced with contributions clustered in three distinct molecular weight regions: [1] $\bar{M}_w$ <1500, [2] $\bar{M}_w$ = 4000–30 000, and [3] $\bar{M}_w$ = 100 000 to several million. The material in the lowest molecular weight region is mainly oligomeric and, while of mechanistic interest, has little preparative utility. The low yields of useful polymer often obtained in solvents such as toluene are troublesome and make the preparation of sufficient material for

subsequent study tedious. Fortunately, many of the polymerization reactions are strongly solvent dependent, and experimentation often results in greatly improved yields of high polymer. This solvent effect on the Wurtz-type polymerization was first described by Miller and co-workers[46] in the preparation of poly(cyclohexylmethylsilane), a material of interest for its imaging characteristics (Table 4, entries 1a–d).[46] In this case, diglyme as an additive not only improves the overall polymer yield but also causes changes in the polymodal molecular weight distribution, producing increased quantities of polymer in the middle molecular weight range [2]. In very low concentration (<5% by volume) diglyme still results in improved polymer yields, but significant quantities (10–15%) of the very high molecular weight fraction are concurrently produced. The use of diglyme in quantities >20–25% by volume again results in a monomodal molecular weight distribution but leads to a further reduction in the molecular weight of the isolated polymer. Similar results were observed in a xylene/diglyme mixture using ultrasonic agitation.

The utility of diglyme as a cosolvent appears general for the polymerization of dialkyldichlorosilanes and is particularly obvious in the preparation of symmetrical dialkyl polymers where low yields of high polymer result in toluene alone (Table 4, entries 3 and 4). This is exemplified in the synthesis of a typical symmetrical dialkyl polymer, poly(di-n-hexylsilane). Interestingly, for this material as well as for related dialkyl derivatives, the improved polymer yields are not always accompanied by a decreasing proportion of the high molecular weight fraction in the high molecular weight range [3].

Initially, it was felt that the solvent effects were best explained by the intermediacy of silyl anions in the polymerization and the cation sequestering effect of the polyether solvent.[46] However, the data in Table 5 suggest that, at least for this particular example, the solvent effect is more complex than simple anion activation. This is demonstrated by the poor yields of low
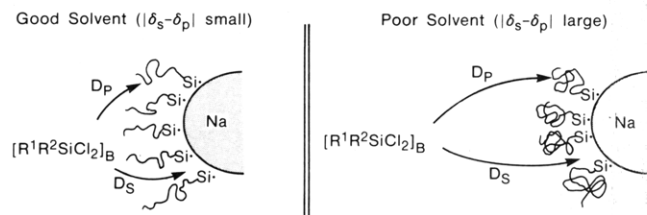
Figure 1. Diffusion model for polymerization using inverse sodium addition mode.

molecular weight material produced by the addition of relatively large amounts of the sodium-specific sequestering reagent 15-crown-5 (Table 5, entries 6 and 7) and the improved yields of high molecular weight polymer when the toluene is diluted with a nonpolar additive such as heptane (Table 5, entry 8). The results suggest that the solvent effects in the polymerization of di-*n*-hexyldichlorosilane might possibly be described as bulk solvent effects. This does not rule out the presence of propagating silyl anions in the present case nor does it necessarily ensure that all solvent effects are bulk solvent effects in every case.

Similar observations on the effect of additives in the polymerization of methylphenyldichlorosilane in a sodium-poor environment (inverse addition) have also been ascribed to bulk solvent effects by Zeigler and co-workers.[51,76] These workers have also formulated a tentative model to explain the bulk solvent effects in a sodium-poor environment, which is shown in Figure 1. Their model rationalizes the observed effects in terms of the effective monomer concentration at the sodium interface. This in turn is determined by the rate of diffusion of monomer to the sodium surface, which depends in part on whether the surface is predominantly open and readily accessible or is covered with growing polymer. In the former case, the monomer concentration at the interface will be the bulk concentration, while in the latter, the concentration will depend on the rate of diffusion through the polymer chains on the surface. In the case of unimpeded access, a large number of initiation steps occur which facilitate the formation of small fragments such as dimers etc. Diffusion of monomer through polymer chains covering the sodium particles, on the other hand, effectively reduces the concentration at the interface, generates fewer reactive intermediates, and promotes reaction at the reactive chain ends in a chain-extension process. The authors rationalize the solvent dependence in the following fashion. After a finite initiation period the sodium particles are undoubtedly covered with growing chains. In a good solvent, that is, one where the difference in the polymer and solvent solubility parameters $\Delta\delta = (\delta_s - \delta_p)$ approaches zero, the chains are predominantly extended, permitting relatively unimpeded access of the monomer to the surface. In a poorer solvent, the attached polymer chains tend to collapse to the surface, forcing monomer to diffuse through the growing chain to reach the surface of the sodium. If, however, the solvent is too poor, the polymer collapses upon itself and precipitates, thus limiting the molecular weight in this fashion. The authors suggest that there is an optimal $\Delta\delta$ for each polymer structure which permits the formation of high polymer in reasonable yield with a controlled molecular weight distribution and that this is responsible for the observed solvent effects. The

optimal $\Delta\delta$ determined empirically for the preparation of poly(methylphenylsilane) using inverse addition is 0.6. Although the reported experimental data refer mainly to poly(methylphenylsilane), the authors suggest that their model is applicable to other polysilane syntheses, although the optimal $\Delta\delta$ will depend on the structure of each polymer.

(b) The Polymerization Process. Mechanistic studies of the sodium-mediated polymerization have been hampered by the general exothermicity of the polymerization reaction and the heterogeneity of the media. The latter is apparently an important feature for the formation of long-chain linear polymers, since homogeneous chemical reductants such as Na/biphenyl produce only oligomeric materials.[51] At this point, it is not clear whether high polymer is not isolated in homogeneous media because the growth step fails or because the polymer rapidly degrades under the reaction conditions.

As described earlier, most polysilane syntheses yield materials with polymodal molecular weight distributions. The lowest molecular weight fractions ($\bar{M}_w \leq 1500$) consist mainly of oligomeric materials, particularly cyclic derivatives. For example, in the polymerization of *n*-hexylmethyldichlorosilane, the major portion of the oligomeric fraction was isolated and spectroscopically identified as a cyclic pentamer present as a mixture of isomers.[41]

Normally the generation of polymeric products with strongly polymodal molecular weight distributions would suggest that more than one mechanism competes in the polymerization process. However, in polysilane syntheses there is some evidence that the heterogeneity of the medium itself can also be responsible for the polymodal distribution in some cases. In this regard, Zeigler[51] has reported that in the preparation of poly-(methylphenylsilane) by inverse addition, constancy in the rate of addition of the sodium is critical. For this particular example, if the sodium addition is deliberately interrupted and restarted, the molecular weight distribution of the isolated polymer becomes increasingly polymodal.

Detailed mechanistic studies are also complicated by the fact that molecular weight changes in the presence of any excess sodium often depend on the length of time that the reaction refluxes after the addition is complete. This is manifested by slight increases in the molecular weight of the highest molecular weight fraction (region [3]) and larger increases in the molecular weights of the lower molecular weight fractions.[41]

In spite of the obvious complexity of the system, a number of important mechanistic observations have been reported. One could envision the possibility of a number of silicon-containing reactive intermediates such as silylenes, disilenes, silyl radicals, silyl anions, radical anions, etc. in the polymerization process. Of these, only the silylenes can be eliminated as major contributors, since the polymerization in the presence of known silylene traps such as triethylsilane[51] or dimethyldimethoxysilane[41] still yields high polymer, although the molecular weight distribution of the crude polymer product is altered. Zeigler and co-workers favor silyl radicals for the chain-extension steps on the basis of the lower molecular weights obtained for polymers whose substituents are prone to hydrogen

abstraction and/or when reactions are run in solvents such as 2,5-dimethyltetrahydrofuran.[51]

Likewise, conclusive evidence for the involvement of silyl anions is also sparse. Although the use of polyether solvents often dramatically increases the yields of many polysilanes in a fashion consistent with anionic intermediates, in at least one case [poly(di-n-hexylsilane)] improvements can also be realized by the addition of the nonpolar additive heptane as a cosolvent. However, recent reports[41] have reemphasized the importance of anionic species in the heterogeneous polymerization reaction. The addition of dialkylmercury derivatives to the sodium dispersion prior to monomer addition greatly accelerates the rate of disappearance of methylphenyldichlorosilane and increases the yield of polymer in the 5000–10000 range at the expense of the very high molecular weight polymer. Since the mercury derivatives produce alkylsodiums upon contact with sodium dispersion, it has been suggested that the presence of the organosodium species increases the number of growing chain ends, thus accelerating the polymerization while resulting in a decrease in the polymer molecular weight. Likewise, similar rate accelerations for the disappearance of n-hexylmethyldichlorosilane and modifications in the resulting polymer distribution are observed in the presence of catalytic amounts of 15-crown-5 and various cryptands, supporting the possible intermediacy of silyl anions in the polymerization reaction.[77]

The isolation of high polymer at low monomer conversions, coupled with the relative insensitivity of the polymerization process to reagent stoichiometry, is inconsistent with a classical condensation polymerization where short fragments generated from monomers are ultimately coupled to yield high molecular weight products only at high monomer conversion levels.[41] This observation of high polymer at low conversions suggests that after initiation, subsequent chain growth must be significantly accelerated. The reactivity of the polymeric chain ends cannot be too high, however, since polymer molecular weight increases are observed with time even after consumption of most of the monomer. The effect of the sodium surface area is also consistent with a slow initiation step followed by rapid chain extension. For n-hexylmethyldichlorosilane, monomer rate profiles as a function of sodium particle size show that the maximum rate observed after initiation is largely independent of the surface area,[41] while the initiation period depends strongly on the surface area of the sodium.

In summary, the heterogeneous polymerization of dichlorosilane monomers is a very complex process that more closely resembles a chain growth process initiated at the sodium surface than a classical condensation polymerization. The overall polymerization process may proceed by competing mechanisms that would rationalize the polymodal molecular weight distributions, and plausible intermediates could be silyl radicals, silyl anions, or perhaps even radical anions polymerizing by a single-electron-transfer (SET) mechanism. Regarding the latter, molecular weight vs conversion profiles that are similar to those observed for the polysilanes have been reported for a number of polymerization reactions believed to proceed via a SET mechanism.[78] Although significant progress has been

made recently, more studies are needed before the operative mechanism(s) and intermediates involved in the sodium-mediated coupling can be ascribed with confidence.

In spite of the demonstrated utility of the Wurtz-type coupling for the preparation of substituted silane homo- and copolymers, the technique has some obvious disadvantages. It has a low tolerance for reactive functionality, stereochemical control in the polymerization is marginal, yields are often low and depend strongly on the steric bulk of substituents, molecular weight distributions can be large and variable, the procedure is somewhat hazardous and difficult to scale up, and the process itself is costly on a large scale. For these reasons there is a need to develop new routes to high molecular weight linear polysilanes, particularly those containing reactive functionality. Recently, there has been some progress in this area, and this work will be reviewed in the following sections.

B. Alternative Procedures

1. Homogeneous Dehydrogenative Coupling

Recently, a number of reports have appeared describing the preparation of low molecular weight polysilane derivatives from substituted silanes using catalytic quantities of early-transition-metal complexes of titanium and zirconium.[79-82] Effective catalysts for this procedure were of the general type Cp_2MR_2 (M = Ti, R = alkyl; M = Zr, R = H or alkyl) and the overall reaction is as follows:

$$n\,R^1SiH_3 \xrightarrow{\text{cat.}} H\left(\begin{array}{c} H \\ | \\ Si \\ | \\ R^1 \end{array}\right)_n H \;+\; (n-1)H_2 \qquad (2)$$
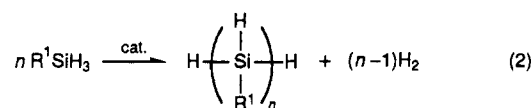
The oligomers prepared by this route are atactic, contain between 10 and 20 silicon atoms, and are terminated by $SiRH_2$ groups. The structure of the chain ends was determined by ^{29}Si NMR using a DEPT pulse sequence and also by IR analysis. Product analyses showed that almost no cyclic materials were produced, and although the dispersities of the linear polymers were low, the distribution was not monomodal. With the titanium catalysts, the introduction of olefins into the reaction mixture led to olefin hydrogenation, thus improving the overall thermodynamics of the process without influencing the polymerization. The use of zirconium catalysts and olefins under similar conditions, however, led to hydrosilylation of the SiH bonds of the product oligomers. The addition of cyclohexene in the polymerization of phenylsilane resulted in hydrosilylation of approximately 50% of the active SiH functionality.

The hydrogenative coupling reaction is highly selective and the steric constraints are significant. Only primary silanes produce the oligomers. Even though secondary silanes react, they produce dimers. A variety of substituents, R = phenyl, tolyl, benzyl, n-hexyl, cyclohexyl, etc., have been successfully utilized. Changes in the catalyst structure also can affect the efficiency of oligomerization. While the incorporation of one pentamethylcyclopentadienyl ligand can be accommodated, the presence of two destroys the catalytic activity. Similarly, while indenyl ligands are active on the

zirconium catalyst, incorporation of these ligands on titanium inhibits the polymerization.

The mechanism of the catalytic cycle is complex and a number of titanium derivatives have been isolated that do not seem to participate in the oligomerization reaction based on rate and product studies.[82] It is currently felt that a silylene complex such as $Cp_2M=SiHR$, either free or more likely bridged, is involved in the oligomerization reaction, although there is little experimental evidence in this regard. The mechanism of termination and the reason why the oligomerization stops at only 10–20 units are questions of current interest. With regard to the latter, it is possible that the polymer itself is subsequently degraded by the catalyst. In one case, it was demonstrated that a linear oligomer derived from benzylsilane was converted into a substituted cyclohexasilane isomer by the zirconium polymerization catalyst.[82]

In summary, homogeneous dehydrogenative coupling is an interesting technique that shows considerable promise. Efforts to generate higher molecular weight polymers using modified catalysts are proceeding in a number of laboratories. The use of optically active catalysts could offer the possibility of better stereochemical control in the polymerization. Even with only 10–20 silicon atoms, the current materials may have interesting electronic properties, and the presence of the reactive SiH functionality should offer the possibility of introducing novel side chains by subsequent hydrosilylation.[82]

2. Ultrasonic Activation

As mentioned, the Wurtz coupling procedure is usually conducted in an inert solvent that boils above the melting point of sodium (97 °C). Recent studies using ultrasound activation to facilitate low-temperature polymerization have provided some interesting results.[43,48,83–85] Matyjaszewski and co-workers[83,84] have shown that the polymerization of methylphenyldichlorosilane yields monomodal high molecular weight polymer ($\bar{M}_w \sim 10^5$) when ultrasonic agitation is utilized during and after the monomer addition. These results are particularly intriguing since the procedure involves the normal addition mode, a technique that usually gives predominantly low molecular weight poly(methylphenylsilane) ($\bar{M}_w = (4–10) \times 10^3$) in a stirred reaction. These and other[48] workers have reported curious substituent effects in the low-temperature ultrasonic polymerizations. While methylphenyldichlorosilane in toluene polymerizes readily near room temperature with ultrasound, dialkyl-substituted monomers such as di-n-hexyldichlorosilane or cyclohexylmethyldichlorosilane do not. In the latter cases, the addition of 25–30% by volume of diglyme initiates rapid polymerization and the production of monomodal high molecular weight ($\bar{M}_w = (4–6) \times 10^4$) polymer. It is also interesting to note that, although di-n-hexyldichlorosilane is basically unreactive in toluene alone, it readily copolymerizes with methylphenyldichlorosilane in the same solvent with ultrasonic agitation.[83,84] Recently, Bianconi and Weidman[43] reported the use of ultrasonic activation for the polymerization of alkyltrichlorosilanes using sodium–potassium alloy. Without the ultrasound, the coupling reaction is incomplete and residual silicon–halogen bonds remain.

The low-temperature, ultrasonic technique warrants closer investigation for preparative and mechanistic purposes. Although the high polymer yields are often comparable to those of stirred polymerizations run at higher temperatures, it does appear to offer some promise as a technique for control of the polymer molecular weight distribution.

3. Polysilane Functionalization

One potentially interesting route to reactively functionalized polysilane derivatives is the chemical transformation of preformed silane polymers. In spite of the attractiveness of such an approach, there has been relatively little work in the area to date. One problem lies with the polymers themselves, since they contain a highly delocalized σ backbone system and as a result have relatively low oxidation potentials (<1.4 V vs SCE).[86] This situation is exacerbated by the apparent instability of the linear polymer structures upon oxidation to radical cations. The redox characteristics of the polymers preclude the use of certain strongly electrophilic reagents and catalysts that are often also strong oxidizing reagents. However, it has been reported that poly(methylphenylsilane) can be efficiently chloromethylated with chloromethyl methyl ether and stannic chloride without significant polymer degradation.[87] This is an important observation, since it allows the introduction of halogen-containing substituents that would normally never survive the standard Wurtz coupling procedure. Similarly, Stüger and West[54] have reported that HX (X = Cl, Br) can be added to the double bond of poly[(2-(3-cyclohexenyl)ethyl)methylsilane] in the presence of Lewis acids without chain degradation.

Recently, Matyjaszewski et al. have shown that over 90% of the pendant phenyl groups of poly(methylphenylsilane) can be replaced by triflate groups by treatment of the polymer with trifluoromethanesulfonic acid.[83,88] The triflate functionality can be subsequently displaced by nucleophiles such as water to produce silanols or by alcohols to generate alkoxy-substituted polysilane derivatives. It has been reported that the phenyl substituents in samples of poly(methylphenylsilane) can be replaced with chlorine using aluminum chloride and HCl.[35] Matyjaszewski et al. have successfully grafted polymeric blocks derived from THF and methyl methacrylate onto samples of poly(methylphenylsilane) that had been modified by treatment with triflic acid.[89] In another study, West et al.[90] demonstrated that oxygen can be inserted into a polysilane polymer without significant chain scission by treatment with m-chloroperbenzoic acid. UV studies suggested that the oxygen insertion was not random but tended to produce block-like regions of polysiloxanes within the polysilane chain. Finally, it has been demonstrated that the active SiH bonds in certain substituted silane homo- and copolymers can be utilized for hydrosilation to introduce a variety of functionality.[35,82] The reactions described demonstrate the potential of the polymer functionalization procedure and suggest that this route deserves more attention in the future.

4. Miscellaneous

The formation of high polymers by reductive coupling under the Wurtz conditions suggests that similar re-

TABLE 6. Solution Light-Scattering Studies on Some Typical Polysilane Derivatives

entry	polymer	solvent	$M_w{}^{LS} \times 10^{-5\,a}$	$M_w{}^{PS} \times 10^{-5\,b}$	$10^4 A_2$	$R_{G,w}^0,{}^c$ nm	C_∞
1	$(n\text{-PrMeSi})_n$	THF	2.1	1.8	2.2	21	19
2	$(c\text{-HexMeSi})_n$	cyclohexane	25.4	8.0	1.2	50	14
3	$(n\text{-Hex}_2\text{Si})_n$	cyclohexane	74.0	22.0	0.5	87	21
4	$(n\text{-Hex}_2\text{Si})_n$	hexane	61.0	19.0	0.8	77	20
5	$(n\text{-Hex}_2\text{Si})_n$	THF	63.0	19.0	0.4	76	20
6	$(n\text{-octyl}_2\text{Si})_n$	THF	32.0	26.0	1.0	59	30
7	$(\text{MePhSi})_n$	THF	0.46	0.19	3.6	15	64

$^a M_w{}^{LS}$ = molecular weight as determined by light scattering. $^b M_w{}^{PS}$ = molecular weight as determined by GPC using polystyrene calibration standards. $^c R_{G,w}^0$ = radius of gyration including corrections for estimated excluded volume effects and corrections of measured $R_{G,z}$ to an average appropriate for comparison with M_w; i.e., $R_{G,z}/R_{G,w} \propto (M_z/M_w)^{0.6}$.

actions should be possible by using controlled-potential electrochemical reduction. In spite of the fact that this technique has been described for the formation of SiSi bonds in monomer synthesis, its application to polymer synthesis has been largely ignored. Although the preparation of high molecular weight polymers from substituted dichlorosilanes by this route has not yet been described, several reports on the preparation of oligomers have appeared.[91,92]

Finally, a recent report suggests that certain substituted silane polymers might be accessible by ring-opening polymerization. In this regard, Matyjaszewski and co-workers have described the production of a high molecular weight polymer ($\bar{M}_w = 10^4$) by the ring-opening polymerization of octamethoxycyclotetrasilane.[83] Finally, the use of α,ω-dilithio acyclic silane oligomers derived from the ring opening of substituted cyclosilanes to prepare block copolymers by condensation with α,ω-dichlorosilane oligomers has been described by Wesson and Williams.[30]

IV. Polymer Properties

Depending on the substitution pattern, polysilane derivatives display a wide variety of polymer properties. Materials with glass transition temperatures ranging from $-76\ ^\circ$C to above 120 $^\circ$C have been produced. For this reason, the polymers themselves range from rubbery elastomers to hard, brittle solids. In general, the incorporation of aryl substituents tends to raise the polymer glass transition temperatures. Copolymers of varying compositions may be prepared in an effort to produce the desired mechanical properties for a particular application.

Substituted silane high polymers are often thermally stable to temperatures above 250 $^\circ$C. Some typical thermogravimetric analyses that show almost no weight loss at temperatures below 300 $^\circ$C are shown in Figure 2. This thermal stability is consistent with the strengths of silicon–silicon (80 kcal/mol) and carbon–silicon (90 kcal/mol) bonds.[93] Although certain aryl-substituted polysilanes such as polysilastyrene and poly(methylphenylsilane) can apparently be melt cast without decomposition, the sterically hindered bisaryl derivatives undergo irreversible changes around 200 $^\circ$C that are not accompanied by significant weight losses. We have observed that symmetrically substituted poly(dialkylsilanes) such as poly(di-n-hexylsilane) thermally decompose with significant weight loss prior to melting.[59]

For the polysilanes, ^{1}H NMR and ^{13}C NMR augmented by the use of ^{29}Si NMR provide invaluable data
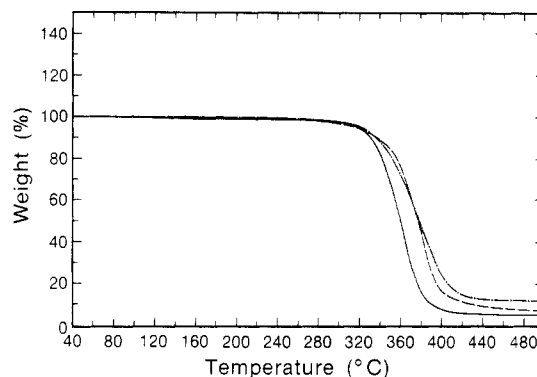

Figure 2. Thermogravimetric analyses (TGA) of some typical polysilane derivatives: (—) poly(cyclohexylmethylsilane); (- - -) poly(di-n-hexylsilane); (-·-) poly(methylphenylsilane).

for the analysis of polymer microstructure. A number of ^{29}Si NMR studies using INEPT pulse sequences on soluble polysilane derivatives in solution have been reported recently. For unsymmetrically alkyl-substituted homopolymers prepared by Wurtz coupling, broad, structured silicon resonances are observed which are characteristic of a random atactic distribution of stereocenters.[62,63] This is apparently not true, however, of polymers with aromatic substituents attached to the backbone such as poly(methylphenylsilane) where the peak intensities within the silicon multiplet suggest a nonrandom collection of stereocenters in the polymer.[64] As mentioned, microstructural analysis of copolymers is more difficult due to the added complexity caused by the need to determine the comonomer sequence as well as stereocenter configuration. For this reason, few substituted silane copolymers have been completely characterized. On the basis of limited data, it has been suggested that the copolymers formed from dialkyl-substituted comonomers are essentially random in nature while those produced from the condensation of methylphenyldichlorosilane and dialkyldichlorosilanes tend to form more blocky type structures.[39,64]

Infrared spectra for a wide variety of substituted silane homo- and copolymers have been measured and the data appear with tentative band assignments in the literature.[50,58b,65,67,75] As these data are for the most part unexceptional, they will not be described further here and the interested reader is referred to the literature cited. The UV absorption characteristics have also been described, and since they are quite extraordinary, these results and their interpretation will be discussed in detail in section VII.A.

While NMR studies have revealed the nature of the polymer microstructure in many cases, preliminary light-scattering studies have provided some information

on the polymer chain structure for some polysilane homopolymers[94] and copolymers[95] in solution. Light-scattering data for some representative polysilane homopolymers are presented in Table 6. A number of interesting features are obvious. Comparison of molecular weights as determined by light scattering and gel permeation chromatography (GPC) shows that the respective numbers are not particularly close and often vary by as much as a factor of 2–3. This confirms that polystyrene, which is used for calibration of the GPC results, is not a particularly good model for the polysilanes. As a result, molecular weights determined by GPC, while useful in a relative sense, should always be compared with data obtained by light scattering or viscometry when a more accurate estimate of the true polymer molecular weight is necessary. The table also lists data on the calculated radii of gyration for a variety of polymers from which the characteristic ratio C_∞ can be calculated. The characteristic ratio is defined as the mean-square end-to-end distance of the polymer ($\langle r^2 \rangle \sim 6R_g$; R_g = polymer radius of gyration) divided by the number of monomer units in the chain times the average silicon–silicon bond length squared (nl^2), and this ratio is often used as a common criterion for polymer stiffness in solution. For comparison, it should be noted that C_∞ for polystyrene has been calculated to be around 10. Since larger values of C_∞ are associated with increasing polymer rigidity, these data suggest that the structure of the polysilanes in solution can be best described as that of a slightly stiffened random coil. As the chain structure of the polysilane derivatives in solution is expected to vary with the type of substituent, there is a need to expand these light-scattering studies to include a wider variety of polysilane derivatives. Finally, it should also be noted that the current light-scattering data[94] were not measured in Θ conditions, thus requiring the incorporation of certain assumptions and approximations in an effort to produce reasonable estimates of the unperturbed chain dimensions. At the Θ point, the polymer–polymer, polymer–solvent, and solvent–solvent interactions are all equal. This point can be approached by changes in either the solution temperature or the solvent. While the current measurements are probably adequate for comparison purposes, they point to the need for more accurate studies performed on polymers of narrow dispersity under Θ conditions.

V. Molecular Structure and Conformation

The molecular structure and conformation of polysilanes in solution and as neat solids are of fundamental importance for their properties and have received considerable attention. The conformations of model parent oligosilanes and, to a lesser extent, of permethylated oligosilanes are now believed to be understood to some degree, although there clearly still is much room for improvement. The conformations of the practically important, tractable polysilanes, i.e., those with longer alkyl (or aryl) substituents on silicon, have not been reliably predicted by theory, although some trends are now apparent. Primarily because of possible side chain–side chain interactions and low torsional barriers in the silicon backbone, it is likely that in these structures, conformations other than the usual trans (180° twist) and gauche (60° twist) may well be important.

A. Parent Oligosilanes (1, $R^1 = R^2 = H$)

Empirical force field,[96-99] semiempirical MINDO/3,[100,101] MNDO,[101,102] and CNDO,[103] and ab initio[104-106] single-determinant molecular orbital geometry optimizations have been performed for several parent oligosilanes.

Among the semiempirical methods, MINDO/3 appears to be superior in that it produces nearly correct SiSi bond lengths, while those predicted by MNDO and CNDO are too short and too long, respectively.[101] Empirical calculations on chains up to 30 Si atoms in length led to the conclusion that the interactions are additive in this approximation and that it is sufficient to evaluate the conformational properties of pentasilane.[97]

Both the empirical and semiempirical methods suffer from a dearth of reliable experimental calibration data, and the single-determinant MO methods suffer from the neglect of electron correlation and thus of dispersion forces. The most recent ab initio calculations[104] probably are the most reliable for the determination of bond lengths and valence angles. They used a relatively small but most likely acceptable basis set (3-21G*) and relied on the SCF approximation in the full geometry optimization step. They were performed up to pentasilane and predict SiSi bond lengths of about 234.6 pm and SiSiSi valence angles of about 111.5°. These results are also in reasonably good agreement with the empirical and the best semiempirical values. The bond lengths and valence angles are quite unexceptional and can be considered reliable. The results obtained in an ab initio band structure calculation[106] for two smaller basis sets with pseudopotentials differ widely and are clearly less reliable.

The difficult part of the calculations is the evaluation of the dihedral angles. Trans and gauche geometries were generally found to represent local minima and were of equal energy within what we consider the credibility limits of the methods (in one of the ab initio studies[105] only the trans geometries were considered). It seems safe to conclude from the collection of calculations that the trans–gauche energy difference is certainly <1 kcal/mol and most likely <0.5 kcal/mol, but we are not convinced that it is known which is the more stable form. The empirical methods of calculation favor the gauche form over the trans form, while the single-determinant MO methods favor the trans form over the gauche form. This trend is understandable since the latter neglect the dispersion forces, which generally favor the more compact gauche geometries. Indeed, a 6-31G* MP2 calculation[104] at the geometries optimized at the 3-21G* SCF level, which includes at least some electron correlation, inverts the stability order in tetrasilane, favoring the gauche form by 0.04 kcal/mol. A more complete consideration of electron correlation would presumably yield an even larger stabilization of the gauche form. However, an indirect experimental gas-phase estimate for tetrasilane is 0.4 kcal/mol in favor of the anti conformer.[107]

All attempts to judge the reliability of the computed minute differences between the trans and gauche conformations should be tempered by the recognition that it is not really the behavior of an isolated gas-phase polymer molecule that is of interest but, rather, the behavior of a molecule in a solvent. Here, it is quite possible that the loss of intramolecular stabilization by

dispersion forces that occurs upon going to the less compact trans conformation is partly or fully compensated by an increase of intermolecular dispersion stabilization by interaction with an increasing number of solvent molecules.

The computed barriers to internal rotation are also very low: the ab initio results[104] are 1.5 ± 0.2 kcal/mol for gauche–gauche and 0.7 ± 0.1 kcal/mol for gauche–anti rotation in tetrasilane. The experimental values are not available; the closest comparison, albeit far from ideal, is with the estimated value of the rotational barrier in disilane, 1.1–1.2 kcal/mol.[108]

A conformational energy map combining empirical force calculations[97] with additional computations employing no relaxation or partial relaxation has been published[98] for the parent polysilane. It is extremely flat, and nearly all regions of the conformational space that are accessible by rigid rotations are located no higher than 2 kcal/mol above the absolute minimum. Although the quantitative details on such a flat surface cannot be taken too seriously, it illustrates nicely the extreme flexibility of the parent polysilane chain.

B. Permethylated Oligosilanes (1, $R^1 = R^2 =$ Me)

Permethylated oligosilanes are the simplest among the peralkylated derivatives that are stable and have been used as models in empirical force field calculations.[97,101] These again yield fairly standard bond lengths (typical values, SiSi, 235 pm; SiC, 187 pm; CH, 110 pm) and valence angles (SiSiSi, 115.4°; SiSiC, 108.5°; SiCH, 110°). The experimental SiSi bond length in poly(di-n-hexylsilane) was determined by EXAFS as 237 ± 2 pm[109] and the valence angle was estimated as 115–118° by a combination of EXAFS, WAXD, and electron diffraction studies.[109-111]

The anti and gauche conformations of permethylated oligosilanes are computed to be close in energy, with gauche slightly favored, the difference again being smaller than the likely error of the calculational method. There is spectroscopic evidence[112] that in neat solution the anti conformer of decamethyltetrasilane is more stable than the gauche conformer by ~0.5 kcal/mol so that both are present in comparable amounts at room temperature and that the barrier to gauche–gauche interconversion is higher than that to gauche–anti interconversion. An attempt[98] to construct a conformational energy map for permethylpolysilane using no relaxation or only partial relaxation but including dispersion corrections suffered from excessive methyl-methyl interactions. The map contained much larger regions of prohibitively high energy than that for the parent polysilane, as could be expected due to the relative bulkiness of the methyl groups. The conformational preferences of the chain were sensitive to the details of the calculation, and we believe that no firm conclusions are possible at this level of approximation. The computed coefficients C_∞ that characterize the degree of chain coiling were less sensitive to the details of the calculation, being ~13 for the permethylated and ~4 for the parent polysilane (cf. polyethylene, 6.7; poly(dimethylsiloxane), 6.4; fully extended chain, ∞).

C. Di-n-hexyl-Substituted Oligosilanes

Full geometry optimization for oligosilanes containing

the more common longer alkyl substituents such as n-propyl, n-hexyl, etc. rapidly becomes very time-consuming already for quite short chains. Semiempirical and ab initio molecular orbital calculations on species of this type now encounter in a particularly severe form the already mentioned problem of how to best treat the dispersion forces between spatially proximate but nonbonded parts of an extended molecule. Dispersion forces between adjacent long alkyl chains may well dictate the overall conformation of the intrinsically very flexible chain in the isolated molecule and possibly even in solution, and the differential solution effects are particularly hard to predict. The treatment of the neat solid polymer would involve a very complex set of intermolecular interactions due to possible side-chain interlocking etc.

Two sets of empirical calculations on a five-silicon chain with two n-hexyl substituents on each silicon and two terminal methyls have been reported.[113,114] The earlier work[113] concluded that the all-trans form was favored, and the later calculation[114] led to the conclusion that the stable form is neither trans nor gauche, but one in which the SiSiSiSi dihedral angle is near 150°, so that the backbone forms a 7/3 helix. In view of the limited reliability of the empirical potentials and the neglect of solvent effects, these calculations, although suggestive, are far from definitive. Interestingly, structural studies on poly(di-n-butylsilane)[115] and poly(di-n-pentylsilane),[116] neither of which displays evidence of significant side-chain crystallization, have suggested that these materials adopt a helical structure (7/3 helix) in the solid state, the structure of which is remarkably similar to that theoretically predicted for poly(di-n-hexylsilane) as an isolated molecule.

D. Arylated Oligosilanes

Two attempts have been reported to compute the conformation of $(SiMePh)_n$.[117,118] In the first calculation,[117] the bond lengths and valence angles were fixed, a torsional barrier of 1.2 kcal/mol was included for the rotations of the SiSi bonds, and the Lennard-Jones 6–12 potential function was used to calculate the nonbonded potential energies. The (up, up, up), (up, down, up), and (up, up, down) arrangements of the phenyl substituents on three successive silicon atoms were considered. Perpetuation of the (up, up, up) sequence corresponds to the syndiotactic polymer, of the (up, down, up) to isotactic segments, and of the (up, up, down) to heterotactic segments.

The trans–trans conformation was generally computed to be favored, with the minima shifted from perfect staggering by as much as 30–40°. Because of this shift, the authors proposed that the "all-up" syndiotactic polymer will form slowly winding helical segments. For the (up, down, up) and (up, up, down) arrangements the approximately trans–trans geometries and those containing approximately gauche turns were calculated to be more nearly comparable in energy, leading to compact helical and looping segments.

The characteristic coefficients C_∞ were calculated for various chain compositions. A high value of 250 was obtained for the syndiotactic polymer and was found to decrease very rapidly upon incorporation of up to about 20% of (up, down, up) or (up, up, down) configurations. The observed[94] value of $C_\infty = 64 ± 20$ is

compatible with a stereoirregular chain.

Chain-end effects on the conformational probabilities were evaluated and predicted to be detectable at room temperature up to 20–40 bonds from chain end for the (up, down, up) and (up, up, down) arrangements. For the (up, up, up) configuration, the trans–trans state is computed to be so highly preferred that there should not be any chain-end effect. The authors proposed that the chain-end effects contribute to the observed red shift of the experimentally observed[119] absorption maximum with the increasing chain length. They attributed the observed[120] sharpening of the absorption peak upon cooling to 77 K to an increase in the probability of the trans–trans arrangement in the segments in the (up, down, up) configuration.

In a more recent investigation by the MM2 method,[118] computations were performed on the model compounds Me–[SiMePh]$_5$–Me and H–[SiH$_2$–SiHPh]$_3$–SiH$_3$, both isotactic and syndiotactic. It was concluded that at room temperature both forms of [SiMePh]$_n$ are nearly exclusively in the all-trans (planar zigzag) conformation, with the TT arrangement ~5 kcal/mol more stable than TG or GG, due to the steric bulk of the substituents. This led to a rodlike polymer with a nonconvergent C_∞ coefficient. The values calculated for $n = 400 \pm 75$ are $C_n = 255 \pm 15$, to be compared with the above-quoted experimental value of 64 ± 20. Although the calculation clearly exaggerates the degree to which the TT conformation is preferred, it also reproduces in a qualitative sense the contrast to the more highly coiled peralkylated polysilanes (experimental C_∞ values, 22 ± 8).[94]

The results calculated[118] for isotactic and syndiotactic [SiH$_2$–SiHPh]$_n$ differ considerably. The former is calculated to prefer T states over G states, particularly the TT arrangement (by about 2 kcal/mol), although not quite as much as [SiMePh]$_n$. The latter is calculated to prefer G states over T states, particularly the G$^+$G$^+$ arrangement. In both forms, the preferred calculated conformations are those that stack the phenyl rings. The conclusion is that the isotactic chain is fairly extended but with just enough bends to form a random coil ($C_\infty = 19$) while the syndiotactic chain forms an inflexible and highly extended helix with a G$^+$G$^+$G$^+$G$^+$ sequence ($C_{400} = 79$).

In view of the uncertainties associated with the empirical force field, the results of both sets of calculations, while of qualitative significance, cannot be considered quantitatively reliable. Unfortunately, it is currently impossible to make meaningful comparisons between the theory and experiment for unsymmetrically substituted polysilanes as the polymers that have been generated to this point have been predominantly atactic materials. Further progress in the area awaits new developments in the synthesis of stereoregular materials.

In summary, the field of conformational analysis of polysilanes is in its infancy, and reliable prediction and interpretation of molecular geometries and conformations represents an exciting challenge. A development of more reliable empirical force fields for molecules containing silicon, hydrogen, and carbon clearly is a task of continuing importance. An extended MM2 force field which also encompasses silanes and polysilanes has recently been reported.[121]
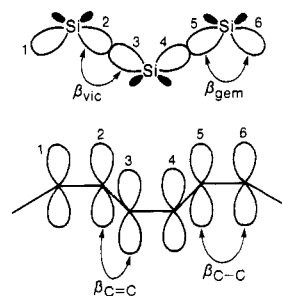
Figure 3. The σ-conjugated linear chain of interacting Si 3sp^3 orbitals in a polysilane (top) and the π-conjugated linear chain of interacting C 2p orbitals in a polyene with alternating bond lengths (bottom).

## VI. Ground-State Properties and Electronic Structure

A. Background

Early work on ground-state properties of oligosilanes used very simple methods such as LCBO (linear combination of bond orbitals),[122–125] Sandorfy model C,[3,126–129] and FE (free electron)[130] and established the fundamental principles for the present understanding of the remarkable "delocalized" electronic structure of polysilanes. More recently, molecular orbital calculations by all-valence-electron semiempirical methods[101,102,123,124,132–134] and pseudopotential[136] as well as all-electron[104,105,139] ab initio methods verified that the simple concepts are fundamentally sound and have helped to fill in some of the missing detail. It has been found that the MNDO method does not describe the electronic structure of these compounds as well as MINDO/3.[101]

These model calculations were performed for oligosilanes with up to 40 silicon atoms. Similar results were obtained from band-theory calculations performed for infinite chains using various semiempirical[103,140–142] and ab initio[106] levels of approximation. In one of these studies, the band structures of several hypothetical unsaturated polysilanes were calculated.[143]

The primary conclusions of all of these studies of the electronic structure of silicon chains agree. The present understanding will now be summarized for the case of an all-trans conformation in terms of the qualitative MO bonding model. We shall use z to label the long axis of the polysilane chain, y for the short in-plane axis, and x for the axis perpendicular to the plane containing the silicon atoms. It now appears quite certain[105,136] that d orbitals play no significant role in the description of the orbitals occupied in the ground state or even the low-energy unoccupied ones.

To a chemist, the bonding in polysilanes is perhaps most naturally described starting with relatively short model chains and extrapolating to higher molecular weights, using a basis set of approximately sp^3 hybrid orbitals located on the silicon atoms and pointing at their neighbors and 1s orbitals on the hydrogens, or other appropriate orbitals on other possibly present substituents, such as sp^3 on a methyl carbon (Figure 3).

The resonance integral between two sp^3 orbitals located on adjacent silicons and pointing at each other, β_{vic}, is responsible for the SiSi σ bond formation. The vicinal interaction splits each such pair of basis orbitals into a strongly bonding σ_{SiSi} and a strongly antibonding
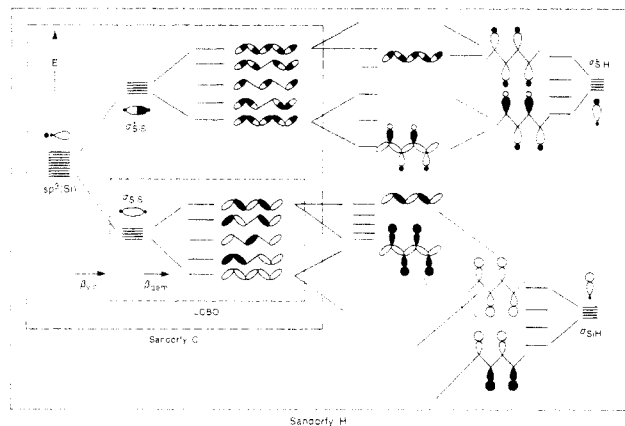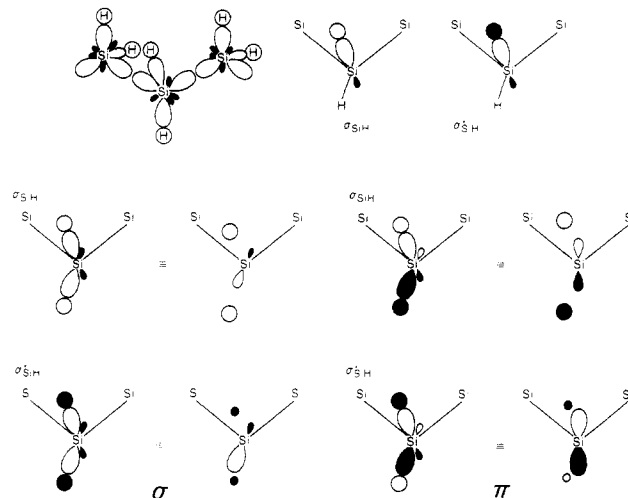
Figure 4. A schematic derivation of the form of the σ-symmetry orbitals of a long, all-trans polysilane chain. Left, backbone orbitals; right, orbitals of the SiH bonds; center, the result of their mutual interaction.

Figure 5. Top: left, the basis set of Si $3sp^3$ and H $1s$ orbitals for the discussion of bonding in a long polysilane; right, the form of the σ_{SiH} and σ^*_{SiH} orbitals. Bottom: two equivalent representations of the σ- and π-symmetry combinations of the two σ_{SiH} and two σ^*_{SiH} orbitals on each silicon atom of an all-trans polysilane, once in terms of the hybrid orbital set and once in terms of the AO set. Schematic.

σ^*_{SiSi} localized bond orbital. A less strongly negative resonance integral β_{gem} between two sp^3 hybrids located on the same silicon atom is responsible for the interaction between localized orbitals carried by the same silicon. A linear chain of mutually interacting localized orbitals results, and the molecular orbitals are delocalized over the whole silicon backbone. The use of this basis set at the Hückel level is known as the Sandorfy model C.[144] When the Si orbitals pointing at the substituents (hydrogens) as well as the substituent orbitals pointing at Si are also included, the Sandorfy model H results. We shall concentrate first on the orbitals of the silicon backbone (model C).

The degree of electron delocalization in the backbone is a function of the ratio β_{gem}/β_{vic}. If the ratio vanishes, the localization of bonds and antibonds between pairs of silicon atoms is complete. If the ratio equals unity, their delocalization is perfect. A well-known analogy is found in the isoelectronic π system of polyenes. When the C–C bond lengths in a polyene are all equal, all resonance integrals are equal and perfect delocalization results. When the bond lengths alternate, so will the resonance integrals, and the π components of the double bonds will be partially localized.

Within the framework of the Sandorfy model C (i.e., incorporating implicitly the corrections for the presence of bonds to hydrogen) and fitting parameters to vertical ionization energies of Si_nH_{2n+2}, $n \leq 5$,[126] the best value for the Hückel one-center Coulomb integral in the parent oligosilanes is $\alpha = -8.6 \pm 0.07$ eV and for the Hückel resonance integrals, $\beta_{vic} = -1.9 \pm 0.1$ eV, $\beta_{gem} = -1.67 \pm 0.02$ eV, with $\beta_{gem}/\beta_{vic} = 0.87$. The corresponding values for carbon in alkanes are $\alpha = -9.6 \pm 0.2$ eV, $\beta_{vic} = -2.5 \pm 0.2$ eV, $\beta_{gem} = -1.90 \pm 0.02$ eV, and $\beta_{gem}/\beta_{vic} = 0.76$, indicating a substantially smaller degree of delocalization in the carbon chain, a correspondingly faster damping of substituent effects, and generally less "π-electron-like" character.

The nodal patterns of the delocalized bonding MOs of the polysilane backbone are identical with those in the isoelectronic polyenes. The most stable orbital has no nodes at the silicon atoms nor at bond midpoints, and the least stable one has them at each silicon atom and at each bond midpoint. As shown in Figure 4, the bonding orbitals do not have nodes at bond midpoints and can be viewed as linear combinations of localized (two-center) σ orbitals σ_{SiSi}, separated by an increasing

number of nodes at Si atoms as their energy increases. In the least stable bonding orbital (the highest occupied molecular orbital, HOMO), there is a node at every silicon atom. This is also the qualitative picture provided by the simplest LCBO model, in which the two-center σ_{SiSi} orbitals represent a basis set from which all delocalized σ molecular orbitals are constructed, and antibonding orbitals are not considered.

The nodal patterns of the delocalized antibonding MOs also are just like those in a polyene. These MOs can be viewed as linear combinations of localized σ^*_{SiSi} orbitals, each of which has a node at a bond midpoint, again separated by an increasing number of nodes on Si atoms as the energy goes up. In the most stable antibonding orbital (lowest unoccupied molecular orbital, LUMO), there are no nodes at the silicon atoms, only between them, at bond midpoints.

The remaining effects on the backbone orbitals to be mentioned are those due to nonneighbor resonance integrals. These are unimportant for the present purposes, but will be essential when we discuss the role of chain conformations.

It is now necessary to consider the orbitals used in the bonding of the substituents to the silicon backbone, as in Sandorfy model H. The two sp^3 hybrids used by each silicon atom for this purpose combine with the orbitals of the substituents into low-energy bonding σ_{SiH} (σ_{SiC}) and high-energy antibonding σ^*_{SiH} (σ^*_{SiC}) orbitals; symmetry adaptation with respect to mirroring in the plane of the silicon atoms yields π-symmetry (antisymmetric) bonding and antibonding combinations and σ-symmetry (symmetric) bonding and antibonding combinations (Figure 5). Relatively weak interactions between such orbitals located at neighboring silicon atoms bring about a perfect delocalization along the length of the chain. Since the SiSi distances are all nearly equal, the overlap and resonance integrals for such delocalization do not alternate in size along the chain. They are larger for the antibonding σ^*_{SiH} orbitals, which are largely localized on silicon atoms, whereas the bonding σ_{SiH} orbitals are primarily localized on the substituent. This is caused by the low electro-

negativity of silicon relative to hydrogen (and carbon) and would not be necessarily true in otherwise substituted polysilane chains. This also makes both the σ- and the π-symmetry combinations of the σ_{SiH} orbitals relatively low in energy, well below the less stable among the SiSi bonding molecular orbitals of the silicon backbone.

The π-symmetry combinations of the σ_{SiH} and σ^*_{SiH} orbitals are not permitted by symmetry to mix with any of the orbitals of the silicon backbone described above, while the σ-symmetry combinations are (Figure 4). The mixing is of some importance but does not modify very significantly the conclusions reached previously for the frontier orbitals. The SiSi bonding backbone orbitals are destabilized by the mixing with the σ-symmetry σ_{SiH} combinations. For the upper bonding backbone orbitals, the mixing is weak not only because of the energy mismatch but also because they have nodes at many Si atoms and, thus, are of the wrong local symmetry to have a nonzero resonance integral with the sp³ hybrids used in the Si–H bonds. As a result, the band of SiSi bonding backbone orbitals is compressed and its center of gravity is pushed to higher energies.

When the σ_{SiH} bond orbitals are included in the LCBO model, it is possible to account for the observed photoelectron spectra quantitatively,[123] while ignoring the σ^*_{SiH} bond orbitals altogether. In particular, the overall shift to higher energies and the compression of the more strongly bonding orbitals cannot be explained without invoking the effect of the σ_{SiH} orbitals. It was first thought that the photoelectron spectra of permethylated oligosilanes fit the LCBO model even without this refinement,[122] but later it was recognized that this is not so when conformational effects are deconvoluted.[123] Still, the net effects of mixing with σ_{SiC} bond orbitals appear to be smaller.

The most stable among the SiSi antibonding backbone orbitals are stabilized by in-phase mixing with the σ-symmetry σ^*_{SiH} combinations (Figure 4). The mixing is now stronger since the energy mismatch is not as bad and, particularly, since these backbone orbitals have nodes at few if any Si atoms and, therefore, consist primarily of silicon 3s and 3p$_y$ contributions (see below), which have the proper local symmetry for strong interaction with the sp³ hybrids pointing to the hydrogen atoms. The SiSi antibonding backbone orbital band is expanded and its center of gravity is pushed to lower energies.

Thus, while in a long all-trans chain the effect of the mixing with σ-symmetry combinations of the σ_{SiH} and σ^*_{SiH} orbitals on the HOMO is negligible, the effect on the LUMO is large. The former has essentially no contribution from Si 3p$_y$ and H 1s orbitals, the latter a significant one. The former is an essentially pure backbone orbital, for which the Sandorfy model C is appropriate; for the latter, the Sandorfy model H is preferable.

Virtually all numerical calculations suggest that the lowest among the σ-symmetry antibonding molecular orbitals of the SiSi backbone is the LUMO. The lowest among the delocalized π-symmetry orbitals resulting from σ^*_{SiH}, primarily composed of in-phase Si 3p$_x$ contributions, is located at higher energy (for a discussion of the possible involvement of Rydberg orbitals in the LUMO, see ref 136). The issue is somewhat
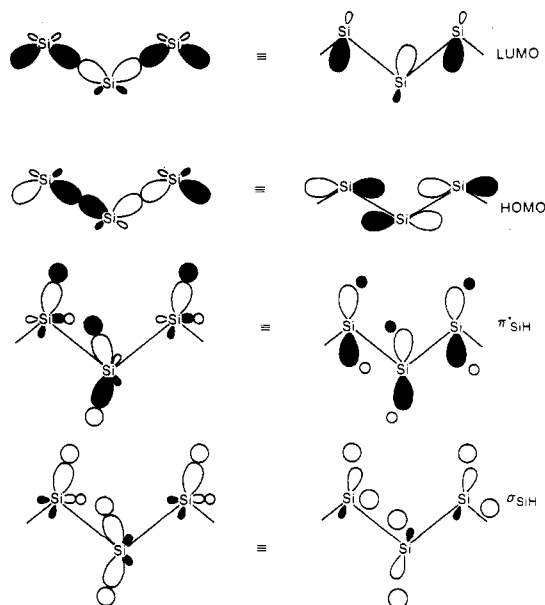
Figure 6. Equivalent representations of the LUMO, HOMO, π^*_{SiH}, and σ_{SiH} orbitals of a long all-trans polysilane in terms of the hybrid orbital set (left) and the AO set (right). Schematic.

clouded by the fact that certain authors[105] have referred even to MOs that are symmetric with respect to mirroring in the backbone plane as π-type orbitals (at least judging by Figure 3 and Table II in ref 105, although the text seems to disagree), presumably because of the significant contributions from the 3p$_y$ orbitals that they contain. This is not a common usage and we shall avoid it.

It should be noted that the description of bonding in polysilanes in terms of a basis set hybridized orbitals is not limited to Hückel theory. The results of any minimum basis set calculation are easily transformed into such a basis set, as was done, for instance, for the INDO/S results of ref 134.

The inverse transformation is equally facile (Figure 6). At those Si atoms where a backbone MO has a node, the two sp³ hybrids enter with opposite signs and their 3s components cancel. At these atoms, the MO has a purely 3p$_z$ character. The least stable among the backbone bonding MOs (the HOMO), as well as the least stable among the antibonding orbitals, which have a node on every Si atom, are therefore of purely 3p$_z$ character in a very long chain.

At those Si atoms where the two hybrids enter with equal signs, their 3s components add up, and the p components add to a 3p$_y$ orbital. At these atoms, the MO then has a strong 3s, 3p$_y$ character. The most stable among the bonding MOs and the most stable among the antibonding MOs (the LUMO), which have no nodes on any of the Si atoms, are therefore largely of 3s, 3p$_y$ character in a very long chain.

This analysis provides a rationale for the energy ordering of the orbitals as a function of their nodal patterns. The absence or presence of a node between Si atoms, at a bond midpoint, is related to bonding and antibonding in σ_{SiSi} and σ^*_{SiSi}, respectively (contribution from β_{vic}). The absence or presence of a node at Si atoms, in orbitals interacting through β_{gem}, is not related to bond formation but rather to the relative weight of the 3s (and 3p$_y$) and 3p$_z$ contributions in the orbital. Since the 3s orbital is much lower in energy, the absence of a node is favorable.

Similar considerations apply to the orbitals used to attach substituents. For instance, the π-symmetry orbitals are of pure $3p_x$ character on silicon and $1s$ character on hydrogen.

For a solid-state physicist, used to descriptions in terms of s bands and p bands, an analysis of polysilanes in terms of a basis set of 3s and 3p atomic orbitals is more natural, as is the use of an infinite chain for the starting point.[103,106,140-142] In the end, however, the same picture of MOs results, with a HOMO of purely $3p_z$ character, consisting of a $3p_z$ orbital on each Si atom, and with a LUMO of largely 3s, $3p_y$ character, antibonding across each SiSi pair and containing some H 1s contribution. Now, the former results from the lower edge of the p band and the latter from the upper edge of the s band. The gap between them originates in the strongly avoided crossing of the s and p bands.

Most of the Hamiltonians used in the band structure calculations were of a very simple semiempirical kind. They, too, placed the π-type conduction band above the σ-type one in energy.

B. Substituent Effects

These have been discussed in quite a few papers either in the context of band structure calculations[140-142,146a] or in consideration of model oligosilanes[147,148] and can be simply summarized as follows (the authors of ref 146a use "orbital hybridization" where it would be more common for chemists to speak of "orbital mixing" or "orbital interaction").

In discussing the electronic structure of parent oligosilanes and polysilanes, we have indicated that the electronegativities of hydrogen and carbon are similar, so that similar results might be expected for the parent and the peralkylated polysilane backbones. However, while the σ CH bond is nonpolar, when attached to an atom with orbitals of π symmetry, an alkyl such as methyl will hyperconjugate and in this regard will be different from hydrogen. In principle, methyl can act both as a π donor and a π acceptor since it has both occupied and empty orbitals of π symmetry relative to its threefold axis. Normally, the former interact strongly with the bonding orbitals and the latter with the antibonding orbitals of the substrate.

The effects of permethylation on the HOMO of the parent oligosilane or polysilane, the least stable of the backbone SiSi bonding orbitals (mostly $3p_z$), on the LUMO, the most stable of the backbone SiSi antibonding orbitals (mostly 3s and $3p_y$), and on the π-symmetry SiH antibonding orbital (mostly $3p_x$) are readily understood (see Figure 7). The energy difference from the methyl donor orbital is smallest for interaction with the HOMO, and the $3p_z$ nature of the latter is perfect for a hyperconjugation, so that a significant destabilization of the HOMO must be expected. This is indeed readily revealed by comparison of photoelectron spectra.[107,122,123] The energy difference to both σ- and π-symmetry antibonding orbitals is larger and they should be destabilized less.

At the same time, the energy separation of these antibonding orbitals from the acceptor orbital of methyl is smaller and interaction with it is likely to dominate, leading to their stabilization. The LUMO, i.e., the σ-symmetry SiSi antibonding orbital of the backbone, with its 3s and $3p_y$ character, has almost exactly the
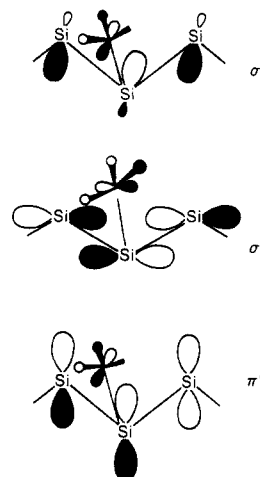

Figure 7. Interaction of the local π-symmetry orbitals of a methyl substituent with the HOMO (σ), LUMO (σ^*), and π^*_{SiH} orbitals of a long all-trans polysilane. Of the two degenerate components of the methyl orbital, only the one whose symmetry is appropriate for the interaction is shown.

wrong local symmetry for any hyperconjugative interaction with the methyl substituent and is not affected much (only the $3p_y$ component can interact and even that is not ideally oriented). The π-symmetry SiC antibonding orbital has much better suited local symmetry and will be affected; numerical results show that the interaction with the antibonding methyl π orbital dominates, so that it is stabilized. If the substituent effect is strong enough, this orbital may become the LUMO, and there indeed is ambiguity in the assignment of the nature of the LUMO of peralkylated oligosilanes.

Evidence for the expected decrease in the HOMO → LUMO gap can be seen in the red shift caused by permethylation in the electronic spectra, as discussed below.

Stronger effects than those of hyperconjugation can be expected for conjugative substituents, whose interactive power is generally stronger. Aryl substituents represent a prime example. Unlike the methyl substituent considered so far, they lack axial symmetry and their effects will depend on their orientation relative to the plane of the silicon backbone (Figure 8). When the aromatic plane is orthogonal to the backbone plane, the conjugating π orbital will be ideally disposed for interaction with the HOMO of the parent, composed primarily of $3p_z$ contributions, but not at all for interaction with its π-symmetry SiC antibonding orbital ($3p_x$). After rotation of the substituent by 90°, the opposite will hold. In neither case will the interaction be ideal for the LUMO, the SiSi antibonding backbone orbital, its 3s component being of the wrong local symmetry. Because of its $3p_y$ component, the LUMO will interact weakly with the aryl substituent in the 90° rotated geometry. Of course, those phenyl π and π^* MOs that have a node at the position of attachment remain virtually unperturbed by the presence of the backbone.

Armed with this knowledge, one can predict aryl substitution effects once the donor and acceptor power of the aryl is known. As was the case for methyl, the antibonding MOs of the polysilane will usually interact most strongly with the π^* orbitals of an aryl and its bonding MOs, with the π orbitals of aryl.
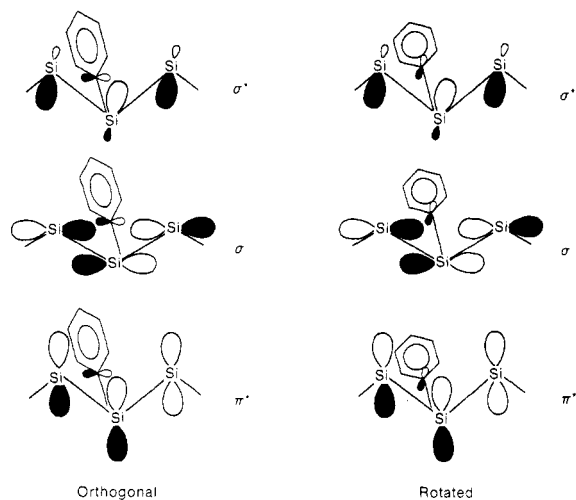
Figure 8. Interaction of a π orbital of a phenyl substituent with the HOMO (σ), LUMO (σ*), and π*$_{SiH}$ orbitals of a long all-trans polysilane. Left: aromatic ring orthogonal to the backbone plane; right, aromatic plane rotated by 90°.

With the aryl substituent orthogonal to the plane of the backbone, we then expect a destabilization of the HOMO. This will be particularly strong for a phenyl that carries a donor group such as p-methoxy. When the aryl donor orbital energy becomes equal to the energy of the backbone HOMO, the orbitals will mix equally. When the energy of the aryl donor orbital is higher than that of the backbone HOMO, the resulting delocalized highest occupied molecular orbital will actually be located mostly on the aryl group.

With the phenyl rotated by 90°, we expect a stabilization of the π-symmetry SiC antibonding orbital and, to a lesser degree, of the LUMO. This will be particularly strong if the phenyl carries an acceptor group such as p-cyano. In actual practice, the orthogonal geometry is believed to be preferred for steric reasons.

A number of experimental studies have appeared that bear on the nature of the electronic ground state and the effect of substituents. The electrochemical redox characteristics of a number of substituted polysilane films have been reported.[86] The measured oxidation potentials of a variety of alkyl polysilanes fall between 1.4 and 1.6 V vs SCE and are relatively insensitive to the nature of the alkyl substituent. Direct bonding of an aryl substituent to the backbone as in poly(methylphenylsilane) reduces the oxidation potential by ~0.4 V to 1.0 V in accordance with the predicted strong destabilization of the silicon backbone HOMO through interaction with a substituent π orbital. Substitution of the aromatic ring with an electron donor (p-OMe) further reduces the oxidation potential of the polymer, also in accordance with the predictions. The destabilization of the HOMO of the polymer through the interaction with the aryl substituent π system is also consistent with the red shifts of UV absorption bands observed for phenyl-substituted polysilane derivatives.[119] If the aromatic group is buffered from the backbone through a saturated carbon bridge, e.g., poly(methylphenylsilane), the oxidation potential and the UV absorption spectrum again mimic those of simple alkylated polysilanes. Loubriel and Zeigler[146a] have studied the photoelectron spectra of a number of polysilanes and have concluded that while alkyl substituents cause little perturbation of the backbone silicon
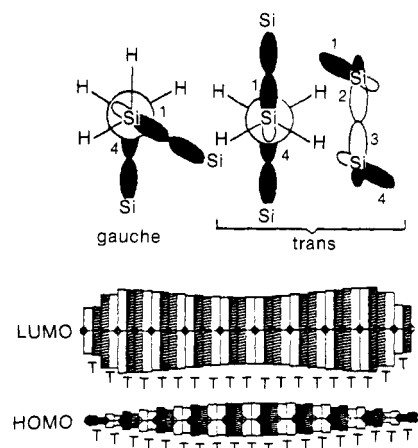
Figure 9. Top: A schematic rationalization of the sign of the resonance integral β_{14} in a polysilane chain as a function of the SiSiSiSi dihedral angle. Bottom: The size (bar length) and sign (bar color) of the coefficients of the backbone Si 3sp^3 orbitals in the HOMO and LUMO of an all-trans conformation of Si$_{20}$H$_{42}$ (INDO/S). The Si atoms are symbolized by small circles.

orbitals, significant orbital interactions result from appending aryl substituents such as phenyl or naphthyl to the backbone. In the latter case, the spectrum indicates that the HOMO is predominantly a naphthalene-type π orbital perturbed by mixing with a lower energy silicon backbone orbital.

C. Conformational Effects

The orbital energies of oligosilanes and polysilanes are very sensitive to molecular conformation. At first, this may be surprising, since they reflect σ conjugation and σ bonds are supposed to have cylindrical symmetry. Yet, this sensitivity is apparent to all levels of calculation that consider interactions beyond β_{gem}, β_{vic}, and β_{13}. Thus, while it does not appear in Sandorfy C and H models, it was first noted in CNDO[123] and subsequently in INDO/S[134] and ab initio SCF[104] calculations. The ab initio study[104] also went beyond Koopmans' approximation and reported ionization energies using electron propagator theory, with qualitatively similar results.

The rationale for the dependence of the orbital energies on the SiSiSiSi dihedral angle is quite simple and is related to the difference between syn- and antiperiplanar interactions, well known in organic chemistry. We follow the argument given in ref 134 (Figure 9). The sign of the overlap between the sp^3 orbitals on central silicon atoms among the four that define the dihedral angle is positive if the angle is zero (eclipsed conformation), yielding a negative value of β_{14}, since the 3p contributions to the two hybrid orbitals are lined up parallel. The overlap is negative and β_{14} positive if the dihedral angle is 180° (trans), since the 3p contributions are then lined up antiparallel. The change of signs does not occur exactly at 90°, since the overlap of the 3s contributions to the hybrids is positive for any angle of twist.

When a correction for a nonzero β_{14} is introduced into the Sandorfy C model, the effects of twisting can be understood very simply by considering the signs of the coefficients with which the various hybrid orbitals enter into an MO. The direction and magnitude of the response to twisting depend on the relative phase of coefficients on hybrid orbitals n and $n + 3$. For the
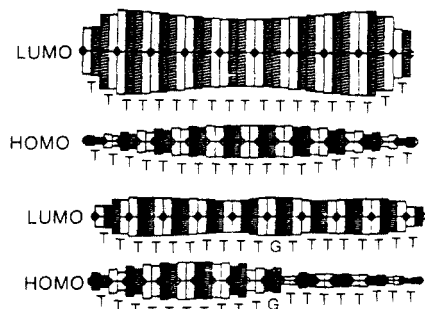
Figure 10. Size (bar length) and sign (bar color) of the coefficients of the backbone Si sp^3 orbitals in the HOMO and LUMO of Si$_{20}$H$_{42}$ (INDO/S). The Si atoms are symbolized by small circles. Top, all-trans; bottom, all-trans except for one gauche turn. T = trans; G = gauche.

HOMO, which has a node on every Si atom and none at SiSi bond midpoints, there will be two nodes between the hybrid orbitals n and $n + 3$ and the coefficient signs will be equal. In an all-trans chain ($\beta_{14} > 0$) all 1–4 interactions in the HOMO will, therefore, be destabilizing; in a gauche chain ($\beta_{14} < 0$), they will be stabilizing. The LUMO has a node at every SiSi bond midpoint but none at the Si atoms, and there will be one node between the hybrid orbitals n and $n + 3$ so that the coefficient signs will be opposite. All 1–4 interactions will stabilize this orbital in the all-trans form and destabilize it in the all-gauche form.

The sensitivity to twisting that a given MO displays depends significantly on the degree to which it contains 3s or 3p character, since only the latter responds to twisting. Thus, the HOMO, which is nearly purely of 3p$_z$ character, is very sensitive, while the LUMO, which has much 3s character, is considerably less sensitive.

Since the energies of oligosilane molecular orbitals converge to their limits relatively rapidly with increasing chain length, the conformational dependence of orbital energies leads to orbital localization if the chain contains both trans and gauche arrangements[134] (or another set of sufficiently different dihedral angles). This localization is much more pronounced for the HOMO than for the LUMO, since the latter responds less strongly to conformational effects in general, as explained above (Figure 10).

Thus, in a 20-silicon chain that is all-trans, the HOMO is perfectly delocalized. However, when a turn is introduced in the center so as to produce an 11-atom and a 9-atom all-trans chain joined in the center in a gauche manner, the HOMO keeps its nodal structure but is essentially purely localized in the longer all-trans segment. There is another MO with the same nodal structure and a somewhat lower energy, essentially purely localized in the shorter all-trans segment. Such localization of the HOMO suggests that in a long polymer chain each approximately all-trans segment in the chain, separated from others by one or more sharper twists, will have "its own HOMO", whose energy will be dictated by the length of the segment and the exact values of the dihedral angles within it. In effect, the strong turns (such as gauche) correspond to regions of unfavorable energy for a positive hole and offer resistance to the motion of such a hole down the chain. Because of the considerable 3s character of the LUMO, the effect of conformational irregularities on the motion of a negative charge down the chain should be small. However, in those substituted polysilanes whose LUMO

TABLE 7. Absorption Characteristics of a Number of Typical Polysilane Homopolymers in Solution

entry	polymer	λ_{max}, nm	ϵ/SiSi
1	(n-PrSiMe)$_n$	306	5600
2	(n-HexSiMe)$_n$	306	5700
3	(PhC$_2$H$_4$SiMe)$_n$	303	9950
4	(n-dodecylSiMe)$_n$	309	5000
5	(c-HexSiMe)$_n$	320	7390
6	(n-HexSi-n-Pr)$_n$	318	10600
7	(n-Bu$_2$Si)$_n$	314	8400
8	(n-Hex$_2$Si)n	317	9700
9	(n-tetradecyl$_2$Si)$_n$	322	8400
10	(n-HexSi-n-octyl)$_n$	318	8785
11	(PhSiMe)$_n$	341	9300
12	(p-MeC$_6$H$_4$SiMe)$_n$	338	8600
13	(p-MeOC$_6$H$_4$SiMe)$_n$	344	8180
14	(p-(n-hexyloxy)C$_6$H$_4$SiMe)$_n$	354	5400
15	(p-biphenylSiMe)$_n$	352	4000
16	(β-naphthylSiMe)$_n$	350	2800

TABLE 8. Absorption Characteristics of a Number of Typical Polysilane Copolymers in Solution

entry	\-(R^{1}R^{2}Si)$_n$(R^{3}R^{4}Si)$_m$- R^1	R^2	R^3	R^4	n/m^a	λ_{max}, nm
1	Me	Me	Me	n-Hex	1.52	303
2	Me	Me	Me	Ph	1.51	330
3	Me	Me	Ph	Ph	1.13	351
4	Me	Me	p-BuC$_6$H$_4$	p-BuC$_6$H$_4$	1.0^b	354
5	Me	Me	p-BuOC$_6$H$_4$	p-BuOC$_6$H$_4$	1.0^b	357
6	Me	c-Hex	Me	PhC$_2$H$_4$	1.49	310
7	Me	c-Hex	Me	p-tolyl	1.77	338
8	Me	PhC$_2$H$_4$	Me	Ph	1.77	326
9	Me	c-Hex	Me	t-Bu	1.0^b	312
10	Me	Me	Me	TMS	1.0^b	295
11	Me	Ph	Me	TMS	1.0^b	308
12	Me	Me	Me	α-naphthyl	0.6	300

^{a} Monomer ratios in polymer as determined by ^{1}H NMR analyses unless otherwise noted. ^{b} Monomer feed ratio in the polymerization reaction.

actually is of the SiC antibonding π type, represented by 3p$_x$ orbitals on the silicons, chain twisting will have the potential for interrupting conjugation by reducing their overlap on neighboring silicons and should lead to LUMO localization.

In summary, while the present theoretical understanding of the electronic nature of oligosilanes and idealized polysilanes in terms of molecular orbital theory is fairly satisfactory, much remains to be done on the theory of substituent effects and of the effects of conformational variation and other defects on properties of long polysilane chains, such as hole or electron conduction.

VII. UV Spectroscopy and Photophysics

A. Absorption Characteristics

The existence of strong near-UV absorptions for oligosilanes[2,146b] and polysilanes[119] is the main reason for the interest these materials have attracted. All soluble high molecular weight polysilane derivatives absorb strongly in the UV[119] as shown in Tables 7 and 8, which present the long-wavelength absorption characteristics of some representative homo- and copolymers. A number of features are obvious from examination of these data. As indicated by the large extinction coefficients calculated per SiSi bond at the λ_{max}, the UV transition is very intense. Although values between 5000 and 10000 are quite typical, numbers in excess of

TABLE 9. Long-Wavelength Absorption Characteristics of a Number of Poly[bis(alkylphenyl)silanes] in Solution

polymer	λ_{max}, nm	$\epsilon \times 10^{-3}$/SiSi
[structure]	390	10.2
[structure]	395	26.6
[structure]	390	16.2
[structure]	376	3.4
[structure]	397	23.3
[structure]	400	21.3
[structure] n-C_6H_{13}	394	18.6
[structure]		
$(PhMeSi)_n$	340	9.0
-[$(Ph_2Si)_x$-co-(n-HexMeSi)$_y$]$_n$[a]	350	5.5

[a] Monomer feed ratio in the copolymerization was 1:1.

Figure 11. Absorption wavelength maxima (λ_{max} (●, O)) and extinction coefficients (ϵ_{SiSi} (■, □)) as a function of oligomer/polymer chain length of n units [$(SiR^1R^2)_n$]: (●) $Me(Me_2Si)_nMe$; (O) ([n-dodecyl)(Me)Si]$_n$; (■) $(PhSiMe)_n$; (□) [(n-dodecyl)(Me)Si]$_n$.

20 000 have been measured for certain diaryl-substituted polysilane derivatives where the absorption bands are quite narrow (vide infra).[53] The shape of the long-wavelength absorption band of typical polysilanes is usually very broad and devoid of vibrational fine structure. In this regard, bandwidths of 25–40 nm are not unusual.

Studies have revealed certain trends for the position of the long-wavelength maximum as a function of the polymer substituents.[119] In room-temperature solution, the absorption peak of dialkyl-substituted polysilanes appears from 300 to 325 nm. However, it is difficult to separate the direct effects of the substituents on the electronic structure and absorption spectra from indirect effects, mediated by substituent effects on chain geometry and conformation. Aromatic substituents directly attached to the silicon backbone cause a 25–35-nm red shift in the position of the absorption maximum. This appears to be at least in part due to a direct effect of electronic substituent perturbation by the aryls since similar effects have been noted previously in phenyl-substituted oligomeric silanes.[147] When the aromatic substituent is buffered from the chain by insulating carbon atoms, the absorption spectra again resemble those of simple alkyl-substituted derivatives.[119] In the alkyl series, the position of the λ_{max} for the long-wavelength transition also appears to depend on the steric bulk of the substituents. This was first noted by Trefonas et al., who ascribed the effect to changes in the backbone geometry and/or conformations.[119] Zeigler et al.[49,50] have reported an approximate linear correlation between the position of the absorption maximum and the sum of the radii of the substituents on the silicon backbone.

The UV absorption spectra of soluble poly[bis(alkylphenyl)silanes] are atypical and striking.[53] High molecular weight derivatives absorb at very long wavelengths both in solution and as solid films (see
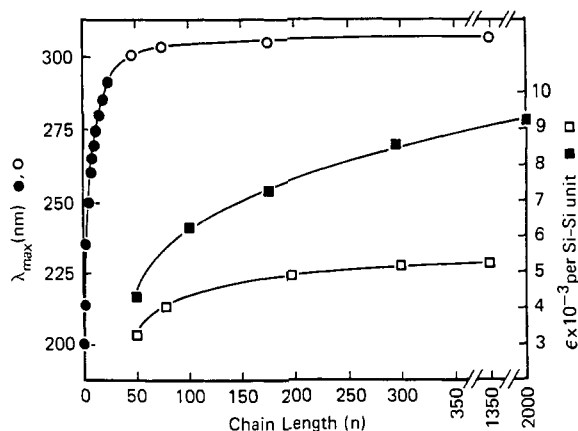
Table 9). Compared with typical monoaryl-substituted materials such as poly(methylphenylsilane), the absorption of the diaryl derivatives is red shifted by more than 50 nm. The absorption band shapes for these materials are also anomalous relative to most polysilanes derivatives in that they are exceptionally narrow (FWHM = 10–15 nm) and the width increases only slightly for solid films. The absorption spectra are relatively insensitive to temperature, although some band broadening is observed at elevated temperatures.

The extraordinary red shifts of the long-wavelength band observed for the diaryl polymers seem too large to be ascribed simply to electronic substituent effects, particularly when compared with the spectra of phenyl-substituted oligomeric silanes. A similar conclusion is drawn from a comparison with the absorption spectra of poly(methylphenylsilane) (λ_{max} = 340 nm) and diphenylsilane copolymers (λ_{max} = 350–355 nm, Table 9). As a result, the authors have tentatively suggested that the red shift in the absorption maxima for the diaryl-substituted silane homopolymers is conformational in origin and have proposed that long trans segments exist even in solution. Consistent with this proposal are the solution light-scattering studies by Cotts et al.,[149] who have measured a persistence length of over 100 Å for poly[bis(p-n-butylphenyl)silane]; such a value is consistent with a stiffened chain structure caused by the presence of extended trans segments. For comparison, earlier light-scattering measurements on poly(di-n-hexylsilane) in solution resulted in persistence lengths of only ~30 Å.[94] The persistence length measured for poly[bis(p-n-butylphenyl)silane] when compared with the calculated mass/unit length for the polymer suggests that approximately 60 monomer units comprise the stiff segments.

The absorption spectra of typical polysilane derivatives also depend somewhat on the degree of polymerization. Both the λ_{max} and the molar extinction coefficients per SiSi bond increase initially with increased catenation but approach limiting values around a degree of polymerization of 40–50.[119] The molecular weight dependence of the spectral properties for some typical polysilane derivatives is shown graphically in Figure 11. The convergence at high molecular weights allows a direct comparison of substituent steric and electronic effects for a variety of high molecular weight polysilanes. The convergence of the spectral properties with

increasing catenation is adequately rationalized by using the simple Sandorfy theoretical approaches.[3]

Theoretical treatments[134,150,151] that predict significant differences both in the excitation energies and in the degree of energy localization between trans segments and those containing strong conformational twists or kinks suggested that the broadened absorption spectra of typical polysilane derivatives in room-temperature solution could be modeled as a statistical distribution of individual chromophores of varying segment lengths and, hence, differing excitation energies.[134,150,151] By assuming that the segmental chromophores were only weakly electronically coupled through conformational defects, the absorption and emission spectra were modeled by using rotational isomeric state theory and adequate correlations with the experimental data were obtained.[152] The theoretical treatment makes certain basic assumptions such as the following: (i) long chains are assumed to minimize end effects on the rotational distribution; (ii) defect-free conformational runs are effectively insulated by chain defect conformers; (iii) defect-free segments act as independent absorbers; (iv) adjacent defects have the same defect energy as isolated defects; and (v) only the HOMO → LUMO transition is considered.

Although simple molecular orbital theory was adequate to rationalize the gross spectral features and the asymptotic behavior of the λ_{max} and extinction coefficients with increasing molecular weight, more sophisticated theoretical approaches are necessary to properly describe the nature of the electronic transition.

For a period of time, excitations from the least stable SiSi bonding backbond orbital of σ symmetry (HOMO) to either the most stable π-symmetry SiC antibonding orbital, originally proposed to have considerable d-orbital character,[2] or the most stable SiSi antibonding backbone orbital of σ symmetry (LUMO) were both considered as viable candidates.[2,153] The initial interpretations in favor of $\sigma \rightarrow \pi^*$ excitation[154,155] were misled by the excellent correlation of the excitation energy with expectations based on the Hückel treatment of the energy of the antibonding orbital, assumed to be a delocalized orbital of π symmetry built from unspecified vacant orbitals, one on each Si atom. This turned out to be a red herring.

In fact, the data correlate also with the energy differences obtained from the Sandorfy model C, in which the excited orbital is of the σ^* antibonding type, delocalized over the backbone.[3,125-129,156] Gradually, it was realized that the bulk of the evidence, such as a regular increase in the oscillator strength with chain length, favored the $\sigma \rightarrow \sigma^*$ assignment. An excellent summary of the case in favor of this assignment was provided in ref 157, which also pointed out that significant participation by 3d orbitals in the observed strong transitions is out of the question anyway, since the excited state clearly is not of a Rydberg type (the spectra are similar in the gas phase and in solution, the transition energies do not fit expectations and decrease too fast with chain length,[129] etc.). The gradual decrease in the excitation energy, initially attributed merely to an increase in the energy of the HOMO, is in fact about half due to the concurrent stabilization of the LUMO.[129]

An experimental determination of the transition moment direction as parallel to the chain in the stretched polymer[49,109,134] and in streaming solution[150] settled the issue definitively: the observed intense transition in polysilanes is of the σ-σ^* type. Of course, a π-symmetry excited state could be only a little higher in energy and probably would not be noticed, because of its expected low absorption intensity. However, the $\sigma \rightarrow \pi^*$ state clearly is not the known fluorescent lowest excited singlet S_1 of polysilanes, whose fluorescence has strong positive polarization and whose very short radiative lifetime leaves no doubt that the S_0-S_1 transition is strongly allowed. As the all-trans silicon chain gets shorter, the exact order of the two states becomes less certain. In disilanes, and perhaps trisilanes, the experimental evidence does not rule out the possibility that a weaker transition to a σ-π^* singlet state lies below that to the σ-σ^* excited state. However, it is clear that the observed intense absorption peak of oligosilanes should be assigned to the latter.

The experimental absorption spectra of oligosilanes and polysilanes pertain to conformer mixtures and little, if anything, is known with certainty about the spectra of individual conformers and about the effects of conformation on the relative energies of various excited states. The effects of simple substitution on excitation energies have been studied relatively little[158] and may be complicated in the case of longer chains by possible simultaneous substituent effects on conformations. The arguments given earlier for the effect of permethylation on orbital energies suggest that it will lower the energy of the σ-π^* state more than that of the σ-σ^* state. Aryl substitution causes a strong red shift of the σ-σ^* transition. This can be understood readily as a result of the strong destabilization of the HOMO and stabilization of the LUMO, but it is difficult to deconvolute conformational effects on the backbone in a quantitative manner.

The available calculations of excitation energies agree with the experimental $\sigma \rightarrow \sigma^*$ assignment of the observed transition. A possibly dissenting suggestion has been made recently only in ref 105. However, its attempt to draw conclusions about excited-state energies from orbital energy differences alone is not convincing since additional electron repulsion terms enter into the expressions for excitation energy even in the absence of significant configuration interaction.[159] The suggestion[105] that a σ-π^* state might be lowest ignores the evidence from fluorescence and absorption polarization studies and is based on invalid conclusions from the charge-transfer emission experiments on aryl disilanes (the optimal geometries for the charge-transfer states are those at which the two singly occupied orbitals are orthogonal;[160] the charge transfer is from the SiSi σ bond to the ring π orbital and not in the opposite direction[161]).

Numerical calculations of the excitation energies for long-chain polymers used the semiempirical Sandorfy model C (improved by explicit consideration of electron repulsion),[156] INDO/S[134,151] and CNDO/2 (S + DES CI)[132,133] methods, and, on quite short oligosilanes, up to heptasilane, ab initio procedures.[136,139,162,163]

We shall describe the ab initio results first. Calculations for the longest chain, Si_7H_{16}, utilized a minimum basis set and the excitation energies were too high by a factor of 3 (some of the discrepancy may be due to the rather unrealistic geometry assumed).[162] In this

work, effects of variation in bond lengths, valence angles, and dihedral angles were investigated. The other calculations only went up to Si_4H_{10} or Si_5H_{12}, using larger basis sets and either the SCF[136] or SCF-CI[139,162,163] approximation. The agreement with the absolute values of excitation energies was much better, but not perfect. Only CI calculations based on the natural orbitals of the ground and excited states obtained by the MCSCF procedures gave satisfactory agreement.[139,163] The nature of the wave functions remains the same as in the above simpler calculations.

There are two low-energy valence excited singlet states. One is of the $\sigma-\sigma^*$ type and is dominated by a single configuration (HOMO → LUMO), although others contribute as well. The transition is polarized along the silicon chain (z). The excitation energy decreases rapidly with increasing chain length and increases upon twisting from trans to gauche conformation, as expected.[139,162] The other is of the $\sigma-\pi^*$ type. The transition into this state is polarized perpendicular to the plane of the silicon atoms. Its energy does not drop as fast with increasing chain length. In disilane and trisilane it is computed to be the lowest energy valence-shell transition, with several Rydberg states at lower energies.[139] An earlier calculation on disilane[164] assigned four excited states of similar energy to the region of the first observed absorption band, including $\sigma-\sigma^*$ and $\sigma-\pi^*$. In tetrasilane and pentasilane, the $^1\sigma-\sigma^*$ state is calculated to lie below the $^1\sigma-\pi^*$ state.

The inclusion of polarization (3d) orbitals and Rydberg (diffuse) orbitals in the basis set does not improve the agreement of the computed excitation energies with those experimentally observed substantially nor does it significantly affect the description of the strong lowest singlet–singlet transition.[136,139] The lowest triplet state of tetrasilane has also been calculated and found to have $\sigma-\sigma^*$ character, the same as the lowest excited singlet.[163]

Calculations on excited singlet states by semiempirical methods permitted an extension of these investigations to much longer chain lengths. Their results for the lower oligosilanes reproduce quite well the qualitative features of the ab initio computations. The Sandorfy model C, even when improved by explicit consideration of electron repulsions,[156] suffers from the absence of nonneighbor resonance integrals, necessary for proper description of conformational effects. Also, it can only predict $\sigma-\sigma^*$ transitions. In the INDO/S work,[134,150,151] the lowest excited state was calculated to be of the $\sigma-\sigma^*$ (HOMO → LUMO) type, with a modest amount of configuration mixing. The calculated excitation energy decreases upon permethylation. It also decreases rapidly as the all-trans chain length increases to about Si_7 or Si_8 and reaches a low-energy limit near Si_{10}–Si_{12} (parent oligosilanes,[134] permethylated polysilanes[151]). Further chain extension has a negligible effect on the energy. The calculated energies are all too high; e.g., the computed long-chain limit for permethylated polysilanes is about 50 000 cm^{-1}, while the experimental value is 34 000 cm^{-1}.[165]

The transition is long-axis polarized and its calculated oscillator strength is too high, as usual when using the dipole length formula on an approximate MO wave function. It increases regularly with the chain length. Even after configuration interaction, the transition density has exactly the form anticipated from the nodal
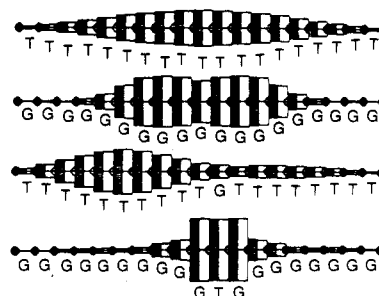
Figure 12. Size (bar length) and sign (bar color) of the coefficients of the backbone Si $3sp^3$ contributions to the transition density of the $S_0{\rightarrow}S_1$ transition in $Si_{20}H_{42}$ (INDO/S). The Si atoms are symbolized by small circles. From top to bottom: all trans; all gauche; all trans with a single gauche turn; all gauche with a single trans turn. T = trans; G = gauche.

properties of the HOMO and LUMO orbitals and consists of a series of dipoles on the silicon atoms, all lined up along the chain axis (Figure 12). Additional $\sigma-\sigma^*$ states involving other orbitals lie somewhat higher in energy but have low calculated oscillator strengths. In these, the transition densities look similar but the local dipole are aligned differently so that they mostly cancel. The lowest $\sigma-\pi^*$ state also lies well above the HOMO → LUMO state and is also only weakly allowed.

The results of the CNDO/2 calculations with singly and doubly excited configurations for the singlet and triplet state of the parent[132] and permethylated[133] oligosilanes, using somewhat different geometries, are generally similar. The doubly excited configurations have very little effect. In this model, possibly because of the different geometries assumed, in particular, larger SiSiSi valence angles, the $\sigma-\sigma^*$ configurations are more strongly mixed. They still produce the lowest excited singlet states of the parent oligosilanes. In the permethylated pentasilane, however, the S_0-S_1 transition is incorrectly calculated to be very weak and to originate in an excitation from the second HOMO to LUMO. On the other hand, the absolute values of the excitation energies agree with experiment better than the INDO/S values.

Because of the nature of the two orbitals involved in the S_0-S_1 and S_0-T_1 transitions, we expect a relatively small S_1-T_1 splitting in the longer polysilanes. The σ orbital is largely composed of silicon $3p_z$ orbitals and the σ^* orbital avoids it in space quite well, being composed mostly of silicon 3s and $3p_y$ and hydrogen 1s orbitals. The overlap density is, therefore, not diagonal in the AO basis and is fairly small everywhere, as is its self-repulsion, which dictates the small magnitude of the exchange integral $K_{\sigma\sigma^*}$. The situation is quite analogous to that encountered with the $n-\pi^*$ transition in pyridine.

The relatively small magnitude of the overlap charge density of the σ and σ^* orbitals suggests that it will have only a small dipole moment so that the singlet $\sigma{\rightarrow}\sigma^*$ excitation will have a relatively small oscillator strength, as is known to be the case for the $n{\rightarrow}\pi^*$ excitation in pyridine. However, as mentioned above, in an oligosilane, this charge density consists of a local dipole on each Si atom, and all of these are lined up in phase along the z axis, so that for the longer chains the resultant electric dipole moment actually becomes quite large and the transition is strongly allowed. This has been discussed in detail.[102]

TABLE 10. Solution Absorption and Emission Properties of Some Representative Polysilane Derivatives

entry	polymer	solvent	λ_{max}, nm absorption	λ_{max}, nm emission	$\Phi_{fl}{}^a$ (τ, ps)
1	$(n\text{-PrSiMe})_n$	hexane	306	340	0.76
2	$(n\text{-HexSiMe})_n$	hexane	306	337	0.61
3	$(n\text{-dodecylSiMe})_n$	hexane	310	337	0.67
4	$(\beta\text{-phenethylSiMe})_n$	hexane	305	338	0.14
5	$(c\text{-HexSiMe})_n$	hexane	317	345	0.42 (140)^c
6	$[(TMS)SiMe]_n{}^b$	hexane	294	335	0.026
7	$(n\text{-Hex}_2\text{Si})_n$	hexane	318	342	0.42 (130)^d
8	$(PhSiMe)_n$	2-methyltetrahydrofuran	337	353	0.25 (70)^c
9	$(p\text{-MeOC}_6\text{H}_4\text{SiMe})_n$	tetrahydrofuran	346	361	0.5
10	$(\beta\text{-naphthylSiMe})_n$	tetrahydrofuran	351	373^e	f
11	$(p\text{-}(TMS)C_6\text{H}_4\text{SiMe})_n$	cyclohexane	338	357	0.03
12	$(p\text{-}(TMS)CH_2C_6\text{H}_4\text{SiMe})_n{}^b$	cyclohexane	341	354	0.05
13	$[(p\text{-}n\text{-BuC}_6\text{H}_4)_2\text{Si}]_n$	cyclohexane	390	400	0.55
14	$[(p\text{-}n\text{-BuOC}_6\text{H}_4)_2\text{Si}]_n$	3-methylpentane	323	412	0.60

^{a} The fluorescence quantum yields of many polysilane derivatives vary with excitation wavelength. Wherever possible we have selected values that have been reported for long-wavelength excitation and, hence, approach the maximum fluorescence quantum yields. ^{b} TMS = trimethylsilyl. ^{c} Reference 167. ^{d} Reference 150. ^{e} The major emission of this material peaks at 473 nm and has been attributed to excimer emission. The main emission contains a shoulder at 373 nm, which has been assigned as the naphthalene-like monomer emission. ^{f} No monomeric emission quantum yield was reported.

So far, the discussion has been restricted to the all-trans conformers of polysilanes and vertical excitations. As was anticipated by various authors from the conformational dependence of orbital energies,[123] ab initio[139,162,163] and INDO/S[134] calculations of the $\sigma \rightarrow \sigma^*$ excitation energy indeed predict a dramatic increase in the transition energy upon twisting towards the gauche and synperiplanar geometries. This is readily understood from the already discussed strong stabilization of the HOMO and the weaker destabilization of the LUMO upon such twisting and from the nearly pure HOMO $\rightarrow$ LUMO nature of the excitation.

A comparison of an all-trans with an all-gauche oligosilane chain at the INDO/S level[134] revealed that the former converges to a much higher excitation energy limit than the latter as the chain length grows. The calculated difference was 10 000 cm^{-1}, but this is probably exaggerated. As a result of the much higher excitation energy of the gauche conformation, in a mixed conformation chain the lowest excited state localizes quite strongly in the regions that are in the trans conformation (Figure 12). Already a single trans link in an all-gauche Si_{20} chain draws nearly all the transition density into its immediate vicinity. In a similar vein, a single gauche link near the middle of an all-trans Si_{20} chain effectively breaks this chromophore in two. Judging by the transition densities, the lowest energy excitation is localized on the longer segment, and a higher energy excitation is localized on the shorter segment. These results suggest that the localization of singlet excitation on an actual polysilane chain will be substantial and will be dictated by the conformation irregularities. Relatively long-chain segments that are all-trans and nearly planar are likely to represent the lowest energy chromophores.

Little theoretical work has been done on the effects of simple substitution on the electronic spectra of polysilanes. Some of the solid-state physics work[166] belongs in this category. Aryl substitution has received more attention[140-142] but only in the one-electron approximation, which does not account properly for excited electronic states of substituted phenyl rings.

To summarize, the present theoretical understanding of the excited states of polysilanes is rather incomplete. Although a clear picture is beginning to emerge for the
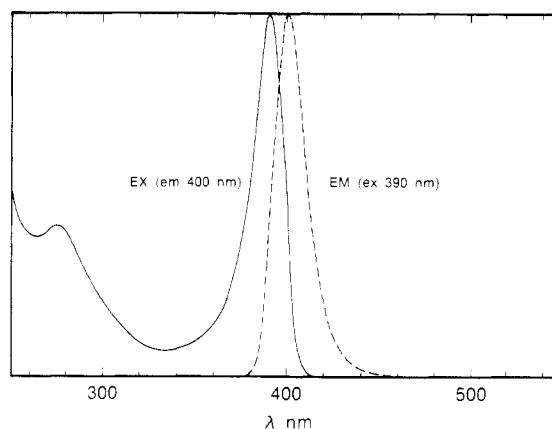

Figure 13. Fluorescence emission (EM) and fluorescence excitation (EX) spectra of poly[bis(p-n-butylphenyl)silane] in cyclohexane at room temperature.

energies and the order of singlet states in the parent oligosilanes as a function of conformation, very little is known about the triplet states and about substituent effects. A quantitative description of the separation of a long polysilane chain into a series of interacting chromophores by conformational and possibly also other defects is lacking, as is information on the rates of electronic energy transfer, geometrical relaxation of the excited segments, etc.

B. Polysilane Emission Studies in Solution

The emission properties of substituted high polymers in solution have been studied in some detail.[49,50,57,65,66,120,134,150-152,167,168] In this section we will restrict our discussion to data obtained for fluorescence in fluid solution at room temperature since cooling samples to low temperatures (both in solution and in the solid state) often leads to thermochromic changes that significantly complicate the interpretation. The emission characteristics of a number of polysilane derivatives in solution have been studied and some representative data are reported in Table 10. Similar studies on copolymer derivatives have been reported but they are far less numerous.[50,65,66]

The emission data for the soluble bis(alkylphenyl)-substituted polysilanes are not reported in the table but
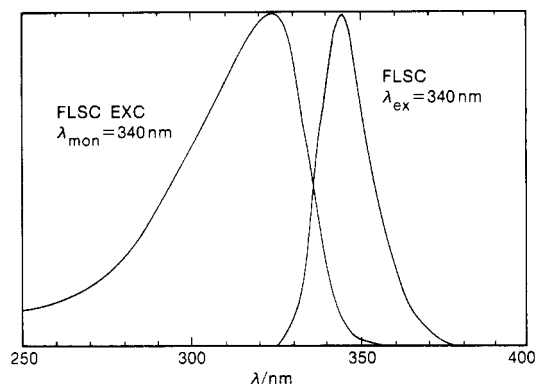
Figure 14. Fluorescence (FLSC) and fluorescence excitation (FLSC EXC) spectra of a typical dialkyl polysilane [poly(di-n-hexylsilane)] in 3-methylpentane at room temperature.

Figure 15. Change in fluorescence quantum yield as a function of excitation wavelength for poly(di-n-hexylsilane) in 3-methylpentane; ABS = absorption spectrum.

they are typical (see Figure 13) with very small Stokes shifts ($\sim$10 nm, peak to peak).[169] A careful study of the total emission at room temperature produced no evidence of long-wavelength excimer emission in spite of the close proximity of the aromatic substituents in the polymer structure.

In almost every homopolymer studied a slightly Stokes shifted unstructured emission is observed that is much narrower (15–30 nm) than the corresponding absorption band (see Figure 14). Two notable exceptions are poly(methyl-β-naphthylsilane) (Table 10, entry 10)[49,152] and the copolymer poly(methyl-α-naphthylsilane-co-dimethylsilane).[65,66] In these cases, a broad, strongly Stokes shifted emission similar to that previously reported for poly(2-vinylnaphthalene) is observed which has been attributed to an intramolecular excimer. In both cases, a much weaker emission on the blue tail of the excimer emission was associated with a monomeric naphthalene-like emission.

For the other polysilane derivatives the narrow and structureless emission was taken to be indicative of an extensively delocalized excited state. The fluorescence lifetimes that have been measured are very short (75–200 ps)[134,150,167,168] and the emission quantum yields often vary with the excitation wavelength.[49,150,151] The latter seems a general characteristic of most polysilane derivatives in solution at room temperature, and increases in the fluorescence quantum yields by factors of 2–3 upon going from short-wavelength excitation to a position on the red tail of the long-wavelength absorption band are common. This variation of fluorescence quantum yield with excitation wavelength for a typical polysilane derivative (poly(di-n-hexylsilane)) is shown in Figure 15. The "plateau effect" for short-wavelength excitation seems also to be a common feature for most polysilane derivatives. Various suggestions have been tendered in an effort to rationalize this curious behavior. For poly(methylphenylsilane), Harrah and Zeigler[49] have suggested that such behavior constitutes evidence that the long-wavelength band is resolvable into at least two noncommunicating transitions that have different emission efficiencies. Another possibility also acknowledged by these authors is that long-wavelength excitation preferentially excites chains or portions of chains with more extensive delocalization, larger oscillator strengths, and, hence, enhanced emission yields more competitive with intersystem crossing and other competing processes. In this regard, the emission spectra of dialkyl-substituted polysilanes are
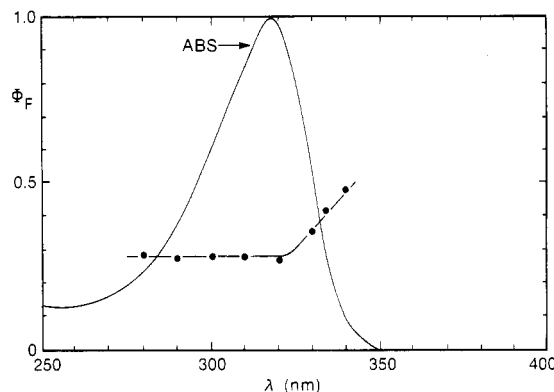
also somewhat wavelength dependent and the maxima weakly blue shift for shorter wavelength excitation.[134,150] A model for a polysilane chain in solution composed of discrete chromophoric segments each with its own absorption and emission characteristics is also consistent with fluorescence depolarization studies[120,134,150,151] (see section VII.C).

Finally, the possibility that photochemical decomposition may be wavelength dependent and other competitive photochannels are opened for short-wavelength excitation must be considered. This is discussed more completely in section IX.C.

In general, the fluorescence emission quantum yields for polysilanes in solution are quite high (0.1–0.7). Recently, however, it has been reported that the attachment of silyl substituents to the polymer backbone, e.g., poly[methyl(trimethylsilyl)silane], causes a marked drop in the emission quantum yield (Table 10, entry 6).[57] Similarly, reduced emission yields were reported for certain copolymers containing trimethylsilyl substituents. In a similar fashion, we have also observed significantly lower fluorescence quantum yields (0.03–0.05) for poly[(m- and p-(trimethylsilyl)phenyl)-methylsilane] and poly[(m- and p-((trimethylsilyl)-methyl)phenyl)methylsilane] relative to parent poly(methylphenylsilane) (0.12) in solution when measured in the short-wavelength plateau region.[169] On the basis of the low emission quantum yield for poly[(trimethylsilyl)methylsilane] coupled with its enhanced photolability, Zeigler and Harrah have invoked a substituent heavy-atom effect that they propose increases the intersystem crossing rate to a photoreactive triplet state.[57] However, attempts to directly correlate low emission yields and photolability are risky as evidenced by the observation that while the copolymer poly(cyclohexylmethylsilane-co-tert-butylmethylsilane) has a very low emission yield (0.034),[57] its relative photolability, as determined by the rate of spectral bleaching, is not significantly enhanced. Obviously, the pathways competing with emission are myriad and complex, and a low emission efficiency does not necessarily signify the increased competitiveness of photochemical decomposition routes.

The high quantum yields for fluorescence coupled with the narrow emission bandwidths and lack of vibronic structure are consistent with considerable delocalization of the excitation. This has prompted the suggestion that the singlet excited state of the polysilane derivatives may not be responsible for their observed
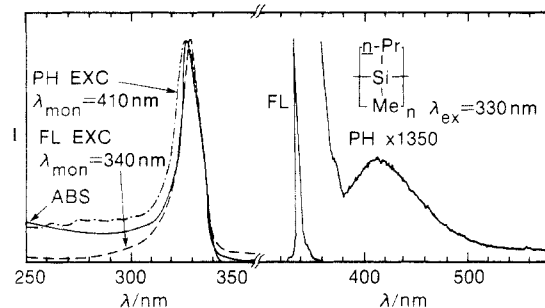
Figure 16. Fluorescence (FL), phosphorescence (PH), fluorescence excitation (FL EXC), phosphorescence excitation (PH EXC), and absorption (ABS) spectra of poly(methyl-n-propylsilane) in 3-methylpentane at 77 K. The wavelengths at which emission was excited (λ_{ex}) and monitored (λ_{mon}) are given.

photolability.[49,50,120,128,150–152] Emission studies in rigid media show a weak, broad phosphorescence for a number of polysilane derivatives.[49,150–152] In every case, this emission is very weak and long-lived (1–5 ms). Estimates of the phosphorescence quantum yields suggest values as low as 10^{-4}. Harrah and Zeigler have reported indications of discernible vibrational fine structure[49,50,152] in this emission for a number of poly(dialkylsilanes). For poly(methyl-n-propylsilane), this band is centered around 440 nm, with principal vibrational spacings of 722/667 cm^{-1}. On the basis of the spectral bandwidth and the vibrational coupling, these authors assume a highly localized triplet state and have proposed that this state is the source of the observed photoreactivity. Other workers[120,151] have also reported weak phosphorescence emissions for a number of dialkyl polysilane derivatives in rigid media. In the latter studies, however, no evidence of any vibrational fine structure was reported. Although no definitive explanation for this discrepancy has been offered, it is possible that differences in the instrumentation (pulsed laser vs lamp/monochromator excitation) may be responsible. In the case of poly(methyl-n-propylsilane) Michl and co-workers[151] have measured a phosphorescence excitation spectrum (Figure 16) that closely resembles the absorption spectrum, thus making it likely that the emission is intrinsic and not due to an impurity, although some doubt still lingers because of its weakness. The extrapolated energy of the origin of this phosphorescence (75–80 kcal/mol) is comparable with the dissociation energy of the silicon–silicon bond,[93] which makes the triplet state an energetically viable candidate for the photochemical cleavage.

Attempts to directly implicate the triplet state in the photodegradation of dialkyl polysilanes (as monitored by the decrease in the intensity of the original long-wavelength absorption maximum) have produced inconclusive results. In the case of poly(di-n-hexylsilane),[151] there is no quenching of the fluorescence nor of the rate of disappearance of the original polymer absorption in neat piperylene, a known and effective triplet quencher with a triplet energy of about 60 kcal/mol. On the other hand, for poly(methyl-n-propylsilane)[151] and poly(methylphenylsilane)[151] a significant decrease in the rate of photodegradation was observed, with no apparent quenching of the polymer fluorescence. In this case, at least, there seems to be good evidence for the involvement of the triplet state in the photodegradation. It is possible that for poly(di-n-hexylsilane) the lifetime of the triplet state at room temperature is too short in solution to allow effective quenching even in neat piperylene. Clearly, more detailed and quantitative analyses of the quenching processes in solution are warranted.

C. Fluorescence Polarization Studies

Some insight into the electronic nature of the polysilane chain in solution has also been obtained by fluorescence polarization studies. For poly(di-n-hexylsilane), Michl and co-workers have reported that the degree of polarization (P) is remarkably wavelength dependent.[134,150,151] P ranges from a value close to the theoretical limit of 0.5 for long-wavelength excitation to near zero (no correlation between the absorbing and emitting transition moments) at short excitation wavelengths. Such an observation would be consistent with the concept of polysilane chain in solution as consisting of a collection of weakly interacting chromophores absorbing at different wavelengths and communicating by rapid energy transfer. A model proposed as consistent with these results is a chain composed of a series of trans (or nearly trans) links of varying lengths and, hence, differing excitation energies that are electronically insulated to some extent from one another by conformational twists or kinks. Irradiation into the red edge of the absorption band would address only the longest chromophores, thus minimizing the opportunities for energy transfer and maximizing the spectral correlation between the absorbing and emitting transition moments. On the other hand, irradiation at the blue edge would preferentially excite the short, high-energy chromophores, leading to rapid energy transfer to the longer chromophores, resulting in the lower values for the polarization degree as observed for short-wavelength excitation. It is also possible that the short segments are photochemically more reactive as well, which would rationalize the substantial decreases observed in the measured fluorescence quantum yields for short-wavelength excitation. A similar solution model has been proposed by Johnson et al.[120] also on the basis of fluorescence polarization studies. INDO/S calculations support the proposed model for poly(di-n-hexylsilane)[134,150,151] in solution and strongly suggest that the primary chromophores are all-trans or nearly all-trans segments separated by strongly nonplanar conformational kinks. Furthermore, these studies indicate that considerable localization of the excitation occurs even on very short segments (see section VII.A for details).

Photophysical measurements have also been used to obtain information on the length of the emitting chromophores.[150,151,167] The observed fluorescence quantum yield for poly(di-n-hexylsilane) and the measured fluorescence lifetime imply a very high oscillator strength of about 1.8 for the emitting chromophore. From the corresponding absorption spectrum, one derives an average increment of roughly 0.09 per SiSi bond for the oscillator strength. These numbers suggest a maximum of about 20 silicon atoms in the lowest energy chromophores absorbing around 335 nm. The number could be smaller, perhaps only 10 or so, if the emitting chains have an extended all-trans geometry and are thus likely to have a disproportionately large increment per SiSi bond for the oscillator strength.[150,151] In a similar fashion, Hochstrasser et al. have estimated a energy

localization length of ~36 silicon atoms for poly(di-*n*-hexylsilane) in solution.[167] The calculated excitation localization depended somewhat on the nature of the polymer substituents and ranged from 30 to approximately 60.[167]

Recently, picosecond time-resolved fluorescence and fluorescence anisotropy measurements have been reported on poly(methylphenylsilane).[167] The authors have identified at least two anisotropic decay regimes: (i) sub 10 ps and (ii) 20–30 ps. Measurements at longer times (>500 ps) were precluded by the short emission lifetime of poly(methylphenylsilane). However, for alkyl-substituted polymers, which have significantly longer fluorescence lifetimes, additional decay of the anisotropy proceeds on a nanosecond time scale. The origin of the temporally distinct decay regimes is not clear at this time. The authors propose that the polymer chain is composed of a distribution of chromophores of varying chain segment lengths and that energy transfer to the longer, low-energy segments is responsible for the ultrafast decay of the anisotropy. They furthermore suggest that the subsequent decay in the anisotropy observed in the 20–30-ps time regime may be caused by energy transfer along the backbone possibly involving segments where the silicon–silicon bonds are not precisely collinear with each other. Torsional motions of the polymer chain were rejected as a source of the anisotropy decay based on the fact that such motions in ground-state polyalkanes occur in the nanosecond frequency regime. While this proposal seems quite reasonable based on ground-state models, it neglects the possibility that torsional motions within excited segments may be much more rapid, being driven by the strong tendency toward segment planarization in nearly trans segments upon photoexcitation. We believe that such planarization could account for the initial rapid anisotropy decay, with energy transfer being responsible for the rest.

It seems, therefore, that although there is general agreement that the polysilane chain in solution is composed of chromophoric segments with different excitation energies, the actual nature of the segments and their dynamic behavior, particularly upon excitation, seems to be a topic for further investigation.

D. Solution Thermochromism

Spectroscopic studies suggest that polysilane derivatives in solution exist as a collection of loosely electronically coupled chromophores. It has been proposed[134] that trans or nearly trans segments are likely chromophores and the presence of nonplanar conformations (gauche and/or gauche-like) partially decouples the interaction between the segments, creating a statistical collection of chromophores of varying lengths and, hence, different absorption characteristics.

In such a model of inhomogeneous conformational broadening caused by the presence of varying segment lengths and possibly also varying segment structures isolated by defects, one might expect to observe thermochromic changes in solution. Thermochromism in solution has indeed been reported by two groups. Trefonas et al. have reported three distinct types of thermochromic behavior for dialkylsilanes in saturated hydrocarbon solvents, depending on the polymer substituents.[170] For highly unsymmetrical, atactic materials
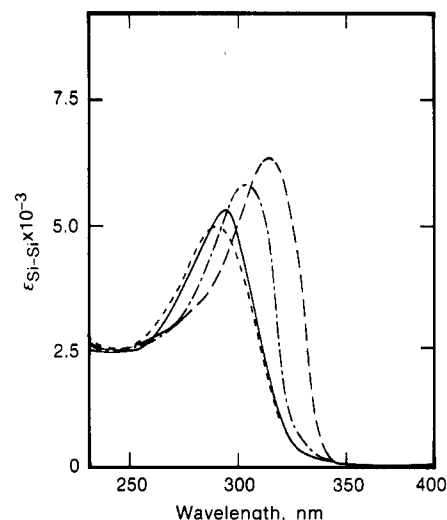
Figure 17. UV spectra of a 0.0035% solution of poly(*n*-hexylmethylsilane) in isooctane: (- - -) 92 °C; (—) 24 °C; (- · -) –17 °C; (- - - -) –67 °C.

such as poly(*n*-hexylmethylsilane), the absorption maximum steadily red shifts from the room-temperature value of 306 nm and approaches a limiting value of ~330 nm at low temperatures (see Figure 17). The bathochromic shift is also accompanied by a significant narrowing of the absorption band. It was proposed that such behavior is consistent with increases in the relative population of trans polymer segments at lower temperatures. A second type of behavior is demonstrated by unsymmetrical materials with sterically demanding substituents (e.g., poly(cyclohexylmethylsilane), poly(methylphenylsilane), poly(isopropylmethylsilane), etc.). The absorption maxima of these materials do not red shift upon cooling and in fact slight hypsochromic shifts are often noted. This has been rationalized as a decrease in the average persistence length due to the disruption of trans sequences in the polymer backbone. A third type of behavior is observed for many symmetrically substituted dialkyl polysilane derivatives and is manifested by a striking thermochromism that is discontinuous with temperature. This effect was first reported for poly(di-*n*-hexylsilane)[152,170,171] and is illustrated in Figure 18. Following a continuous but small bathochromic shift with decreasing temperature, a temperature is reached where the original broad absorption band is replaced by a very narrow, strongly red-shifted peak at 354 nm. The transition temperature range can be very narrow, as observed for poly(di-*n*-hexylsilane) in alkane solvents (a few degrees), or it can be much broader, depending on the polymer structure and solvent. Below the transition temperature, poly(di-*n*-hexylsilane) rapidly precipitates from solution. Zeigler and Harrah have ascribed this behavior to a unimolecular coil to rod transition, the rod form being responsible for the narrow, red-shifted absorption.[171] Trefonas et al. have also suggested that the spectral changes may be conformational in origin (i.e., the spectral red shifts are associated with the formation of trans or nearly trans segments) but have also acknowledged that aggregation effects may possibly be involved.[170] A recent study by Thorne et al.[168] reports that the emission lifetime of the narrow red-shifted absorption (354 nm) of poly(di-*n*-hexylsilane) measured in rigid media (77 K) is short and similar to that ob-
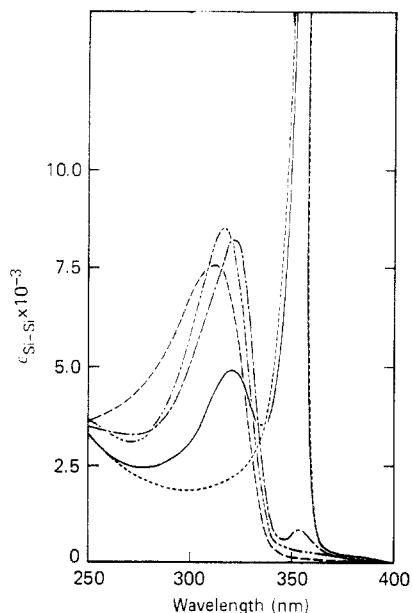
Figure 18. UV spectra of a 0.045% solution of poly(di-*n*-hexylsilane) in hexane: (— — —) 56 °C; (— - - —) 24 °C; (- - -) -23.5 °C; (—) -24.2 °C; (- - - -) -54.5 °C.

Figure 19. Thermochromism of poly[bis(*p*-butoxyphenyl)silane]: (a) in *tert*-butylbenzene; (b) film.

served for poly(di-*n*-hexylsilane) in fluid solution at room temperature. This, coupled with the observation that the measured lifetime of poly(di-*n*-hexylsilane) as a solid suspension is relatively long, led the authors to conclude that the thermochromism is a result of a unimolecular conformational change. However, these authors also note that the decay curves from the species observed at 77 K were nonexponential and varied with cooling rate, suggesting the possibility of some aggregation.

The complete understanding of the abrupt thermochromism displayed by a number of polysilane derivatives will require the answers to at least two important questions. The first concerns the nature of the transition; i.e., is this really a monomolecular event? In this regard, the controversy closely resembles that recently described for the solution thermochromism of certain soluble poly(diacetylene) derivatives.[172] Perhaps the answer to this question lies in careful, variable-temperature, light, neutron, and X-ray scattering studies.

The second question deals with the potential driving force of such a transition if it could be demonstrated to result from a unimolecular conformational change. This has recently been considered by Schweitzer,[173-176] who has proposed that such a transition could be "polarization driven" and caused by the enhanced polymer–solvent induced-dipole van der Waals interactions caused by the large increase in the polymer polarizability resulting from conformational changes to the more extended "all-trans" conformation. Recent theoretical studies have supported the suggestion that the polarizability of the polymer greatly increases in the extended form. Schweitzer proposes that the solvent sensitivity of the thermochromism hinges on a coupling parameter V_D/ϵ which is both solvent and polymer dependent. The author defines V_D as the delocalized backbone contribution to the attractive polymer–solvent interactions when the polymers is in the fully extended, all-trans form. This term will obviously depend on the nature of both the polymer substituents and the solvent. The term ϵ is defined as the increase in free
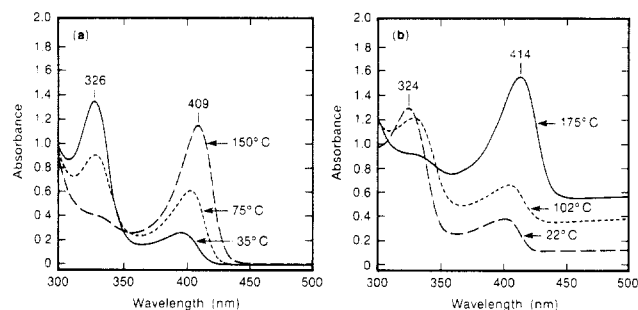
energy upon creation of a conformational defect (in this case a gauche or gauche-like conformational kink) and, hence, should be relatively insensitive to solvent. The statistical model predicts an abrupt phase change type behavior, similar to that observed for a number of dialkyl polysilanes, for large values of the solvent coupling constant. It also rationalizes other less dramatic thermochromic changes, the nature of which depend on the polymer substituents and solvent. Furthermore, the theory predicts that solvent polarizability is an important contributor to the solvent–polymer interactions and establishes a correlation between the predicted thermochromic transition temperatures and the solvent refractive index.[152,175]

In summary, although some progress has been made toward the understanding of the abrupt thermochromism shown by a number of dialkyl polysilanes in solution, more structural evidence is necessary before this interesting phenomenon can be conclusively described as a monomolecular conformational event.

A different type of solution thermochromism that does not result in polymer precipitation has recently been described by Miller and Sooriyakumaran.[52] These workers have described anomalous variable-temperature spectra of poly[bis(*p*-alkoxyphenyl)silanes] which, in stark contrast to the poly[bis(*p*-alkylphenyl)silanes], absorb strongly at much shorter wavelengths (λ_{max} 320–325 nm) with only weak absorption observed around 400 nm at room temperature. The short-wavelength absorption was quite unexpected for diaryl-substituted polysilane derivatives. These materials are, however, thermochromic at elevated temperatures both in solution and in the solid state. Upon heating, the short-wavelength absorption is gradually replaced by a strong band around 400 nm (see Figure 19). This thermochromism is continuous, is completely reversible, and in the solid state does not appear to be initiated by a phase change. Consistently, no significant thermal transitions were observed by DSC in the polymer films in the temperature region where the thermochromism is observed. Interestingly, the limiting absorption spectra of the poly[bis(*p*-alkoxyphenyl)silanes] at elevated temperatures closely resemble those of the corresponding poly[bis(alkylphenyl)silanes] at comparable temperatures, although the absorption maxima of the former are red shifted by 5–10 nm. The authors have tentatively suggested that the backbone for the bis(*p*-alkoxyphenyl) polymers may be strongly twisted at room temperature and postulate that this distortion may be caused by unfavorable substituent dipole interactions present in the all-trans form (see Figure 20). Some support for this proposal is generated by the
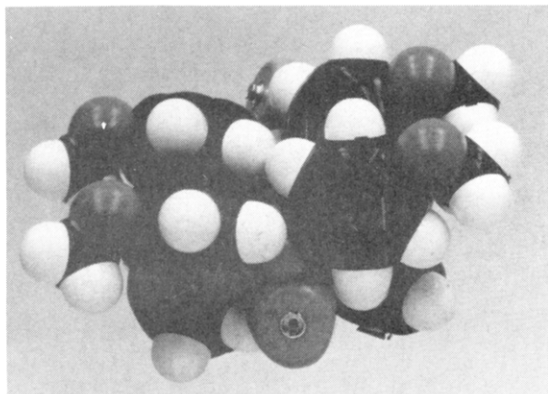
Figure 20. A space-filling molecular model of poly[bis(p-methoxyphenyl)silane] showing alignment of the p-alkoxy substituents when the backbone conformation is all trans.

Figure 21. UV absorption spectra of a thin film of poly(di-n-hexylsilane): (·−·) solution in hexane; (−−−) thin film run immediately after baking at 100 °C; (—) thin film after standing at 20 °C for 3 h.

observation that bis(m-alkoxyphenyl)polysilane derivatives absorb strongly around 400 nm and are not thermochromic. In these cases, because of the meta substitution, the substituent dipoles can be oriented to avoid an unfavorable alignment by rotation of the aromatic rings around the SiC bond even when the polymer backbone is planar zigzag.

VIII. Structure and Electronic Properties in the Solid State

A. Poly(di-n-hexylsilane)

The observation of thermochromism in the solid state for a number of polysilane derivatives has piqued the research community's interest. The first report of such thermochromism by Miller et al. resulted from UV spectroscopic studies on films of poly(di-n-hexylsilane).[177] While films of freshly baked poly(di-n-hexylsilane) show a typical broad absorption maximum at 317 nm, upon standing at room temperature a long-wavelength absorption (λ_{max} 370–375 nm) gradually appears at the expense of the original absorption (see Figure 21). This effect is thermally reversible and brief heating restores the short-wavelength band to its original intensity. The growth of the long-wavelength band was also accompanied by a strong birefringence in the sample which decreased with heating but did not completely disappear prior to polymer decomposition above 250 °C. DSC analysis of the solid polymer revealed a strong endotherm upon heating, peaked around 42 °C (ΔH = 5.0 kcal/mol). The thermal behavior was reversible with a strong cooling exotherm observed around 28 °C, but the exact position depended somewhat on the molecular weight of the sample, cooling rate, etc. The thermal behavior was typical of a first-order phase change in a polymeric system, and visual observation of the sample showed that it did not melt to an isotropic liquid prior to polymer decomposition. It was originally proposed[177] that the changes in the UV spectrum were associated with a change in the polymer backbone conformation and that the long-wavelength absorption was most likely associated with the formation of planar trans segments in the chain.

Largely as a result of this curious thermochromism, poly(di-n-hexylsilane) has been extensively studied in the solid state by FT-IR,[177,178] Raman,[110,178] EXAFS,[109] wide-angle X-ray diffraction (WAXD),[111,178] electron diffraction,[111] and ^{13}C and ^{29}Si solid-state NMR,[181,182]
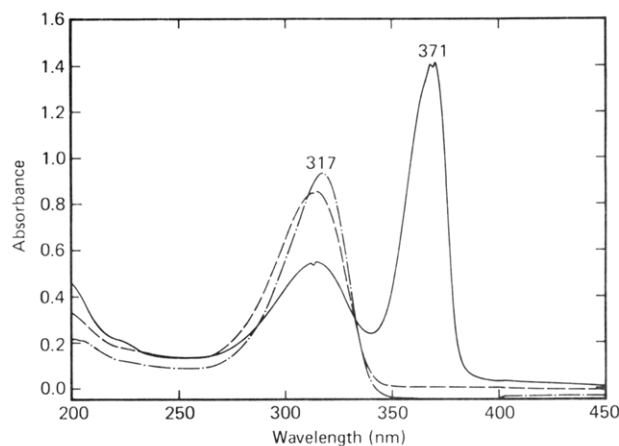
both below and above the transition temperature. Initial IR studies[177,178] on solid films showed a number of sharp strong bands at room temperature. These vibrations were roughly grouped into two types by frequency. Those above 700 cm^{-1} are attributable mainly to vibrations involving the n-hexyl side chains, while those below 700 cm^{-1} involve silicon. This was confirmed by isotopic labeling and by Raman scattering studies[110,178] in which the low-frequency bands were intensified due to the enhanced polarizability associated with silicon vibrations. Polarized Raman studies[110] on uniaxially oriented films allowed the assignment of many of the bands in the room-temperature spectrum. These assignments were also supported by studies of isotopically labeled poly(di-n-hexylsilane).[110] Variable-wavelength excitation confirmed the enhancement of many of the bands that are associated with the electronic transition. This preresonance enhancement is caused by the long-wavelength UV–visible absorption of the low-temperature form. Above the transition temperature all the IR and Raman bands were greatly reduced in intensity and were significantly broadened. Vibrational analysis of bands above 1000 cm^{-1} suggested that the side chains were extended and crystallized at room temperature. The intensity ratios in the CH stretching region are suggestive of an orthorhombic subcell structure for the n-hexyl groups. Analysis of the polarized Raman data on a uniaxially oriented film was consistent with a planar zigzag polymer backbone at room temperature and suggested, furthermore, that the plane of the side chains is not exactly perpendicular to the plane of the silicon backbone.[110] This rotation around the silicon–carbon σ bond apparently relieves some steric interactions between the side chains. The observation of additional bands in the region of the SiSi vibrations around 450–485 cm^{-1} may be indicative of the presence of some nonplanar conformers perhaps attributable to an amorphous component or the presence of another phase. Consistently, the UV spectra of unoriented films always show residual absorption around 317 nm whose intensity varies with the processing conditions. The thermal analysis and IR and Raman studies strongly suggested that side-chain crystallization causes the ordering of the polymer backbone, which is in turn responsible for the observed UV spectral changes.

A number of NMR studies on poly(di-*n*-hexylsilane) in the solid state have been reported. Gobbi et al. have described the variable-temperature ^{29}Si CPMAS NMR behavior of poly(di-*n*-hexylsilane).[181] Below room temperature, a single broad resonance is observed for the silicon backbone at −20.8 ppm relative to TMS. Heating the sample causes the appearance of a much sharper upfield signal at −24.1 ppm, which has been attributed to the silicon backbone resonance in a mobile or conformationally disordered phase. The upfield chemical shift suggests the presence of nonplanar backbone segments, and the narrowness of the signal and the shorter relaxation time are consistent with increased backbone conformational mobility. Related ^{29}Si NMR studies have also been described by Schilling et al.,[182] who have offered a similar explanation. The variable-temperature ^{13}C MAS NMR spectra of poly-(di-*n*-hexylsilane)[181,182] also support the presence of two phases, one mobile and one static or crystalline. Above 24 °C only the mobile phase is observed and the hexyl substituents appear as a six-line pattern. At lower temperatures, the ^{13}C spectra are considerably more complex. By varying spectral parameters, the signals from either phase can be selectively enhanced.[182] The carbon resonances in the mobile phase are upfield from those in the crystalline phase, consistent with the incorporation of gauche conformations into the side chains. Interestingly, Schilling et al.[182] report splitting in the carbon spectra of the crystalline phase, which they have tentatively rationalized as two alternative modes of chain packing in the same polymer molecule. The chemical shifts of the *n*-hexyl substituent carbons above 42 °C are similar to those observed for the mobile phase at room temperature (although the line widths are narrower at elevated temperatures), suggesting a close similarity for the polymer structure in each case.

The structure of poly(di-*n*-hexylsilane) has also been studied extensively by WAXD[110,111,178] and also by electron diffraction.[111] Samples for the latter have been prepared by solvent recrystallization, polymer precipitation, and thermal annealing of cast films. Uniaxially oriented films can be prepared by drawing polymer films above the transition temperature (42 °C), and draw ratios of 100–1000% were obtainable. For the electron diffraction, thin films (<50 nm) that had been uniaxially aligned and coated with evaporated carbon were employed.

Poly(di-*n*-hexylsilane) is an unusually crystalline organic polymer. Powder diffraction patterns show more than 30 reflections over an angular range (2θ) between 5 and 45°. Figure 22a shows a typical powder pattern for poly(di-*n*-hexylsilane) at room temperature (top) and at 60 °C (bottom).[110,178] At 60 °C most of the sharp reflections are lost and a diffuse halo appears. However, even at elevated temperatures a strong, sharp reflection remains at 13.5 Å. Even given the large number of useful reflections available, it was necessary to obtain a fiber pattern to index the reflections and determine a unit cell. Figure 22b shows a fiber pattern[110] for poly(di-*n*-hexylsilane) at room temperature for which over 40 reflections have been indexed. The layer line spacing indicative of the polymer repeat distance suggests a planar zigzag backbone with a 1,3-repeat distance of 4.07 Å. A similar conclusion was reached from electron diffraction studies, although the
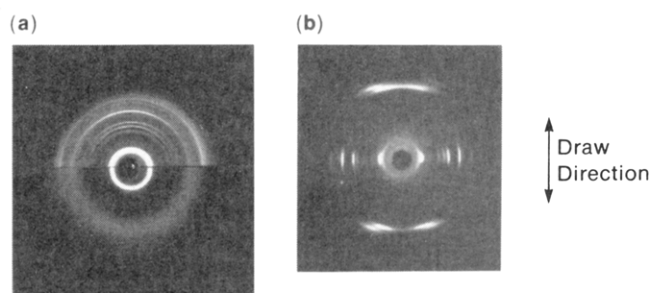
Figure 22. Wide-angle X-ray diffraction (WAXD) patterns of poly(di-*n*-hexylsilane): (a) powder diffraction pattern of PDHS at 60 °C (bottom) and 25 °C (top); (b) WAXD fiber pattern for a stretch-oriented sample.

repeat distance was measured as 4.00 Å.[110] The unit cell was triclinic with cell dimensions $a = 13.75$ Å, $b = 21.82$ Å, $c = 4.07$ Å, and $\gamma = 88°$ with two molecules passing through each unit cell.[110] Using standard SiSi bond lengths of 2.35 Å, the SiSiSi valence angle ranges between 116 and 120° (depending on the value of the 1,3-repeat distance utilized), which is slightly expanded but not unexpected considering the steric bulk of the side chains. The angle is reduced somewhat to 115–118° if a bond length of 2.37 Å as suggested by EXAFS[109] studies is assumed. The strong reflection at 11.8 Å in the crystalline phase was attributed to the distance between the silicon chains. Other strong reflections that disappear upon heating were due to the crystalline side chains. In this regard, a strong reflection on the equator at 4.54 Å is characteristic of the packing of *n*-hexane in a triclinic unit cell. Similarly, off-meridional reflections at 3.85 and 3.55 Å are also observed for monoclinic polyethylene, the chain packing of which is equivalent to triclinic *n*-hexane. Another off-meridional reflection at 3.71 Å is a characteristic reflection in orthorhombic polyethylene. This suggests the possibility of multiple coexisting packing rearrangements for the hexyl groups in the same polymer, a feature consistent with the peak doubling observed by Schilling et al.[182] in the solid-state ^{13}C NMR spectra.

The structure of the polymer above the transition temperature is also of considerable interest. At elevated temperatures IR, Raman, and WAXD studies suggest that the side chains melt and disorder. The appearance of a single, narrow upfield line in the ^{29}Si CPMAS NMR spectra is also indicative of motional averaging in the backbone, and the upfield shift is characteristic of the contribution of nonplanar gauche or gauche-like conformations.[181,182] WAXD studies[110,111,178] indicated that even though the reflections due to the hydrocarbon matrix disappear with heating, a strong interchain reflection remains at ∼13.5 Å. In the X-ray diffractograms[111] this reflection at ∼6.5° (2θ) increases significantly in intensity with heating. No significant arcing results for this reflection in the uniaxially aligned films at elevated temperatures. This information suggests that while the side chains melt above 42 °C and the polymer backbone conformationally disorders, the polymer chains remain in roughly cylindrical alignment. Recent studies of poly(di-*n*-hexylsilane) above 42 °C by optical microscopy and X-ray diffraction[183] suggest that the material is liquid crystalline with hexagonal columnar symmetry ($a = 1.56$ Å). The columns appear to be composed of single polymer chains that appear from analysis of the data to exist predominantly as extended,

highly gauche helices. The intercolumnar space is amorphous and is presumably occupied by the disordered alkyl side chains. Similar conclusions were drawn by Kuzmany et al.[110] and Lovinger and co-workers,[111] although the latter authors have suggested that the conformationally disordered backbone retains vestiges of the original all-trans structure.

Polymer alignment techniques have been used extensively to study the UV transitions for a number of polysilane derivatives. For poly(di-n-hexylsilane) in solution, flow dichroism[150] results show that the molecules undergo easily detectable orientation in the direction of flow, and the observed dichroism (stronger absorption polarized in the direction of the polymer backbone) was consistent with a backbone $\sigma \rightarrow \sigma^*$ transition. Similar observations have also been reported for oriented films: Klingensmith et al.[134,150] have achieved significant orientation of poly(di-n-hexylsilane) on stretched films of polyethylene and have observed large dichroic ratios. Subsequently, Harrah and Zeigler[49] have succeeded in stretching films of poly(di-n-hexylsilane) deposited on a poly(methyl methacrylate) substrate. Again, the dichroic ratios $(A_{\parallel}/A_{\perp})$ were very large. For the polyethylene alignment, the anisotropy observed for the small residual absorption at 317 nm, while nonzero, was significantly less than that observed for the long-wavelength band at ~370 nm associated with the crystalline phase. Similar UV polarization effects were observed on thin films of poly(di-n-hexylsilane) prepared by uniaxial shear-induced alignment using a glass rod and viscous solutions.[109] Inner core C 1s and Si 2s spectroscopic studies on these films were consistent with the results obtained by the UV polarization studies. From the inner core studies it was also deduced that the alkyl side chains were roughly perpendicular to the silicon polymer backbone of the polysilane in the low-temperature crystalline phase and that the plane of the silicon backbone in the cast films was parallel to the substrate. The anisotropy in the C 1s spectra, which is large in the low-temperature phase, is largely lost in the more mobile high-temperature phase. Polarized EXAFS studies beyond the Si K edge yielded a SiSi bond length of 2.37 ± 0.02 Å and a value of 1.81 ± 0.03 Å for the SiC bond length in the crystalline phase. This value for the SiSi bond length, while considerably longer than that reported for disilane (2.32 Å), confirms the theoretical lengthening predicted for disilane upon methylation.[184]

In summary, poly(di-n-hexylsilane) has been studied extensively both in solution and in the solid state. Studies in the solid state have confirmed the crystallization of the alkyl side chains and the planar zigzag nature of the silicon backbone at room temperature. Above the side-chain melting transition, the substituent groups become disordered and conformationally mobile. Similarly, the backbone also conformationally disorders as manifested by the large blue shift in the UV spectrum but does not become amorphous or isotropic according to the WAXD results. The structure of the polymer in the high-temperature phase has been described as columnar liquid crystalline with hexagonal symmetry. Crystallization of the side chain results in the regeneration of the all-trans silicon backbone. Current evidence indicates that significant intermolecular interactions (i.e., side-chain crystallization) are

necessary to drive the backbone into the planar zigzag conformation for this sterically encumbered example.

Although many structural and electronic questions have been resolved for poly(di-n-hexylsilane), the difference between the position of the UV absorption maximum of the proposed rod form in solution at low temperatures[170,171] and the crystalline polymer[177] remains unanswered. In solution, the so-called "rod" form absorbs at much shorter wavelengths than the crystalline phase at room temperature (λ_{max} 354 vs 370–375 nm). Since the backbone conformation of the crystalline phase at room temperature is known to be planar zigzag, this would suggest that either the structure of poly(di-n-hexysilane) in solution below the transition temperature is composed of shorter trans segments than are observed in the solid state or that the backbone segments in solution are not strictly trans coplanar. This assumes, of course, that the thermochromic changes observed in solution are single-molecule events that do not involve polymer aggregation. An alternative explanation would be that the UV absorption spectrum of poly(di-n-hexylsilane) in the crystalline phase is in fact perturbed by solid-state effects that are responsible for the spectral red shifts. These may be intermolecular or intramolecular in origin. In this regard, it is known that the SiSiSi bond angle in the crystalline phase is somewhat larger (115–118°) than anticipated. Although one might suspect that changes in bond lengths and/or valence angles could strongly perturb the electronic spectrum of a σ-delocalized chromophore, it is not yet clear in which direction. INDO/S calculations on parent and permethylated oligosilanes containing up to 20 silicon atoms suggest that the excitation energy for all of the low-energy $\sigma-\sigma^*$ transitions should progressively *increase* as the valence angle increases, at least for angles in the range from 101 to 120°.[185] On the other hand, ab initio calculations on trisilane[139] suggest that an increase of the SiSiSi valence angle will cause the $\sigma \rightarrow \sigma^*$ transition energy to decrease and that of the $\sigma \rightarrow \pi^*$ transition to increase. Thus, it appears that the explanation for the red shift observed for poly(di-n-hexylsilane) as a crystalline solid vs low-temperature solution will require additional structural studies, particularly in fluid solution, before the spectral effects can be adequately rationalized.

B. Structural Studies on Other Alkyl-Substituted Polysilane Derivatives

Although by far the major structural efforts have been devoted to poly(di-n-hexylsilane), studies on related polysilane derivatives have also produced some interesting results. Miller et al.[116] have recently described some surprising results for poly(di-n-pentylsilane). This material, even though it differs from poly(di-n-hexylsilane) by only one methylene unit per side chain, absorbs at 314 nm and is not significantly thermochromic in the solid state. Differential scanning calorimetry revealed a weak ($\Delta H \sim 0.5$ kcal/mol) reversible endotherm peaked around 75 °C, above which the UV absorption spectrum broadens with little change in the peak position. IR and Raman studies on poly-(di-n-pentylsilane) at room temperature also revealed significant differences between this material and poly-(di-n-hexylsilane). The former shows no evidence of significant side-chain crystallization, and the intense

(a)

(b)
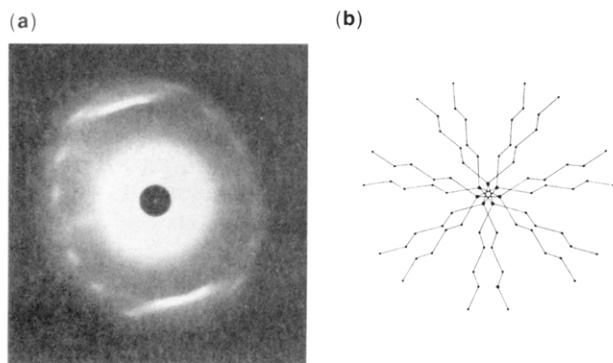
Figure 23. (a) WAXD pattern for stretch-oriented poly(di-*n*-pentylsilane) at 25 °C; (b) pictorial representation of the 7/3-helical structure suggested by the WAXD studies. The large dots represent the silicon atoms of the polymer backbone while the smaller dots symbolize the carbon atoms of the side chains.

Raman band around 690 cm^{-1} that had previously been assigned as a silicon–carbon vibration of the all-trans form in poly(di-*n*-hexylsilane)[110] is missing. In addition, there were also marked differences in the region of the silicon–silicon stretches (350–450 cm^{-1}) relative to poly(di-*n*-hexylsilane). ^{29}Si CPMAS NMR studies on poly(di-*n*-pentylsilane) showed a single upfield resonance at −29.2 ppm (vs −23.0 ppm for PDHS) at room temperature. At elevated temperatures, a narrow time-averaged resonance appeared downfield around −23.5 ppm at the expense of the upfield resonance. The ^{13}C and ^{29}Si spectra above the transition temperature closely resembled those of poly(di-*n*-hexylsilane) at elevated temperatures. All of the spectral evidence for poly(di-*n*-pentylsilane) at room temperature suggested a regular albeit nonplanar backbone conformation below the transition temperature.

Fiber diffraction patterns for a stretch-oriented sample showed sharp reflections out to ~4 Å (Figure 23). Layer line spacing of 13.8 Å and strong near-meridional reflections on the third layer line were consistent with a 7/3 helical conformation (Figure 23). In this conformation the silicon backbone deviates from trans planar by an ~30° twist around each SiSi bond. It is remarkable that such a small deviation from the all-trans geometry even in a regular structure causes a blue shift of almost 60 nm relative to all-trans poly(di-*n*-hexylsilane), although the SiSiSi valence angle is not known with certainty for poly(di-*n*-pentylsilane) in the solid state. Interestingly, both the ^{29}Si NMR and WAXD results on the high-temperature phase of poly(di-*n*-pentylsilane) (above 75 °C) indicate that the polymer structure is very similar to that of poly(di-*n*-hexylsilane) at comparable temperatures. Recently, a similar 7/3 helical structure has also been proposed for poly(di-*n*-butylsilane) at room temperature on the basis of X-ray studies.[115] A transition temperature for this material was observed around 90 °C (transition midpoint temperature). Interestingly, recent isolated molecule conformational calculations on poly(di-*n*-hexylsilane) have predicted strong minima at nontrans conformations[114] very similar to those observed experimentally for poly(di-*n*-pentylsilane) and poly(di-*n*-butylsilane). These results are in conflict with earlier results of Damewood[113] which predict an energetic minimum for the all-trans conformer. It is possible that the agreement between theory and experiment could be in this case fortuitous, since the structural studies
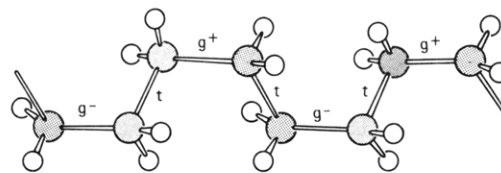
Figure 24. Ball-and-stick model representation of the TGTG′ backbone conformation of poly(di-*n*-tetradecylsilane) as determined from WAXD studies.

pertain to materials in the solid state while the calculations deal with the isolated molecules.

Polysilane derivatives with *n*-alkyl side chains longer than *n*-hexyl have also been studied. For the C$_7$ and C$_8$ homologues, side-chain crystallization results in the adoption of an all-trans backbone and strongly red shifted absorption spectra.[178] However, recent evidence on longer homologues suggests that alternative backbone conformations can result even in the presence of significant side-chain crystallization. This behavior was first observed for poly(di-*n*-decylsilane) for which at least two thermochromic crystalline phases were observed (λ_{max} 350 and 378 nm).[186] The solid-state composition varied with molecular weight, thermal history, etc. When the side-chain length was increased to 14 carbon atoms, a single thermochromic crystalline phase ($T_m \sim$ 55 °C, λ_{max} 345 nm at room temperature) resulted. IR and Raman studies suggested that the backbone of poly(di-*n*-tetradecylsilane) was again nonplanar in spite of the side-chain crystallization ($\Delta H \sim$ 8 kcal/mol). WAXD studies[187] on stretch-oriented fibers confirmed the nonplanarity of the backbone and indicated a TGTG′ (Figure 24) rather than trans-planar conformation. It is proposed that for longer *n*-alkyl substituents the side-chain crystallization need not involve the entire chain, but perhaps only those portions remote from the backbone. This would allow some flexibility for the backbone to adopt a conformation other than the all-trans form.

The structural studies imply that the observation of significant thermochromism in the solid state is consistent with, but not limited to, changes involving the formation of an all-trans conformation. It also suggests that there may be a range of different regular backbone conformations for dialkyl-substituted polysilanes resulting in absorption maxima between 315 and 380 nm and that the position of the UV absorption maxima need not be uniquely associated with a particular backbone conformation in every case. Recent studies on unsymmetrically substituted derivatives such as poly(*n*-hexyl-*n*-pentylsilane) and poly(*n*-hexyl-*n*-octylsilane) show that they are each thermochromic (λ_{max} 316–354 nm) with transition temperatures below 0 °C. Preliminary FT-IR and Raman studies on these materials below their respective transition temperature suggest that the backbone conformations are not identical with any regular form previously described.[188]

In summary, structural studies in the solid state have shown that the electronic properties of poly(dialkylsilanes) depend strongly on the polymer backbone conformation, which, in turn, may be altered by subtle changes in the appended substituents (see Table 11). This behavior is unique for a polymer system, since the substituents themselves cause minimal electronic perturbations but serve mainly to alter the backbone conformations through intramolecular interactions.

TABLE 11. Summary of the Structural, UV Absorption, and Thermal Properties of Some Polysilane Derivatives in the Solid State

$-(R^1R^2Si)_n-$	polymer backbone	λ_{max},[a] nm (film)	DSC transition temp, °C		ΔH,[b] kcal/mol
$R^1 = R^2 = n$-butyl	7/3 helix	313–315	83	0.36	backbone disordering
$R^1 = R^2 = n$-pentyl	7/3 helix	313–315	75	0.45	backbone disordering
$R^1 = R^2 = n$-hexyl	trans planar	375	42	5.0	side-chain melting backbone disordering
$R^1 = R^2 = n$-octyl	trans planar	375	47	4.7	side-chain melting backbone disordering
$R^1 = R^2 = n$-tetradecyl	TGTG'	345	55	8.4	side-chain melting backbone disordering
$R^1 = n$-hexyl; $R^2 = n$-octyl (atactic)	?	354	−19	1.4	side-chain melting backbone disordering
$R^1 = R^2 = $ 4-methylpentyl	disordered	316			

[a] Absorption maximum below the transition temperature. [b] Enthalpy change of the thermal transition when observable.

Such a situation offers the unprecedented opportunity to study the relationship between backbone conformation and the spectral properties without the complications often caused by substituent perturbations.

There have been very few structural studies on aryl-substituted polysilane derivatives in the solid state. Recently, Ovchinnikov and co-workers have suggested that the backbone conformation of poly(diphenylsilane) exists in an all-trans conformation in the solid state on the basis of an analysis of X-ray powder pattern data using solid-state parameters derived from the study of a number of crystalline perphenylated silane oligomers.[189] This proposal is consistent with the conclusions of Miller and Sooriyakumaran[53] based on studies of soluble poly[bis(alkylphenyl)silane] derivatives.

C. Poly(arylalkylsilanes)

Structural data on unsymmetrically substituted aryl polysilanes have not been reported, presumably due to the problems caused by the atactic nature of such polymers. Even the spectroscopic studies on materials of this type in the solid state have also revealed certain complexities and ambiguities.

While the interpretation of the polarization data for poly(di-n-hexylsilane) in oriented form seems quite straightforward and is consistent with the assignment of a $\sigma \rightarrow \sigma^*$ transition for the long-wavelength band, the results for some aromatic polysilanes are less clear-cut. Harrah and Zeigler[49] have prepared stretched films of poly(methylphenylsilane), poly[(p-methoxyphenyl)-methylsilane], and poly(methyl-β-naphthylsilane) and have recorded their dichroic UV spectra. While the first two examples were strongly dichroic, their difference spectra $(A_{\parallel} - A_{\perp})$ showed red-shifted maxima. The authors have proposed that these data, in concert with the observation that the fluorescence quantum yields were strongly wavelength dependent, imply that the long-wavelength absorption is resolvable into at least two transitions, but other explanations are plausible as well. For example, chain segments of different lengths or conformations could differ in their average degree of orientation. The oriented poly(methyl-β-naphthyl-silane) spectra are not dichroic, which is not surprising since absorption–emission studies in solution suggest that the excitation resides primarily on the side chains which are apparently randomly oriented for the β-naphthyl-substituted polymer.[49]

Emission studies on unoriented poly(methylphenyl-silane) in the solid state have produced some conflicting results. Kagawa et al.[190] have observed two short-lived

emissions from films of poly(methylphenylsilane) at 77 K: a strong emission peaked in the ultraviolet at 350 nm and a much weaker, broad emission at ~480 nm. On the basis of band structure calculations on poly-(methylphenylsilane) it was concluded that the long-wavelength band was intrinsic to the system and was best described as a $\sigma\pi^*$ charge-transfer emission. Harrah and Zeigler[191] have reinvestigated the emission properties of poly(methylphenylsilane) films at room temperature and have similarly confirmed the existence of two short-lived emissions: normal fluorescence emission peaked around 360 nm and a much weaker broad band at 540 nm. Although this emission is in the same spectral region as the normal phosphorescence emission (454 nm), the latter is easily distinguished by its relatively long lifetime ($\tau = 1.5 \times 10^{-3}$ s). These authors suggest that the long-wavelength, prompt emission originally assigned as charge transfer is not intrinsic to the polymer but instead results from photodegradation. This emission band grows and red shifts with prolonged irradiation at the expense of the normal fluorescence absorption band at 360 nm. Although no estimate of the amount of photoimpurity produced by photoscanning was possible, it was suggested that little would be necessary to produce the emission results, since the long-wavelength emission is emphasized by energy transfer from the photoexcited poly(methyl-phenylsilane). It is important to note that the latter study was performed at room temperature where photodegradation is expected to be more efficient, while the original spectroscopic studies on poly(methylphenyl-silane) were done at 77 K or below. However, Kagawa et al.[190] also note in their paper that the polymer is rapidly degraded at unspecified temperatures >77 K and that this is manifested by a decrease in the standard polysilane fluorescence emission at 350 nm and an increase in the low-energy luminescence in a manner similar to the observations Harrah and Zeigler.

D. Miscellaneous Properties

1. Electrochemistry

Diaz and Miller[86] have studied the electrochemical oxidation of a variety of polysilane derivatives deposited as thin films (400–700 Å) on platinum electrodes. All of the polymers studied oxidized irreversibly, and the peak potentials are listed in Table 12. There is a significant substituent effect observed when an aryl group is attached directly to the silicon backbone, which is manifested by an anodic shift in the peak potential of

TABLE 12. Electrochemical and UV Absorption Data for Some Substituted Polysilane Films

| compd	peak potential,[a] V	absorp max, nm
poly(methylphenylsilane)	1.0	342
poly[(p-methoxyphenyl)methylsilane]	0.69	344
poly(methyl-β-phenethylsilane)	1.30	308
poly(cyclohexylmethylsilane)	1.42	320
poly(n-hexylmethylsilane)	1.44	303
poly(di-n-hexylsilane)	1.60	317
poly(dimethylsilane)	1.0[b]	295

[a] Film thicknesses 400–650 Å. [b] Extrapolated value.

0.3–0.6 V. Poly[(p-methoxyphenyl)methylsilane] is more easily oxidized than poly(methylphenylsilane) by almost 0.3 V. For the aryl derivatives, the oxidation must involve the silicon backbone, since the peak potentials are much more anodic than those of alkyl- and silyl-substituted model compounds. For poly(methylphenylsilane) comparison of the charge involved in oxidation with the amount of polymer on the electrode surface suggested that ~1 electron is removed for approximately every 10 monomer units. ESCA studies of the oxidized electrode surface showed that the polymer was removed in the oxidation process. No silicon could be detected and only a small amount of residual carbon and oxygen remained. It is interesting that the oxidation potentials for the alkyl polymers are considerably more cathodic than both those measured for permethyl-substituted silane oligomers and the extrapolated value proposed for poly(dimethylsilane). The authors suggest that this might be due to kinetic limitations caused by the bulky alkyl groups which provide some separation between the platinum surface and the silicon backbone.

2. Photoelectron Spectroscopy

Loubriel and Zeigler[146a] have measured the photoelectron spectra of a number of polysilane derivatives deposited on tantalum substrates and have compared the measured binding energies with those of relevant hydrocarbons in the gas phase. In spite of the considerable band overlap, the authors conclude that for the alkyl polysilanes the photoelectron spectra can be interpreted in terms of backbone and side-chain levels that do not mix extensively. With aromatic substitution, such as in poly(methylphenylsilane) and poly(methyl-β-naphthylsilane), the photoelectron spectra provide evidence of interaction between the substituent orbitals and those of the silicon backbone. This observation is also consistent with absorption and emission data. The authors further suggest that insulation of the silicon chain orbitals from those of the side chain may be responsible for the increased photosensitivity of alkyl-substituted polysilanes relative to aromatic derivatives observed in the solid state, although the solution photolability[119] of aryl polysilanes remains unexplained.

3. Spectroscopic Hole Burning

Spectroscopic hole burning at 1.4 and 77 K in a sample of poly(di-n-hexylsilane) dissolved in methylcyclohexane has been demonstrated by Trommsdorff et al.[192] Cooling poly(di-n-hexylsilane) rapidly results in a thermochromic absorption shift and the formation of a narrow absorption band (FWHM = 285–500 cm^{-1})
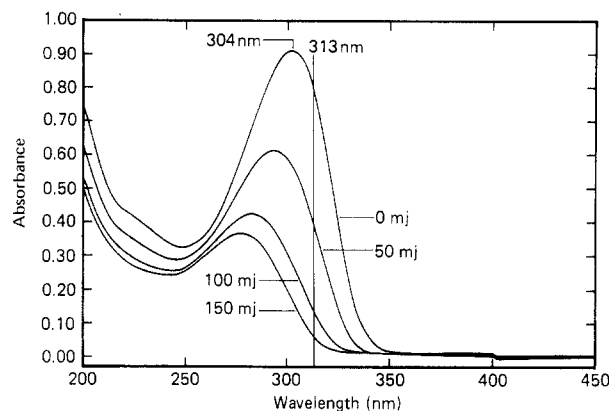
Figure 25. Photochemical spectral bleaching of a film of poly(n-hexylmethylsilane) upon irradiation at 313 nm.

centered at 350.5 nm. Irradiation at 355.11 nm results in the burning of a spectral hole in the absorption spectrum. The width of this hole varied from 4 to 125 cm^{-1} at 1.4 and 77 K, respectively. The authors conclude that the inhomogeneous line width probably results from a distribution of chromophore segment lengths. Addressing certain segment lengths with the laser light causes selective photodestruction, although some rapid energy transfer occurs, leading to photochemistry at the low-energy edge of the laser line. This photochemistry becomes less efficient as the most photoreactive regions are destroyed. This study represents the first example of hole burning in a molecular system at temperatures as high as 77 K and as such constitutes an exciting recent development.

IX. Photochemistry of Polysilane Derivatives

A. Background

Although the curious spectroscopic properties of high molecular weight polysilane derivatives have attracted considerable attention, it is their photochemical lability and sensitivity to ionizing radiation that is responsible for many of the proposed applications.

The first suggestion that linear, high molecular weight polysilanes might be photolabile was a report by West and co-workers,[31] who found that cross-linking of the copolymer polysilastyrene occurred in polymer solutions left standing in sunlight. This phenomenon, which was manifested in solution by the formation of a gelatinous precipitate, has been utilized in the solid state to provide dimensional stability and decrease the loss of volatiles in the pyrolytic conversion to β-silicon carbide (vide infra). Soon afterward, it was reported that solutions and films of high molecular weight polysilanes bleached strongly upon exposure to UV light.[119] An example of this for a typical polysilane film is shown in Figure 25. The observation of a progressive blue shift in the absorption maximum suggested that the polymer molecular weight was being continuously reduced upon exposure by some type of chain scission process. This result is demonstrated in Figure 26, which shows the progressive decrease in molecular weight of a typical polysilane derivative upon UV exposure. Spectral bleaching upon irradiation occurs both in solution and in the solid state, although the rate is much faster in the former. Oxygen can also play a role in the photodecomposition of polysilane derivatives, particu-

TABLE 13. Quantum Yields for Photolysis of Polysilane Homopolymers, $(R^1R^2Si)_n$

entry	R^1	R^2	solvent	$\bar{M}_w{}^0 \times 10^{-3}$ [a]	λ_e,[c] nm	solution Φ_s	solution Φ_x	solid film Φ_s	solid film Φ_x
1	c-Hex	Me	toluene	41.4	355	1.2	0.06	0.022	0
2	n-Hex	n-Hex	toluene	44.6	353	0.6	0		
3	PhC$_2$H$_4$	Me	toluene	208.9	347	0.97	0.08		
4	n-dodecyl	Me	toluene	185.1	347	0.54	0		
5	n-Pr	Me		3900				0.011	0.0013[b]
					190			0.015	0.0013[b]
6	Ph	Me	THF	245	313	0.97	0.12	0.015	0.002
7	p-t-BuC$_6$H$_4$	Me	toluene	633.6	367	1.00	0.18		

[a] Molecular weights were determined by GPC analyses and are based on polystyrene calibration standards. [b] Reference 197. [c] Irradiation wavelength.
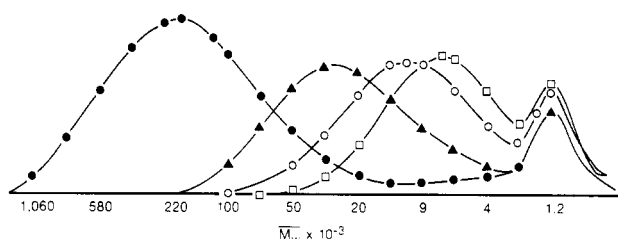

Figure 26. Change in molecular weight distribution of a 0.006% solution of poly(dodecylmethylsilane) upon irradiation at 313 nm: (●) 0, (▲) 2, (O) 4, and (□) 8 mJ/cm^2.

larly in the solid state. Zeigler et al.[50] have shown by IR studies that irradiation of thick films of the copolymer poly(cyclohexylmethylsilane-co-dimethylsilane) at 254 nm in air leads to the appearance of IR bands at 3401, 2173 and 1021 cm^{-1} attributed to the formation of SiOH, SiH, and SiOSi bonds, respectively, the latter being ascribed to the generation of cyclic siloxanes. Similarly, Ban and Sukegawa[193] have also reported the formation of SiOSi linkages upon irradiation of both poly(methyl-n-propylsilane) and poly(methylphenylsilane) in air, which they attribute to the generation of lower molecular weight siloxane polymers. In addition to these observations, it is now quite apparent that polysilane derivatives also undergo substantial spectral bleaching and that chain scission occurs in the absence of oxygen, even in vacuo.

B. Quantum Yields for Photodecomposition of Polysilanes

For polymers that undergo significant changes in molecular weight upon irradiation, the quantum yields of scission and cross-linking can be simultaneously determined by using a standard set of equations; (3) and (4).[194] Using this technique, quantum yields for a va-

$$\frac{1}{\bar{M}_n} = \frac{1}{\bar{M}_n{}^0} + \phi(s) - \phi(x)\frac{D}{N_A} \quad (3)$$

$$\frac{1}{\bar{M}_w} = \frac{1}{\bar{M}_w{}^0} + \frac{\phi(s) - 4\phi(x)}{2}\frac{D}{N_A} \quad (4)$$

$\bar{M}_n{}^0$ = initial number-average molecular weight

$\bar{M}_w{}^0$ = initial weight-average molecular weight

D = dose

N_A = Avogadro's number

riety of polysilanes have been measured both in solution and as thin films, and some representative examples are reported in Table 13.[119,195,197] In solution, all of the polysilane derivatives that have been studied quantitatively predominantly undergo chain scission, although

cross-linking becomes relatively more important for those polymers where aromatic substituents are directly attached to the backbone. In the solid state the respective quantum yields for both processes are much lower (50-100 times) than the solution values.[119,195,197] Recently, Taylor et al.[196] have reported that the respective solid-state quantum yields for both chain cleavage and cross-linking measured for the copolymer poly(cyclohexylmethylsilane-co-dimethylsilane) are wavelength dependent and increase significantly at short wavelengths (248 nm) relative to broad-band mid-UV excitation (285-350 nm).

In every case, however, the quantum yields for scission are significantly lower[119,195,197] in the solid state. This is unfortunate, since many potential applications utilizing the photolability require solid film configurations, and has led a number of groups to study the effect of additives on the solid-state photochemical processes. Johnson and McGrane[198] have reported the quenching of poly(methylphenylsilane) fluorescence at 77 K by laser dyes such as Coumarin-1 doped into the film and have calculated a quenching rate constant of 2.17×10^{14} cm^3 mol^{-1} assuming a value of 1 ns for the polymer fluorescence lifetime. They suggest that although the quenching rate is somewhat larger than predicted by Förster theory, the enhancement is not large, signifying that exciton migration does not extend over large distances. The authors do not comment on the effect, if any, of the quenchers on the rate of photodecomposition of the polymer in the solid state at room temperature. Miller and co-workers[46] have reported that the addition of a variety of halogenated sensitizers, such as 2-4, to
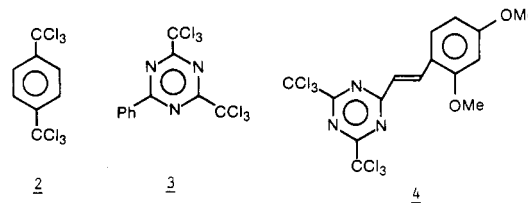
poly(methylphenylsilane) greatly increases the rate of polymer degradation as monitored by the rate of spectral bleaching. The accelerated bleaching is, however, apparently not a general phenomenon and depends on the structure of the polymer. Incorporation of the same sensitizers into aliphatic polysilanes such as poly(cyclohexylmethylsilane) did not significantly accelerate the rate of bleaching. The mechanism of the enhanced photodecomposition of poly(methylphenylsilane) is poorly understood and will require additional studies. The authors tentatively suggest that electron transfer may be involved in the case of poly(methylphenylsilane), a proposal that is supported to some extent by the enhanced reducing power of photoexcited

poly(methylphenylsilane) relative to poly(cyclohexyl-methylsilane) ($E^*_{1/2}{}^{red}$ = -2.54 vs -2.40 V), but other possible mechanisms, including those involving silyl radical formation, have not been ruled out.

The role of electron-transfer processes involving substituted silane high polymers in the presence of electron acceptors is worthy of further investigation. It seems likely that such pathways exist in light of the recent demonstrations of the occurrence of photochemical electron-transfer processes for both hexamethyl-disilane[199] and dodecamethylcyclohexasilane[200] in solution, but such reactions have not yet been unambiguously demonstrated for the high polymers themselves.

## C. Photochemistry and Reactive Intermediates

The photochemistry of short-chain silicon catenates itself constitutes a suitable topic for review and as such a comprehensive discussion of the subject is beyond the scope of this discussion. For this reason, only very few model reactions that are relevant to the photochemistry of the high polymers have been selected and the reader is directed to two excellent reviews of the photochemistry of oligosilanes for further information.[10,11]

The simplest catenated silane derivative is one that contains the disilane unit. Alkyl-substituted disilanes absorb in the deep and vacuum ultraviolet, but aromatic substitution causes significant spectral red shifts into the accessible UV region. It is generally agreed that the primary process in the photochemical decomposition of disilane derivatives is simple homolysis of the silicon–silicon bond to produce silyl radicals. These radicals undergo many characteristic reactions such as hydrogen and halogen abstraction, addition to unsaturated vinyl, acetylenic, or aromatic functionality, abstraction of hydrogen or alkoxy groups from alcohols, etc.[201,202] For the hydrogen abstraction reactions, the relatively low bond energies for most SiH bonds (81–90 kcal/mol)[93] mean that abstractions from typical hydrocarbons are somewhat endothermic except for the most highly activated carbon–hydrogen bonds. Encounters between silyl radicals can lead to dimerization and/or disproportionation, the latter being energetically driven by the formation of a silicon–carbon double bond, worth ~39 kcal/mol.[9] In an early study by Boudjouk et al.,[203] the disproportionation reaction was unambiguously demonstrated in the photolysis of 1,1,2,2,2-pentaphenyl-1-methyldisilane in methanol (MeOH(D)). More recently, Hawari et al.[204] have demonstrated that dimerization and disproportionation are competitive in the reactions of pentamethyldisilyl radicals. Other studies on trimethylsilyl radicals[202] both in solution and in the gas phase have also shown that dimerization and disproportionation are competitive. Studies by Ishikawa and co-workers[10,11] on phenyl-pentamethyldisilane have demonstrated that phenyl-substituted silyl radicals can in principle undergo ortho silyl radical addition to produce unstable silene derivatives that can be subsequently trapped and identified, although the process could also be rationalized as a concerted 1,3-shift. The proposed silene has also recently been detected by transient spectroscopic techniques.[205]

Additional silicon catenation opens a new photochemical channel: chain abridgement by the extrusion of monomeric silylene fragments. Kumada and co-workers[10,11] have studied the photochemical decomposition of a number of cyclic and acyclic polysilane derivatives in the presence of trialkylsilane trapping reagents and have concluded that both monomeric silylenes and silyl radicals are concurrently produced as intermediates. The former were identified by trapping, while the latter were implicated by the formation of silane derivatives that contained fewer silicon atoms than the starting materials and were also terminated with SiH. It was also suggested that the relative proportion of radical vs silylene products increased with increasing chain length for acyclic silanes.[206]

In spite of the extensive studies of the photochemistry of oligomeric silane derivatives, there have been relatively few studies on substituted silane high polymers. Ishikawa and co-workers have studied the photodegradation of a number of disilane polymers such as 5 and 6[207-210] in which the photoreactive disilane unit

5a   Z = 0   6a   R = Et

5b   R = CH₂=CH—   6b   R = Ph

5c   R = CH₂=CHCH₂—

5d   R = CH₂=CHCH₂CH₂—
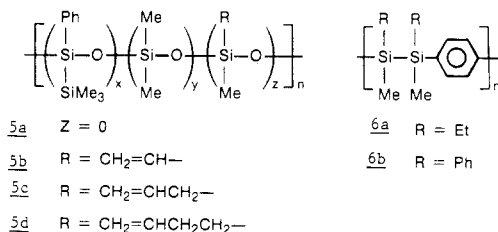
is either pendant or incorporated into the polymer backbone. While these polymers are not strictly analogous to the polysilanes under discussion, their photochemical behavior is relevant in some ways.

Pendant polymers such as 5a–d absorb strongly around 235 nm due to the presence of the phenyldisilanyl chromophore. Irradiation leads to rapid bleaching and the insolubilization of the polymer through cross-linking. Studies on the polymers themselves as well as on monomeric model compounds suggested that silyl radicals are produced by homolysis of the silicon–silicon bond and that backbone radicals are responsible for the polymer cross-linking.[207,208] Neither the polymers nor the model compounds produced any evidence of trimethylsilyl radical readdition to the ortho position of the phenylsilyl chain radical as has been reported in the photolysis of monomeric phenylpentamethyldisilane. The mechanistic conclusions were drawn mainly from the solution behavior of the model compounds coupled with spectroscopic studies on the polymer photoproducts.

Ishikawa et al. have also extensively studied the irradiation of the main-chain disilanyl polymers 6a,-b.[208-210] Photodegradation of these polymers results in the spectral bleaching of the characteristic absorption bands at 262 and 254 nm, respectively, again suggesting that silicon–silicon bond homolysis is occurring. For 6a,b, unlike 5a–d, the photodegradation products remain soluble in common organic solvents, facilitating characterization of the fragments.

When the polymers are irradiated in solution, molecular weight decreases are observed. IR and NMR examination of the photoproducts shows that new SiH functionality is introduced. Studies of the photodegradation in MeOH(D) were consistent with silicon-silicon bond homolysis followed by disproportionation of the incipient silyl radicals. Little SiH (IR analysis) was produced upon irradiation of solid films of 6a in air. Instead, new IR bands characteristic of SiOH and SiOSi functionality were detected in the photodegraded polymer, suggesting that the silyl radicals initially

TABLE 14. Products from the Exhaustive Photolysis (254 nm) of Poly(di-n-butylsilane), Poly(n-hexylmethylsilane), and Poly(cyclohexylmethylsilane) in Cyclohexane Containing Triethylsilane as a Trapping Reagent

product	yield, %		
	$R^1 = n$-Bu $R^2 = n$-Bu	$R^1 = n$-Hex $R^2 = $ Me	$R^1 = $ c-Hex $R^2 = $ Me
$Et_3SiR^1R^2SiH$	59	70	71
$HSiR^1R^2SiR^1R^2H$	11	11	14
$Et_3SiSiR^1R^2SiEt_3$	a	3	a
$HSiR^1R^2OSiR^1R^2H$	a	a	2
$Et_3SiOSiR^1R^2SiR^1R^2H$	a	a	3

^{a} Product yields were <2%.

produced are efficiently intercepted by oxygen prior to disproportionation. Similar results were observed for the irradiation of films of **6b** in air, except that more SiH-containing fragments are produced, suggesting that some silenes are produced competitively. The authors conclude that the photodegradation of **6a** and **6b** both in solution and in the solid state results in the formation of silyl radicals that then react via radical disproportionation (presumably recombination is also occurring competitively) or are intercepted by oxygen when it is present in the medium.

The photodegradation of a number of substituted silane homo- $(R^1R^2Si)_n$ and copolymers $((R^1R^2Si)_m$-$(R^3R^4Si)_n)$ at 254 nm in solution has also been reported.[211] In this study, the polymers were exhaustively degraded in the presence of trapping agents such as triethylsilane (Et_3SiH) and various alcohols. The results from the irradiation of the homopolymers in Et_3SiH are shown in Table 14. In each case, the major product was the disilane $R^1R^2HSiSiEt_3$ expected from the trapping of monomeric dialkylsilylenes by Et_3SiH. Also produced in respectable yields were the hydrogen-terminated disilanes of structure $HR^1R^2SiSiR^1R^2H$. Copolymers produced similar product mixtures in ratios that were consistent with the original copolymer composition. Similar types of photoproducts were isolated from the irradiation of poly(n-hexylmethylsilane) in the presence of methanol or 2-propanol as shown in Table 15.

On the basis of this study the authors conclude that monomeric silylenes and silyl radicals generated by chain homolysis are intermediates in the exhaustive irradiation. The former were confirmed by the isolation of characteristic trapping adducts while the latter were implicated by the formation of the hydrogen-terminated disilanes. On the basis of this evidence the mechanism shown in Scheme 1 was proposed. It was reasonably assumed that silyl radicals produced by silicon–silicon bond homolysis abstract hydrogen from the trapping reagents and continue to be photodegraded until the fragments no longer absorb significantly at 254 nm. More recent studies, however, suggest that the source of hydrogen is *not* the trapping reagent (vide infra). The mechanism shown in Scheme 1 was proposed to rationalize the expected intermediates. It is not meant to imply that both silyl radicals and silylenes are generated from the absorption of a single photon. Indeed, one photon of 254-nm radiation possesses insufficient energy to simultaneously form two silyl radicals and one molecule of substituted silylene based on a silicon–silicon bond energy of $\sim$80 kcal/mol, even considering the stabilization energy for the silylene fragment, $\sim$28 kcal/mol.[93] Simple thermodynamic considerations

TABLE 15. Products from the Exhaustive Photolysis (254 nm) of Poly(n-hexylmethylsilane) in Methanol and in 1-Propanol

product	yield, %	
	R = Me	R = n-Pr
$Me{-}\underset{H}{\overset{n\text{-}C_6H_{13}}{Si}}{-}OR$	65	39
$Me{-}\underset{OR}{\overset{n\text{-}C_6H_{13}}{Si}}{-}OR$	0	5
$H{-}\underset{Me}{\overset{n\text{-}C_6H_{13}}{Si}}{-}\underset{Me}{\overset{n\text{-}C_6H_{13}}{Si}}{-}H$	7	7
$H{-}\underset{Me}{\overset{n\text{-}C_6H_{13}}{Si}}{-}\underset{Me}{\overset{n\text{-}C_6H_{13}}{Si}}{-}OR$	15	20
$RO{-}\underset{Me}{\overset{n\text{-}C_6H_{13}}{Si}}{-}\underset{Me}{\overset{n\text{-}C_6H_{13}}{Si}}{-}OR$	7	12

SCHEME 1. Mechanistic Scheme for the Exhaustive Photodegradation of Polysilanes at Short Wavelengths in the Presence of Triethylsilane Trapping Agent
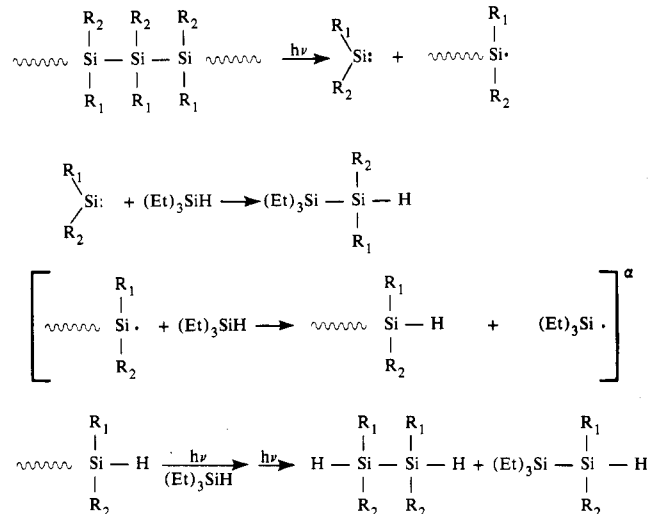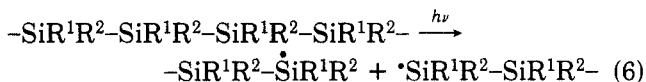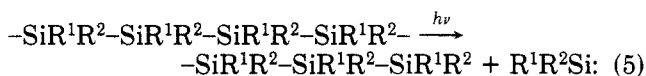

^{a} Subsequent experiments with isotopically labeled substrates and solvents suggest that this reaction is not competitive with radical disproportionation.

predict that the processes generating silyl radicals and silylenes should be uncoupled and competing.

Although the experiments described suggest that the photochemical degradation processes for substituted silane high polymers resemble those previously reported for oligomeric silanes, recent studies indicate that the photochemistry of the polymer systems is more complex than at first envisioned. In this regard, Michl, Miller, et al.[151,212] have studied the solution degradation of poly(di-n-hexylsilane) and poly(di-n-butylsilane) at a variety of exposure wavelengths and report that the photochemistry is strongly wavelength dependent. At 248 nm (pulsed KrF excimer laser) or 254 nm (mercury lamp) in the presence of Et_3SiH, the trapping adducts Et_3SiSiR_2H (R = Bu or Hex) and the homolytic cleavage products $H(SiR_2)_nH$ ($n = 2, 3$; R = Bu or Hex) are produced as previously reported. The formation of the

adduct Et_3SiSiR_2H is, however, wavelength dependent and the quantum yield drops rapidly, approaching zero for wavelengths >300 nm. Polymer degradation still occurs at the longer wavelengths as evidenced by the formation of persistent silicon-centered radicals (vide infra) and the rapid bleaching of the original polymer absorption at 316 nm. Chain scission at the longer wavelengths was also confirmed by GPC analysis of the irradiated solutions. When Et_3SiD was employed, irradiation at 248 nm produced Et_3SiSiR_2D, but the silanes of structure $H(SiR_2)_nH$ (n = 2, 3) remain undeuterated. Using deuterated trapping reagents and/or solvents for the long-wavelength irradiations (λ > 300 nm) resulted in no deuterated products by IR analysis, which demonstrates that the silyl radicals generated from chain scission abstract hydrogen from the polymer rather than from the trapping reagent or the solvent. Long-wavelength irradiation of poly(di-n-hexylsilane) specifically deuterated in the α positions of the side chains (α-d_2) produced products containing –SiD but no –SiH bonds, suggesting that the SiD-containing products arise by Si radical disproportionation. Similar experiments at short wavelengths produce both SiH- and SiD-containing products. However, since the former are suppressed in the presence of excess TES, it has been proposed that the SiH products are produced by intramolecular insertion reactions of di-n-hexylsilylene.[212]

The wavelength studies confirm that the photochemical processes producing silyl radicals and silylenes (eq 5 and 6) are decoupled, consistent with thermodynamic

$$-SiR^1R^2-SiR^1R^2-SiR^1R^2-SiR^1R^2- \xrightarrow{h\nu}$$
$$-SiR^1R^2-SiR^1R^2-SiR^1R^2 + R^1R^2Si: \quad (5)$$

$$-SiR^1R^2-SiR^1R^2-SiR^1R^2-SiR^1R^2- \xrightarrow{h\nu}$$
$$-SiR^1R^2-\overset{\bullet}{Si}R^1R^2 + {}^\bullet SiR^1R^2-SiR^1R^2- \quad (6)$$

considerations. The failure to observe silylene-type products upon irradiation at λ > 300 nm, where polymer degradation is still evident, further demonstrates that silylenes are also not generated to an appreciable extent from the silyl radicals in solution at room temperature (eq 7). This result is also consistent with

$$-SiR_2-SiR_2-SiR_2{}^\bullet \nrightarrow -SiR_2-SiR_2{}^\bullet + R_2Si: \quad (7)$$
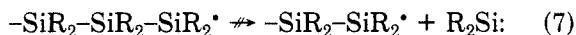
recent results reported for pentamethyldisilyl radicals.[204] The authors stress that, while the wavelength-dependent solution photochemistry is unusual,[213] the results fit nicely with the photophysical model of polysilane derivatives in solution described earlier. In this model, the polysilane chain was described as a weakly interacting statistical collection of chromophores composed of trans or nearly trans units partially electronically decoupled by conformational kinks. With this model, the wavelength-dependent photochemistry could be rationalized as follows. Irradiation at longer wavelengths selectively excites the longest chromophores, which undergo bond homolysis to produce silyl radicals. Short-wavelength excitation, on the other hand, excites the shorter or high-energy chromophores, which can either transfer energy to the longer chromophores which subsequently decompose by bond homolysis, or decompose directly by the extrusion of a silylene fragment. The homolytic cleavage could be simultaneously occurring in both the long and short chromophores or
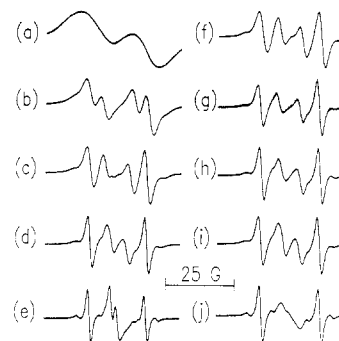
Figure 27. ESR spectra of irradiated polysilanes $(R_2Si)_n$ in n-octane (a–c in n-pentane); (a–e) R = 4-methylpentyl [(a) 200 K; (b) 220 K; (c) 260 K; (d) 300 K; (e) 350 K]; (f) R = n-$C_{14}H_{29}$; (g) R = n-$C_{10}H_{21}$; (h) R = n-C_8H_{17}; (i) R = n-C_6H_{13}; (j) R = n-C_4H_9. T = 300 K.

exclusively from the former. In the latter case, rapid energy transfer would be required in the short-wavelength irradiation to rationalize the results.
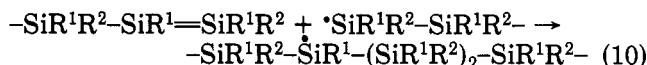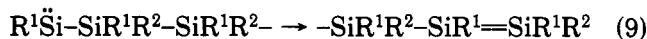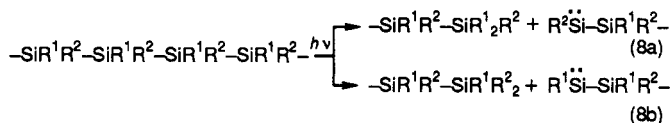
Although the intermediacy of substituted silylenes in the irradiation of polysilane derivatives at short wavelength seems firmly established based on the isolation of characteristic trapping adducts, the evidence for the production of silyl radicals is more indirect and is based mainly on the observation of SiOH and SiOSi-containing fragments upon irradiation in the solid state in the presence of oxygen,[50,193,214] the isolation of SiH-terminated fragments ascribable to radical disproportionation upon exhaustive irradiation in solution,[211] and the successful photoinitiation of vinyl polymerizations.[231,232]

Recently, however, Todesco and Kamat[66] have reported the formation of a long-lived transient (300 μs) from the copolymer poly(methyl-α-naphthylsilane-co-dimethylsilane) using nanosecond flash photolytic techniques. The authors rejected the possibility of silylene intermediates in the flash photolysis on the basis of the λ_{max} of the transient (380 nm) and the failure to observe any visible absorption characteristic of silylenes upon irradiation at 77 K in a variety of organic glasses. In a related study, these authors also report the observation of a complex ESR signal associated with the UV transient upon irradiation of the copolymer in 2-methyltetrahydrofuran at 77 K. The complex shape of the signal was ascribed to the presence of at least two radical species, and the apparent g value (2.0039) was suggestive of silyl radicals containing β-silicon atoms. The measured g value of the radical(s) coupled with the spectral similarity of the UV transient with the absorption spectra of 1-(α-naphthyl)ethyl and acenaphthenyl radicals led to a structural assignment for the transient species absorbing at 380 nm as the silyl radical(s) expected from polymer chain scission α to a naphthyl side chain.

McKinley et al.[215] have also reported the observation of radical species produced during irradiation of a variety of di-n-alkyl polymers [(poly(di-n-hexylsilane), poly(di-n-butylsilane), poly(di-n-tetradecylsilane), poly(di-n-octylsilane), and poly[bis(4-methylpentyl)silane]] in hydrocarbon solvents. These are persistent for hours and even days (see Figure 27). The radical spectra, which are similar for each irradiated polymer, are complex, temperature dependent, and clearly not consistent with those expected from simple homolytic cleavage of the silicon backbone. The structure of the

persistent radicals has been assigned as $-SiR_2\dot{S}iRSiR_2-$ as determined from their ESR and ENDOR spectra. The variable-temperature studies were conducted on the radical derived from poly[bis(4-methylpentyl)silane], which remains soluble at low temperatures. In the low-temperature limit, the spectrum is composed of two doublets due to splitting by the two nonequivalent hydrogens on the α-carbon of the alkyl substituent on the presumably nearly planar silicon radical center. At higher temperatures, the spectra begin to average due to the rocking of the alkyl side chain attached to the center, although complete averaging is never obtained even at the highest convenient temperatures. The following values for the g factor and for the hyperfine couplings were obtained by ESR, ENDOR, and triple-resonance techniques for the persistent radical derived from poly(di-n-hexylsilane) $(C^\beta_2Si^\alpha)$-$\dot{S}i^i$-$C^\alpha H^{\alpha'}H^{\alpha''}CH^\beta_2 CH^\gamma_2-$: (a) $g = 2.00472$; (b) ^{29}Si satellites: $a_\alpha = 5.8$ G (2Si), $a_i = 75$ G, assigned to $-(Si^\alpha)_2-Si^i$; (c) proton couplings: $a_{\alpha'} = 11$ G (1 H), $a_{\alpha''} \approx 3$ G (1H) near the low-temperature limit and $a_\alpha \approx 6.99$ G (2H) near the high-temperature limit, $a_\beta = 0.34$ G, $a_\gamma = 0.13$ G, sgn a_α = sgn a_γ = –sgn a_β, assigned to $-CH^\gamma_2-CH^\beta_2-CH^{\alpha'}H^{\alpha''}-\dot{S}i$; (d) carbon coupling: $a_\beta = 4.12$ G, assigned to $-C^\beta_2Si-\dot{S}iC^\alpha-SiC^\beta_2-$.

The source of these persistent radicals is a question of some interest. Simple photochemical silicon–carbon bond homolysis was considered unlikely based on the lack of literature precedent and the failure to detect any n-alkane or 1-alkene in the photolysis mixtures. A 1-alkene would not survive the reaction conditions, but an n-alkane would. The authors suggest the possible route shown in eq 8–10. It should be noted that, while

$$-SiR^1R^2-SiR^1R^2-SiR^1R^2-SiR^1R^2-\overset{h\nu}{\longrightarrow}\begin{cases}\longrightarrow -SiR^1R^2-SiR^1{}_2R^2 + R^2\dot{\ddot{S}}i-SiR^1R^2- \quad (8a) \\ \longrightarrow -SiR^1R^2-SiR^1R^2{}_2 + R^1\dot{\ddot{S}}i-SiR^1R^2- \quad (8b)\end{cases}$$

$$R^1\dot{\ddot{S}}i-SiR^1R^2-SiR^1R^2- \rightarrow -SiR^1R^2-SiR^1{=}SiR^1R^2 \quad (9)$$

$$-SiR^1R^2-SiR^1{=}SiR^1R^2 + {}^\bullet SiR^1R^2-SiR^1R^2- \rightarrow \\ -SiR^1R^2-\dot{S}iR^1-(SiR^1R^2)_2-SiR^1R^2- \quad (10)$$

the first step (chain scission by 1,1-reductive elimination) is a well-known thermal pathway for oligosilane decomposition,[216,217] the photochemical variant seems not to have been reported. The subsequent rearrangement of the silylsilylenes to disilenes is known to be rapid[218] and silyl radical addition would be expected at the less hindered site to produce the observed persistent radical.

In support of the proposed mechanism, the authors have obtained evidence for the operation of 1,1-photoelimination chain scission processes in the photodegradation of a high molecular weight polysilane derivative. Exhaustive irradiation at 248 nm of poly(cyclohexylmethylsilane) produces ~10–15% of volatile products that contain trialkyl terminal groups. In this case, the following products were identified by GC–MS (R^1 = cyclohexyl, R^2 = Me); H(R^1R^2Si)$_2$H (49%); H-(R^1R^2Si)$_3$H (19%); $R^1_2R^2SiH$ (2%); $R^2_2R^1SiR^1R^2SiH$ (5%); $R^1_2R^2SiR^1R^2SiH$ (7%).

D. Photochemical Theory

On the basis of photochemical studies in solution, it seems that there are at least three photoprocesses that
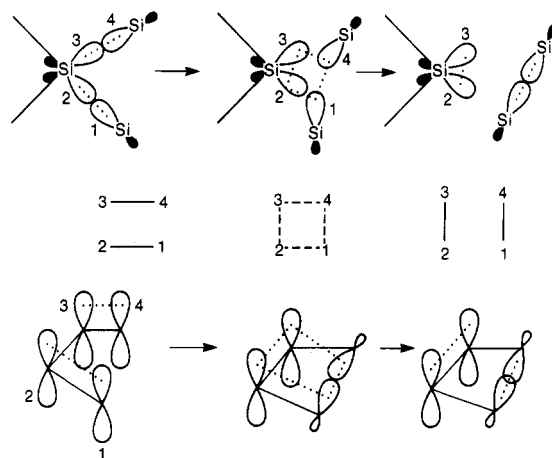
Figure 28. Topological equivalence between the orbitals involved in the extrusion of the central SiH_2 unit from Si_3H_8 (top) and in the disrotatory electrocyclic ring closure of 1,3-butadiene. The primary bonding interactions are indicated by dots.

lead to polymer molecular weight reduction: (i) chain abridgement by silylene extrusion, which occurs only at short wavelengths; (ii) chain scission by silicon–silicon bond homolysis occurring at all wavelengths absorbed by the polymer; (iii) chain scission by photochemical reductive 1,1-elimination. Additional mechanistic studies are necessary to determine whether these solution pathways also occur for polymers in the solid state.

Early theoretical attention focused on chain abridgement by silylene extrusion reaction (i). On the basis of a correlation diagram for the reaction path, it was suggested[219] that this stereospecific[220,221] reaction proceeds from a σ–σ^* excited state, since then it would be orbital symmetry allowed. The proposed conclusion that this is the lowest excited state of oligosilanes does not really follow, since crossings and avoided crossings of states might occur along the reaction path with minimal or no barriers.

The early suggestion was supported in more recent work on two trisilanes at an ab initio SCF level using the pseudopotential approximation[136] and a relatively small basis set which, however, included Rydberg functions. This confirmed the important features of the earlier deduced correlation diagram and showed that d orbitals play a negligible role in the theoretical description of the lowest excitations.

Recently, ab initio CASSCF-CI calculations were performed at a series of points along the asymmetrical (C_{2v}) reaction path.[139,163] These confirmed that the state correlation diagram is indeed just that expected for a ground-state-forbidden and excited-state-allowed photochemical process, such as the disrotatory electrocyclic ring opening in cyclobutene. As shown in Figure 28, the two are actually isoconjugate, with the σ-conjugated system of trisilane assuming the role of the π-conjugated system of 1,3-butadiene, the σ bond in the disilane product playing the role of the π bond in cyclobutene, and the two "nonbonding" orbitals of silylene playing the role of the σ bond in cyclobutene. The hybridized nonbonding orbitals of silylene are the sum and the difference of the usual orbital pair consisting of a 3p orbital and an s–p hybrid with mostly 3s character.

The ground, π–π^* singly excited, and $\pi\pi$–$\pi^*\pi^*$ doubly excited states of butadiene correspond to the ground, σ–σ^* singly excited, and $\sigma\sigma$–$\sigma^*\sigma^*$ doubly excited states of trisilane. The ground, π–π^* singly excited, and $\pi\pi$–
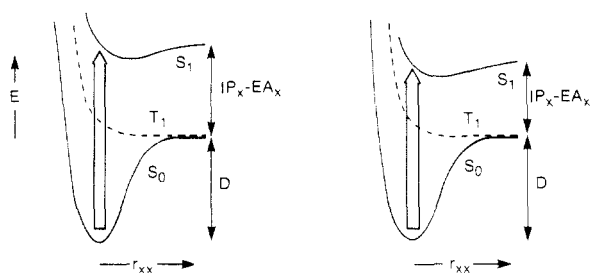
Figure 29. Schematic representation of the dissociation of bonds between two C sp^3 orbitals (left) and between two Si $3sp^3$ orbitals (right) in their S_0, T_1, and S_1 states.

$\pi^*\pi^*$ doubly excited states of cyclobutene have their excitation localized on the π bond. The corresponding three states of the silicon products have the excitation localized on the silylene and are the ground, 3s–3p, and 3s, 3s–3p, 3p excited states.

The state correlation diagram exhibits the expected smooth downhill correlation of the σ–σ^* excited state of the trisilane with the 3s–3p state of the silylene. The ground configuration of the trisilane attempts to correlate with the 3s, 3s–3p, 3p doubly excited configuration of the products, whose ground configuration originates in the $\sigma\sigma$–$\sigma^*\sigma^*$ doubly excited configuration of the trisilane. The intended crossing is avoided, resulting in a barrier in the ground state and a minimum in the lowest excited singlet state, just as in the well-known case of butadiene disrotatory ring closure. It has been proposed[139] that the photochemical process proceeds via return to S_0 from this minimum. As the chain gets longer and the initial σ→σ^* excitation energy decreases, it becomes harder to reach the minimum from the well in the initially reached vertical excited state, and it has been suggested that this provides an opportunity for other processes to compete in longer polysilanes, in particular, fluorescence and intersystem crossing to the triplet manifold. This would account for the decrease of the quantum yield of reaction (i) in long-chain polysilanes as the wavelength of excitation is increased. For wavelengths above 300 nm, only the long chromophores in the chain are excited, and the extrusion process (i) is suppressed.

Ab initio calculations[139,163] on the homolytic cleavage reaction path (ii) show the expected behavior. The S_0 and T_1 states have a common dissociation limit, a pair of polysilyl radicals. The former state is bound, the latter dissociative. The S_0–T_1 excitation energy is approximately equal to the bond energy, so that the T_1 surface does not provide much driving force for the dissociation, but it also offers no resistance to it. The excited singlet state is weakly bound and goes to a high-energy dissociation limit (Figure 29). These calculations thus support the suggestion[49] that the homolytic dissociation process proceeds by intersystem crossing from the initial S_1 state to the T_1 state, followed by bond scission.

These results also suggest a simple qualitative explanation for the much lower singlet excitation energy of the Si–Si σ bond relative to the C–C σ bond. Attempts to attribute this to a smaller separation between the σ and σ^* orbitals in the Si–Si bond than in the C–C bond ("weak bond effect"[108]) are not convincing since the C–C and Si–Si bond strengths in linear chains are comparable. Thus, while the σ–σ^* transition in $Me_3SiSiMe_3$ lies at least 30 kcal/mol and possibly far

below that in Me_3CCMe_3,[157] the Si–Si bond strength in the former is 80 kcal/mol,[93,222a] and the C–C bond strength in the latter is 70 kcal/mol.[222b]

As indicated by Figure 29, a quantity directly related to bond strength is the $^3\sigma$–σ^* triplet excitation energy. The S_0 state and the T_1 state have a common dissociation limit (a radical pair). Both are well-correlated states, nicely described by the valence-bond structure X·X at all geometries of interest. The triplet excitation energy should in general exceed the ground-state bond energy, since the σ^* orbital is more antibonding than the σ orbital is bonding, at least at small internuclear separations, but one would certainly be justified to expect a simple correlation between bond strengths and S_0–T_1 $^3\sigma$–σ^* excitation energies.

However, as Figure 29 also shows very clearly, the $^1\sigma$→σ^* singlet excitation energy should not be simply related to ground-state bond strengths. In the absence of Rydberg states, the $^1\sigma$–σ^* configuration would go to a different dissociation limit, X^+X^-→X^-X^+, and has a highly zwitterionic character already at ordinary internuclear separations. It represents a much less well correlated wave function than S_0 or T_1 and the large difference in correlation energy invalidates the use of simple MO concepts. Instead, the S_1 energy can be related in an approximate fashion to the difference of the ionization potential (IP) and the electron affinity (EA) of X, which define the location of the X^+X^- dissociation limit above the X·X limit of the σ^2 and $^3\sigma$–σ^* configurations. As the nature of X is changed, even if the ground-state bond strength remains constant, the $^1\sigma$–σ^* excitation energy will change. In the first approximation, the change will be dictated by the difference IP_X – EA_X for the participating orbitals localized on the two atoms. This is equal to 210 kcal/mol for a silicon sp^3 orbital and 303 kcal/mol for a carbon sp^3 orbital.[223] We conclude that the lower singlet excitation energy of the Si–Si bond can be understood as primarily due to the lower ionization potential (and higher electron affinity) of silicon.

The process of chain scission by photochemical reductive elimination (iii) has only been detected relatively recently. According to recent CASSCF-CI ab initio calculations,[139,163] it is analogous to the extrusion process (i), with an alkyl carbon now playing the role of one of the silicons involved in the process. The photochemical pathways will surely require additional future attention by theoreticians, as will numerous others, such as intersystem crossing. The theoretical understanding of the photochemical degradation of polysilanes is still quite primitive.

X. Applications of Polysilane Derivatives

The emergence of soluble, castable polysilane homo- and copolymers has spurred the search for new applications. This research has resulted in the identification of a number of areas in which polysilane derivatives may play a useful role. A number of the more promising potential applications are discussed in the following sections.
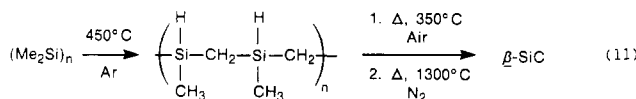
A. Thermal Precursors to Silicon Carbide

Silicon carbide is a useful ceramic material made commercially by the high-temperature solid-state re-

action between silicon dioxide and graphite. Material prepared in this manner is infusible, intractable, and not applicable for the preparation of fibers or films.

The use of a preformed polysilane, in particular poly(dimethylsilane), for the generation of β-silicon carbide fibers was first described by Yajima and co-workers.[20-27] The Yajima process entails essentially a two-step thermal conversion which is shown in eq 11.

$$(Me_2Si)_n \xrightarrow[\text{Ar}]{450°C} \left(\begin{array}{cc} \overset{H}{\underset{|}{Si}}-CH_2-\overset{H}{\underset{|}{Si}}-CH_2 \\ CH_3 \quad\quad CH_3 \end{array} \right)_n \xrightarrow[\substack{2.\ \Delta,\ 1300°C \\ N_2}]{\substack{1.\ \Delta,\ 350°C \\ Air}} \beta\text{-SiC} \quad (11)$$

The low-temperature pyrolysis converts the intractable poly(dimethylsilane) into a soluble carbosilane which can be processed into forms, films, or fibers. The mechanism of this transformation is obviously quite complex and is poorly understood. Potential intermediates in this transformation are silyl radicals, carbon radicals, silylenes generated by thermal 1,1-eliminations, etc. It was originally assumed that the transformation proceeds in a manner similar to that first suggested by Kumada[224] for the rearrangement of certain disilane precursors, i.e., thermal generation of α-carbon radicals followed by insertion into an adjacent Si–Si bond and subsequent hydrogen abstraction by the incipient silyl radical, but the mechanism remains largely unsubstantiated. An attractive mechanistic alternative would be 1,1-elimination followed by CH insertion of the silylene. Unfortunately, the structure of the polycarbosilane thus obtained is more complex than shown. In addition to the presence of some oxygen in the carbosilane polymer produced by oxidation, it has also been suggested that there may be some cross-linking[24,26] and perhaps even some cyclic structures[225] present in the polymer. The soluble carbosilanes thus produced are fractionated by solvent precipitation and can be melt spun into fibers. These fibers are then surface oxidized at temperatures between 350 and 400 °C to provide dimensional stability for further processing and fired to 1300 °C in an inert atmosphere to ultimately produce β-silicon carbide. The pyrolysis of the carbosilanes is also a very complex process and involves at least three stages: (i) condensation of the polymer chains, (ii) elimination of small fragments such as hydrogen and methane from the side chains, and (iii) the elimination of oxygen as oxides of carbon and the crystallization of β-silicon carbide. High-strength silicon carbide fibers are now manufactured commercially by this procedure and are sold under the trade name Nicalon.

The separate steps necessary to produce first carbosilanes and then to oxidize to provide dimensional stability can be circumvented by the use of processable polysilane derivatives other than poly(dimethylsilane).[29,30,226] West and co-workers have described the use of poly(methylphenylsilane) and poly(methylphenylsilane-co-dimethylsilane) ("polysilastyrene") in melt form to impregnate silicon nitride ceramic structures prior to firing.[227] The silicon carbide whiskers thus produced greatly strengthen the ceramic materials. Silicon carbide powder can be slurried with polysilane melts, injection molded, and fired to improve the machinability of silicon carbide.[228] In a similar fashion, poly(methylphenylsilane) and polysilastyrene can also be melt extruded into fibers and fired to yield silicon

carbide.[229] In this process a photochemical cross-linking step is employed to provide dimensional stability prior to the high-temperature conversion. In mechanistic studies[230] on the conversion of linear polysilastyrene to silicon carbide it was reported that initial polymer decomposition to lower molecular weight silicon hydrides is followed by recombination at high temperatures. In the case of materials that had been either partially or completely cross-linked prior to pyrolysis, complete depolymerization does not occur. In this regard, it was noted by thermogravimetric analysis that while linear polysilastyrene lost $\sim$75% of its weight at 500 °C, the weight loss of photo-cross-linked materials was only $\sim$37%.

The considerable research in the area of pyrolytic transformations of polysilane derivatives to silicon carbide has demonstrated that while the process may be complex and mechanistically poorly understood, it has unquestionable practical utility.

B. Photoinitiation of Vinyl Polymerizations

The photochemical decomposition of polysilanes in solution produces both substituted silylenes and silyl radicals. The intermediacy of the latter suggested the possible utility of substituted silane polymers as broad-spectrum photoinitiators for vinyl-type polymerization reactions. Depending on the nature of the substituents, polysilane derivatives have been prepared that absorb strongly over the entire spectral region from 200 to 400 nm.

West and co-workers[231,232] have demonstrated that a variety of vinyl monomers can be polymerized when certain polysilanes are incorporated as photoinitiators. The photopolymerization of acrylic acid and the lack of reactivity of ethyl vinyl ether were taken as suggestive of silyl radical initiation. The former is resistant to anionic type initiation while the latter is efficiently polymerized by cationic initiators. Although this particular experiment does not address the possibility of initiation by silylene intermediates that are undoubtedly produced concurrently, at least for short-wavelength initiation, the polydispersities observed for poly(ethyl acrylate) and polystyrene thus produced mimic those produced with known free radical initiators. The polymer molecular weights vary with the sensitizer employed in a manner that depends on the absorption characteristics of the initiator and the irradiation wavelength. For poly(methylphenylsilane), the initiation efficiency f (fraction of polymer chains produced per photon absorbed) is low ($\sim$1 × 10^{-3}) relative to that observed for a standard photochemical free radical initiator such as α,α-dimethoxydehydrobenzoin ($f \sim 0.275$). In this regard, typical free radical initiation efficiencies for vinyl polymerization range from 1.0 for di-$tert$-butyl peroxide to 10^{-4} for acetone. The low efficiency observed for poly(methylphenylsilane) has been rationalized in terms of competitive disproportionation reactions between the photogenerated silyl radicals and the steric hindrance intrinsic to the initiation reaction. The efficiency problem is ameliorated, to some extent, by the very large extinction coefficients and wide effective spectral range of the polysilanes. In addition, photopolymerizations initiated by polysilane derivatives are uncharacteristically insensitive to oxygen. The

sensitivity can be further reduced by the addition of antioxidants such as tertiary amines or phosphines. The in situ production of potential silicon-containing oxygen scavengers such as silylenes or silenes which could be generated from the initial silyl radical pair by disproportionation is proposed to explain the low oxygen sensitivity of the photopolymerization.

The wide spectral sensitivity, intense UV absorption, and insensitivity to oxygen quenching suggest that polysilanes may find utility in photoinitiated radical polymerization reactions, particularly for thin-film applications.

C. Electrical Conduction, Photoconduction, and Charge Transport

The unusual absorption spectra of the polysilanes suggest potentially interesting conducting and photoconducting characteristics. The band gap in many common silane polymers approaches 4 eV in contrast to a typical band gap of almost 8 eV for a saturated carbon skeleton. Although the polysilanes are insulators in the pure state, West and co-workers[31] have demonstrated that the copolymer polysilastyrene can be doped to a semiconducting level with arsenic pentafluoride. The preparation of other electrically conductive polysilanes by doping has been reported by Naarman et al.[233] Conducting films have recently been prepared from a variety of polysilanes by heating to high temperatures in sulfuric acid.[234] Also, Du et al. have described conductivity studies on a series of ferrocene-containing polysilanes both in the doped and undoped states.[235] A number of other workers have studied the photoconducting[236,237] and charge-transporting[238-241] characteristics of a variety of polysilane derivatives. Theoretical studies suggest that localized intergap states which are spontaneously generated by bond-order polaron formation are available for addition or excitation of electrons or holes.[242]

Workers at Sandia National Laboratories[236] and Nippon Telegraph and Telephone[237] have studied a variety of polysilane derivatives and found them to be excellent photoconductors. In each study, only holes were found mobile and nondispersive transport was observed with measured mobilities of around 10^{-4} $cm^2/(V s)$ at room temperature. Similarly, workers at Xerox have also reported hole generation in a variety of polysilanes by charge injection from amorphous Se and have observed nondispersive transport with comparable mobilities as measured by classical time-of-flight (TOF) techniques.[238-240] The insensitivity of the hole mobilities measured at room temperature to the nature of the polymer substituents led to the conclusion that hole transport occurs via the σ electronic states of the silicon backbone rather than by hopping between side-chain substituents. The measured hole mobilities depend on the applied electric field and are sensitive to temperature. The drift mobility is thermally activated, and activation energies of 0.25–0.28 eV have been measured for poly(methylphenylsilane). Similar activation energies for hole transport in poly(methylphenylsilane) have also recently been measured by thermally stimulated current techniques (TSC).[241] The measured activation energies are among the lowest values reported for amorphous solids and the drift mobilities are quite high, approximately 4 orders of
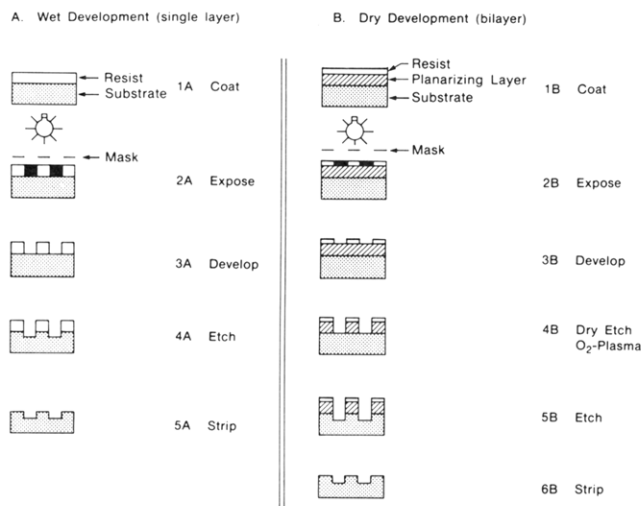
magnitude higher than reported for poly(N-vinylcarbazole).[238] In photoconductivity studies on poly(methylphenylsilane) Kepler et al.[236] have estimated that the hole generation quantum efficiency approaches 1% at high electric fields and that the carrier lifetimes are in excess of several milliseconds. Carrier lifetimes are affected by impurities and decrease substantially in the presence of certain electron-donor dopants. Kepler has proposed that the holes are generated photochemically when singlet excitons generated in the sample by light absorption diffuse to the surface of the polysilane sample and has estimated an exciton diffusion length of approximately 500 Å.

In summary, preliminary studies have indicated that the polysilane derivatives represent an interesting new class of photoconducting and charge-transporting materials. In addition, the favorable discharge characteristics of the materials coupled with the high hole mobilities suggest possible xerographic applications.

D. Polysilanes for Microlithography

Polysilane derivatives have a number of unique characteristics that make them suitable for many potential lithographic applications.[243] The polymers are soluble in common organic casting solvents and can be coated as high optical quality films. They are thermally and oxidatively stable, yet are photochemically labile over a broad spectral range. While the intense optical absorptions permit efficient harvesting of incident radiation, polymer degradation results in significant spectral bleaching, allowing uniform irradiation throughout the entire sample. Finally, these materials, by virtue of their high silicon content, are quite resistant to oxygen etching in plasma environments. The O_2 etch resistance of these polymers has been ascribed to the rapid formation of a thin layer of SiO_x at the polymer surface, which retards subsequent material removal.[244] This last characteristic is particularly important for multilayer resist schemes that employ oxygen reactive ion etching (O_2-RIE) for the transfer of the mask image into a thick planarizing polymer layer.[245] Multilayer techniques have been proposed for the future production of high aspect ratio (feature height/width), high-resolution images over chip topography.[246]

To provide some basic lithographic background, Figure 30 shows a comparison between a classical single-layer positive-resist process and one employing a multilayer scheme. In the single-layer process, a layer of the resist (1–2 μm) is coated over the substrate and imaged through a lithographic mask. The use of a single thick layer, particularly over chip topography, often results in inhomogeneous irradiation of the sample due to the presence of optical standing waves, reflections from feature topography, varying optical paths, etc. For a detailed discussion of the potential problems caused by chip topography, see ref 246. Subsequent wet development of the optical images causes loss of line width control due to the intrinsically isotropic nature of the wet development process exacerbated by inhomogeneous exposure of the film and diffraction distortion of the small mask features. In the multilayer process, the chip topography is covered with a thick (1–3 μm), planarizing polymer layer that is not photosensitive. This layer is then overcoated with a thin, photosensitive imaging layer. Because the imaging layer

A. Wet Development (single layer)   B. Dry Development (bilayer)

Resist / Substrate — 1A Coat

Mask — 2A Expose

3A Develop

4A Etch

5A Strip

Resist / Planarizing Layer / Substrate — 1B Coat

Mask — 2B Expose

3B Develop

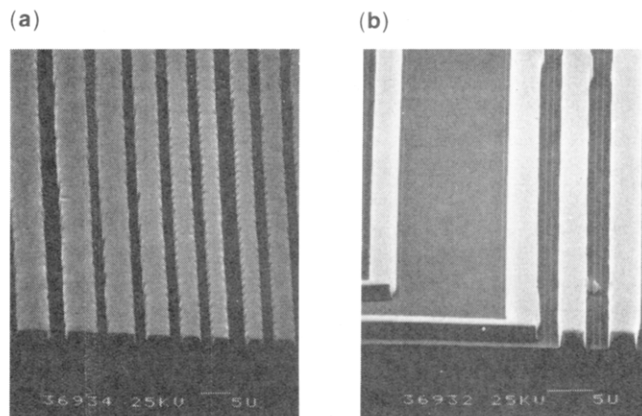4B Dry Etch O₂-Plasma

5B Etch

6B Strip

Figure 30. Schematic representation for the lithographic processing of positive resists: (a) single layer, wet development; (b) bilayer processing.

(a)   (b)

Figure 31. Al–Cu lines deposited using a trilayer configuration with poly(methylphenylsilane) as an O_2-RIE barrier layer: (a) imaging layer patterned by e-beam exposure; (b) imaging layer patterned with a step-and-repeat exposure source (436 nm).

is quite thin (0.1–0.5 μm), high-resolution images can be printed and developed to the planarizing polymer either by ablative imaging (vide infra) or by classical wet development. The images are then transferred through the thick planarizing layer using O_2-RIE etching techniques. Depending on the choice of plasma conditions, this etching process can be highly anisotropic, leading to features with near-vertical wall profiles.[247] The aggressive plasma conditions require imaging materials that are much more resistant to the O_2-etching conditions than the planarizing polymer layer. Three-layer variants of this procedure where the planarizing polymer layer is coated first with a thin inorganic oxygen-etch-resistant barrier of silicon nitride, silicon oxide, spin-on-glass, etc. and finally with a thin photosensitive imaging layer have been employed, but this technique adds considerable complexity to the process.[248] In the trilevel configuration, the photogenerated image must be transferred after development through the barrier layer using a fluorocarbon plasma prior to the final O_2-RIE processing.

The substituted silane polymers, which are strongly absorbing, imageable in a positive mode (i.e., irradiated areas become more soluble), and resistant to O_2-RIE conditions, are ideally suited to many multilayer-type lithographic applications. For these reasons they have been intensively investigated for lithographic purposes. To date, the polysilanes have been exercised as (i) soluble O_2-etch barrier alternatives in trilevel schemes, (ii) combination imaging and O_2-RIE barrier layers in bilayer configurations utilizing both wet and dry development techniques, (iii) short-wavelength contrast-enhancing layers, and (iv) new resist materials for ionizing radiation. These applications will be discussed in more detail in the following sections.

1. Soluble O₂-Etch-Resistant Barriers for Trilevel Lithographic Schemes

As mentioned, a number of silicon-containing inorganic ceramic materials have been employed as etch barriers in trilayer lithographic processes. In this regard, thin layers of refractory materials such as silicon dioxide or silicon nitride have been employed with some success.[248] These compounds, however, require vacuum techniques such as sputtering or chemical vapor deposition (CVD) for application. This is inconvenient and time-consuming. In addition, problems such as poor adhesion and layer cracking are often observed. The inconvenience created by the need for vacuum or vapor-phase deposition techniques can be circumvented by using soluble, spin-on-glass (SOG) formulations, but poor adhesion and cracking remain as problems.

In principle, soluble polysilane derivatives that form adhesive, noncracking coatings upon spinning could be substituted for the inorganic materials. For this application, however, high glass transition temperature materials are required to prevent feature deformation during plasma processing and subsequent metal deposition. While this material requirement is a problem for many soluble polysilane derivatives, Hiraoka et al.[249] have successfully demonstrated the utility of poly(methylphenylsilane) and other aromatic polysilane derivatives in trilevel lithographic processes involving subsequent metal deposition (see Figure 31).

2. Imageable O₂-Etch-Resist Layers for Bilayer Lithography

Polysilane derivatives have also been successfully utilized as a combination imaging and oxygen-etch-resistant barrier layer in a number of bilayer lithographic processes. For these applications, the initial photoimages have been developed either by classical wet development techniques or by "all-dry" processes involving photoablative imaging.[250] In the latter, the photoimages are first generated by exposure to high-intensity laser radiation that leads to ablative image self-development and are subsequently transferred through the planarizing polymer layer by O_2-RIE. This process, which requires no solvent development, is referred to as an "all-dry" process. For those processes employing an initial wet development step, high-resolution images have been produced by using either near-UV (350–400 nm)[47] or mid-UV (300–340 nm)[46–48,73,251,252] exposure by varying the spectral characteristics of the polysilane absorber. An example of vertical features produced in a standard bilayer configuration by mid-UV exposure is shown in Figure 32.

In principle, there is no reason why the polysilane derivatives could not be utilized in a bilayer configu-
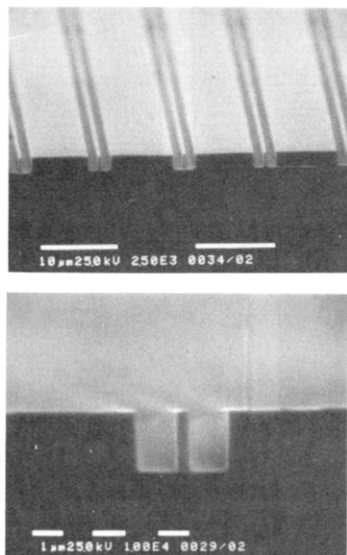
Figure 32. Submicron features generated in a bilayer of 0.2 μm of poly(cyclohexylmethylsilane) coated over 2.0 μm of a hard-baked AZ-type photoresist using mid-UV projection lithography; 100 mJ/cm^2; image transfer was accomplished by O$_2$-RIE.
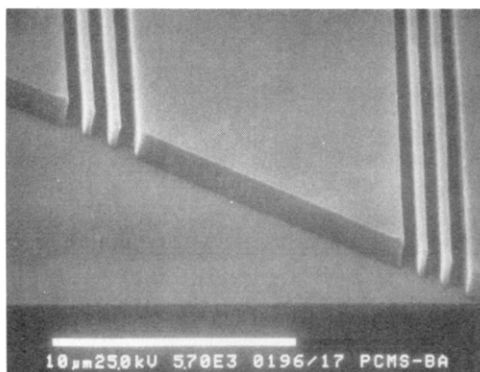
Figure 33. Images generated in a bilayer of 0.17 μm of poly-(cyclohexylmethylsilane) coated over 1.0 μm of a hard-baked AZ-type photoresist: upper left, 0.45 μm; lower right, 0.5 μm. Deep-UV excimer laser exposure (248 nm), 150 mJ/cm^2; image transfer was accomplished by O$_2$-RIE.

ration for deep-UV exposure (220–280 nm), thus realizing the improved resolution intrinsic to shorter wavelength exposure sources.[253] Although the spectral bleaching of polysilanes in the deep-UV is less efficient for normal lithographic doses (50–150 mJ/cm^2), the reduced absorption of the dialkyl polysilanes in the deep-UV relative to the mid-UV would ensure homogeneous irradiation of thin films (150–350 nm), even in the absence of significant spectral bleaching. Initial attempts at deep-UV lithography using polysilane derivatives were disappointing. In this regard, Taylor et al.[196] have described the production of images in thin films employing certain polysilane copolymers upon deep-UV excimer laser exposure (248 nm) but report poor submicron image qualities and excessive dose requirements. Recently, however, Miller et al.[254,255] have demonstrated that clean submicron images can be generated in a bilayer configuration utilizing selected polysilane homopolymers and a 248-nm excimer laser exposure source (100–150 mJ/cm^2). Images smaller than 0.5 μm produced in poly(cyclohexylmethylsilane) and subsequently transferred by O$_2$-RIE are shown in Figure 33. The latter experiments clearly demonstrate that while all substituted silane polymers and co-
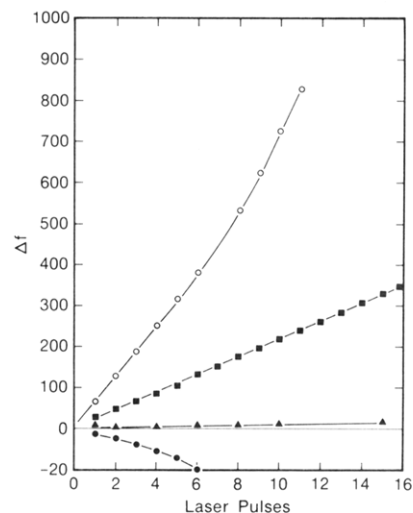
Figure 34. Laser photoablation of poly[(p-tert-butylphenyl)-methylsilane] (248 nm); dependence on incident laser fluence and total energy dose: (●) 34 mJ/cm^2 pulse; (▲) 44 mJ/cm^2 pulse; (■) 54 mJ/cm^2 pulse; (○) 95 mJ/cm^2 pulse. Δf is the difference in the quartz crystal oscillator frequency (in hertz) between irradiated and unirradiated sample. Experiment was performed at 1 atm in air.

polymers may not be suitable for deep-UV lithography, certain derivatives meet the current design requirements.

Hofer et al.[256] first showed in 1984 that polysilane derivatives were self-developed by intense UV exposure from an excimer laser source (308 nm). Subsequently, it was demonstrated that high-resolution images could be produced by such a technique both in a bilayer configuration[244] and also in single layers.[50] Early studies of the ablative imaging process itself originally utilized mechanical profilometers for film thickness measurements.[50] More recently, in situ, real-time thickness monitoring techniques such as a quartz crystal micro-balance (QCB)[244,257] or laser interferometry[258] have been employed. Miller et al. have studied the ablation of poly[(p-tert-butylphenyl)methylsilane] and poly(di-n-pentylsilane) at 248 and 308 nm, respectively, using QCB techniques.[40,46,47,243,244,257] Single-pulse threshold fluences of 40–50 mJ/cm^2-pulse for ablation were measured, above which the material loss per pulse was roughly linear with fluence (see Figure 34). Below the threshold fluence, the polymer ablation rate is negligible even though photobleaching occurs, and slight weight increases were actually recorded for single-pulse measurements. Above the threshold fluence, the ablation rate also depends on the pressure. For poly[(p-tert-butylphenyl)methylsilane] exposed to a single-pulse fluence of 76 mJ/cm^2-pulse, the rate of weight loss is approximately 4–6 times greater in a vacuum (10^{-6} Torr) than at atmospheric pressure. Studies of the ablation process at various wavelengths suggested that the energy deposited per unit volume is an important determinant.

Zeigler and co-workers have also studied the self-development of a number of polysilane derivatives at 248 nm.[50] These authors report a rough correlation between the rate of material loss and the steric size of the substituents. They also suggest that the removal of material at low fluences (<50 mJ/cm^2-pulse) is best described as predominantly photochemical rather than photothermal (photoablative), based on a microscopic

examination of the images. However, more recent studies on three substituted silane copolymers at fluences between 4 and 40 mJ/cm²-pulse (248 nm) suggest that both thermal and photochemical processes are involved.[196] For single-pulse fluences below the ablation threshold, extreme doses (>1 J/cm²) were necessary for film volatilization, and the formation of troublesome silicon-containing residues is often observed.[58b,73,196] A recent detailed study on the ablation of poly(methyl-n-propylsilane-co-isopropylmethylsilane)[258] at both 248 and 193 nm and high fluences (60–200 mJ/cm²-pulse) suggests that high peak power values are necessary to cleanly remove material and that the presence of oxygen is detrimental to this process. At 248 nm and fluences ranging from 60 to 200 mJ/cm²-pulse energy utilization efficiencies of 8–20 J/cm³ were measured. These values were similar to those reported for other common carbon-based polymers.

The composition of the volatilized products produced from a variety of polysilane derivatives has been studied by mass spectroscopy. Zeigler and co-workers have studied the volatiles ejected from poly(cyclohexyl-methylsilane-co-dimethylsilane)[50] upon exposure to low-intensity 254-nm radiation and have concluded that the bulk of the fragments were single monomeric silylene units with small amounts of chain fragments up to pentamers when the irradiation was conducted in vacuo. In the presence of oxygen, a variety of oxygenated materials were produced that were structurally assigned as cyclic siloxanes whose formation was ascribed to the reaction of oxygen with monomeric silylenes produced during the irradiation. Other workers have reported the formation of lower molecular weight siloxane polymers when polysilane films were irradiated in air.[193]

Magnera et al.[259,260] have studied in detail the photoablation of a variety of polysilane derivatives, including some that had been specifically labeled with ¹³C or deuterium, at 308 nm using a XeCl excimer laser. The gaseous products were analyzed with a triple-quadrupole mass spectrometer. Ion formation was by electron impact and also by multiphoton ionization. While most of the experiments were conducted at fluences between 150 and 200 mJ/cm²-pulse, which is well above the single-pulse ablation threshold, some low-fluence experiments were also described.

On the basis of these studies the authors have drawn a number of conclusions. First, under these experimental conditions, there seemed to be little if any compelling evidence that monomeric silylene fragments constitute the bulk of the ejected volatiles. Examination of the mass spectra of the volatile materials showed little contribution from monomeric silylene fragments and higher mass silicon-containing fragments were always observed. Furthermore, attempts to specifically detect the intermediate dimethylsilylene by multiphoton ionization studies (340–520 nm) on the volatiles produced from poly(dimethylsilane) were unsuccessful with no definitive enhancement of a monomeric dimethylsilylene fragment at m/e 58, and higher molecular weight silicon-containing fragments were always observed. Also, cryotrapping of the un-ionized neutrals produced from poly(dimethylsilane) yielded no spectral evidence (UV absorption) for the generation of dimethylsilylene. On the basis of these studies, it was

concluded that the organosilanes are volatilized in a range of sizes containing from one to at least five monomer units upon laser exposure.

Second, studies on the isotopically labeled polymers suggested that considerable scrambling occurs in the fragments, with silicon atoms becoming attached to carbons other than the original α side chain atoms and hydrogens appearing on silicon from sites more distant than the α or β side chain positions.

Third, studies of the silicon-free ions from those polymers containing n-propyl or longer side chain suggested that terminal alkene derivatives were produced in the ablation. This was confirmed by trapping experiments without ionization, and labeling studies showed that hydrogen is transferred specifically from the β side chain carbon to the silicon in the formation of the terminal olefin. Although the ratio of silicon-free to silicon-containing ions decreases with decreasing fluence, the former are still present even below the single-pulse ablation threshold. The failure to detect any n-alkanes concurrently strongly suggests that n-alkyl radicals generated by silicon–carbon bond homolysis are not the source of the olefin products. The authors tentatively suggest instead that the olefins may arise from chain silylsilylenes by β-hydrogen transfer. Such β-hydrogen-transfer reactions have literature precedent in thermal reactions[216] and are thermodynamically feasible ($E_a \sim 30$ kcal/mol), and the silyl-silylene intermediates would be consistent with the observed patterns for isotopic scrambling where CH insertion occurs in competition with fragmentation. They also speculate on two possible routes to the chain-fragmented silylsilylenes: (i) direct 1,1-reductive elimination, proceeding by alkyl transfer, a thermal reaction with considerable literature precedent,[217] and (ii) silicon-silicon chain homolysis followed by radical disproportionation[202–204] and rearrangement of the resulting silylsilene to a chain silylsilylene intermediate.[218] Both proposed routes are thermodynamically feasible and are supported by literature precedent. The suggestion in this paper of a significant thermal component in the photoablation of polysilane derivatives at 308 nm and normal fluences was also supported by the virtual identity of the UV laser desorption and the IR laser pyrolysis (CW CO₂ laser) mass spectra for a typical dialkyl polysilane, poly(di-n-pentylsilane). Furthermore, the observation of significant side-chain loss at higher laser fluences may have important consequences for practical uses. Since the hydrocarbon fragments are volatile, efficient laser ablation need not necessarily be restricted to those polymers with low-mass substituents.

3. Contrast Enhancement Lithography Using Polysilanes

When the wavelength of light incident on a lithographic mask in a projection printing tool is comparable to the mask feature dimensions, the image becomes somewhat distorted due to diffraction effects. This blurred mask image incident on a wafer coated with photoresist often results in severe pattern degradation upon development. Contrast enhancement lithography is a clever technique that utilizes a thin layer of contrast-enhancing material coated on top of a photoresist to sharpen the diffraction-distorted mask image and improve resist resolution (see Figure 35). A detailed
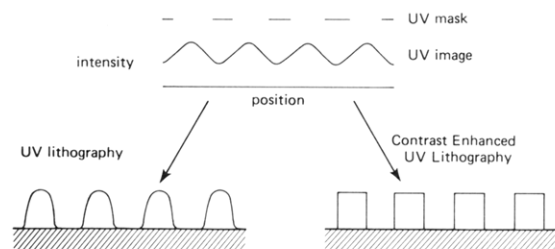
Figure 35. Schematic representation of image improvement by contrast enhancement.

(a) conventional

(b) CEL
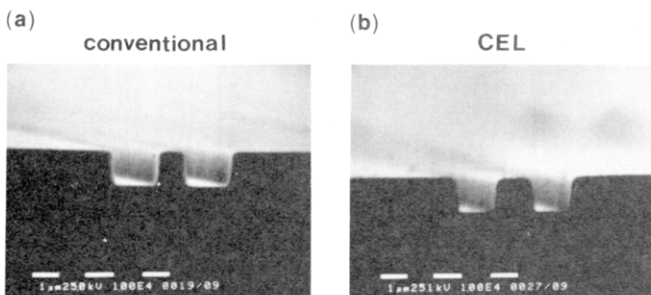
Figure 36. Bilayer of 0.2 μm of poly(cyclohexylmethylsilane) as a contrast-enhancing layer over 1.5 μm of an AZ-type photoresist (AZ-2400). Incident dose, 100 mJ/cm²; mid-UV projection lithography; 1.25 μm line/space array.

description of exactly how this image enhancement occurs is beyond the scope of this review and the interested reader is referred to the original literature.[264,265] However, an effective contrast-enhancing material must possess a number of important characteristics. It should be thermally stable, incompatible with the underlying photoresist, very strongly absorbing at the irradiation wavelength yet readily bleached upon exposure, and ideally removable from the photoresist prior to image development. A number of polysilane derivatives have been discovered that possess these characteristics. In addition, they are also bleached by short-wavelength radiation, which allows the utilization of shorter wavelength exposure sources with their intrinsically higher resolution capabilities. The potential of polysilane derivatives for use as short-wavelength contrast-enhancing materials has been demonstrated in practice by the group at IBM.[244,251,266] Figure 36 shows improved resist images produced by the utilization of poly(cyclohexylmethylsilane) as a contrast-enhancing layer for the mid-UV exposure of a classical diazonaphthoquinone–Novolac photoresist. Similarly, Rosilio and co-workers[58b,73] have recently confirmed the utility of certain polysilane derivatives as contrast-enhancing materials for use with mid-UV exposure.

In principle, since many polysilane derivatives also bleach upon deep-UV exposure, these materials could also be considered as candidates for use as deep-UV contrast-enhancing materials. In practice, however, the alkyl-substituted polysilanes absorb too weakly in the deep-UV to be utilized in thin-film form and the rate of spectral bleaching is considered to be too slow to avoid the unacceptable exposure "dose hit". However, the strong dependence of the absorption characteristics of polysilane oligomers on the extent of catenation coupled with their photolability suggests that substituted silane oligomers or perhaps polymers where short polysilane blocks are interrupted by nonconjugating sequences (block interrupt polysilanes)[267] might find
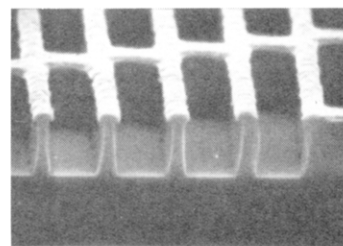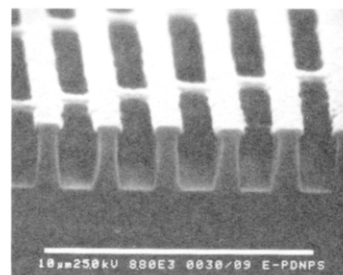
Figure 37. Submicron features generated by e-beam imaging of 0.14 μm of poly(di-n-pentylsilane) over 2.0 μm of a hard-baked AZ-type photoresist; 20 μC; O₂-RIE image transfer.

TABLE 16. Radiation G Values for the ^{60}Co γ Irradiation of a Number of Polysilane Derivatives in Vacuo

polymer	$\bar{M}_n^0 \times 10^{-3}$	G(s)	G(x)	G(s)/G(x)
$[(C_4H_9)_2Si]_n$	304.9	0.42	0.023	18
$[(C_5H_{11})_2Si]_n$	807.6	0.40		
$[(C_6H_{13})_2Si]_n$	971.9	0.42	0.041	10.5
$[(C_{14}H_{29})_2Si]_n$	1472.9	0.86	0.035	24.6
$(PhMeSi)_n$	738.2	0.26	0.014	18.6
$(p\text{-}t\text{-}BuC_6H_4MeSi)_n$	153.9	0.14	0.004	35
$(C_6H_5CH_2CH_2MeSi)_n$	167.3	0.90	0.03	30
PMMA	428.7	1.40		

utility as deep-UV contrast-enhancing materials.

XI. Radiation Chemistry of Polysilanes

Although it has been demonstrated that oxygen can play a significant role in the photodegradation of polysilanes, chain scission and subsequent polymer degradation also occur in vacuo. This has led several groups to investigate the potential of polysilane derivatives for e-beam lithography. The group at IBM has reported the generation of high-resolution images in a bilayer configuration at exposure doses of 10–20 μC/cm² as shown in Figure 37.[48] Similarly, Taylor and co-workers[196] have investigated the e-beam imaging characteristics of three polysilane copolymers but have concluded that they are low-contrast materials. They further speculate that the low contrasts observed upon e-beam exposure may be a result of an enhanced cross-linking component which is exacerbated by the high-vacuum conditions.

In the solid state, in vacuo G values for scission and cross-linking (number of chain breaks or cross-links/100 eV of absorbed dose) have been determined for a variety of polysilane homopolymers subjected to γ-ray exposure. These data are shown in Table 16 in comparison with that for poly(methyl methacrylate) (PMMA), a material whose radiation sensitivity has been extensively studied.[268] The polymers studied undergo predominantly chain scission even in vacuo, and in each case the ratio G(s)/G(x) was >10. Although the measured values for G(s) are not exceptionally large, they do vary with the nature of the substituent. Aromatic

substituents directly attached to the backbone cause significant decreases in the $G(s)$ values as has been observed previously for polystyrene derivatives. The radiation protection afforded by aromatic substituents is, however, apparently restricted to direct backbone substitution, since poly(methyl-β-phenethylsilane) was among the most sensitive of the polysilanes investigated. These studies are quite preliminary and further work is necessary to understand the radiation chemistry of the polysilanes and to access their potential as resists for ionizing radiation.

Pulsed radiolysis techniques have recently been utilized to study the nature of the reactive intermediates produced from polysilane derivatives in solution.[87,269,270] In THF, poly(methyl-n-propylsilane) and poly(methylphenylsilane) produce transients absorbing at 363 and 372 nm, respectively, which have been ascribed to the respective polymeric radical anions. In the absence of another electron acceptor, the lifetimes of these intermediates exceed 150 ns. In the presence of pyrene, rapid electron transfer occurs from the polysilane radical ions to produce the radical ion of pyrene that is observed in absorption. The nature of the radical anion absorption spectra is consistent with considerable electron delocalization over the σ-bonded polymer backbone and depends somewhat on the pendant substituents, with significant red shifts occurring with the introduction of aromatic substituents directly on the silicon backbone.[269] In this regard, a red shift in the absorption maximum to 380–390 nm was observed for copolymers that incorporate the diphenylsilylene monomeric unit. These substituent spectral shifts are in accord with those observed in the absorption spectra of a variety of substituted polysilane homo- and copolymers.[35] Similarly, Irie et al.[270] recently identified the transient (λ_{max} = 365 nm) produced upon pulse radiolysis of polysilastyrene in 2-methyltetrahydrofuran at 77 K as the polymeric radical anion. The absorption maximum for this species is quite similar to that previously reported for the radical anion of poly(methylphenylsilane) in tetrahydrofuran.[87] These authors have also demonstrated that pulsed radiolysis techniques can be used to generate radical cations from substituted silane polymers[270] by using n-butyl chloride as a matrix material at 77 K. For the copolymer polysilastyrene, a transient with an intense UV absorption at 358 nm (half-life ~85 μs) was observed. This intermediate also had an additional band in the infrared region at 2000 nm. The infrared band, which blue shifts upon thermal annealing, was attributed to a charge resonance interaction between two phenyl groups in the radical cation on the basis of previous studies of the radical cation of polystyrene.

XII. Nonlinear Optical Properties of Polysilanes

Considerable interest has been focused recently on organic materials for nonlinear optical purposes due to their intrinsically large nonlinear susceptibilities and rapid response times.[271,272] Materials utilizing second-order nonlinear effects are limited by the need for noncentrosymmetric structures. However, applications utilizing third-order effects have no symmetry requirements, thus expanding the range of useful materials to polymeric systems that often provide ease of fabrication, display good mechanical toughness, and are

resistant to chemical and radiation damage. Several classes of organic polymers containing extensively delocalized π systems possess exceptionally large optical nonlinearities. However, many of these materials also have drawbacks such as limited processability, thermal and/or oxidative instability, nonideal spectral characteristics, etc.

The polysilane derivatives absorb strongly in the UV, the molecular polarizability is strongly anisotropic and conformationally dependent, and electronic substituent effects are transmitted over large distances. In addition, they are thermally and oxidatively stable, soluble in common casting solvents, and imageable to high resolution using standard lithographic techniques. The latter characteristic is particularly important for guided-wave applications. This combination of electronic and physical properties suggests that polysilanes comprise an interesting new class of polymeric materials for nonlinear optical (NLO) studies.

The first NLO measurement on a polysilane derivative was reported by Kajzar and co-workers.[273] They reported a resonant third-order nonlinear susceptibility ($\chi^{(3)}$) value for poly(methylphenylsilane) at 1.06 μm of 1.5×10^{-12} esu as measured by the Maker fringe technique. Some resonance enhancement of this signal was suggested by consideration of the polymer absorption spectrum and the observation that the third harmonic signal measured for the 1.907-μm fundamental was below the detection threshold. Somewhat larger $\chi^{(3)}$ values for poly(methylphenylsilane) of 7.2×10^{-12} and 4.2×10^{-12} esu measured at 1.06 and 1.907 μm, respectively, have been reported by Baumert et al.[274] The latter numbers were dependent on the film thickness and decreased as the sample thickness increased.
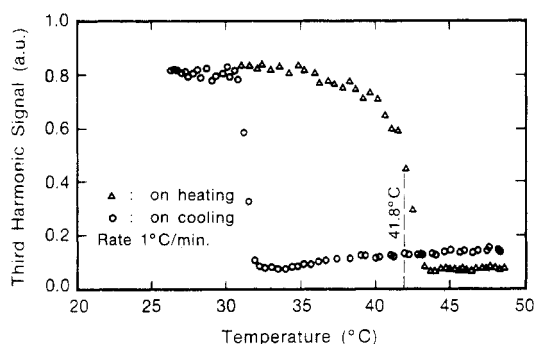
The same authors also studied the third-order susceptibility of poly(di-n-hexylsilane) as a function of temperature. At temperatures below the order–disorder transition (42 °C) where side-chain crystallization enforces an all-trans backbone, a value for $\chi^{(3)}$ of 1.1×10^{-11} esu was measured for the 1.06-μm fundamental. This value is the largest recorded for a polymer transparent in the visible spectral region. Table 17 shows a comparison of the $\chi^{(3)}$ values for poly(methylphenylsilane), poly(di-n-hexylsilane), and a number of π-conjugated polymers.

Above the transition temperature, the measured $\chi^{(3)}$ value for poly(di-n-hexylsilane) decreased by a factor of 2.5. This apparently results from changes in the λ_{max} of the longest wavelength absorption, which blue shifts from ~370 nm to around 317 nm at elevated temperatures. This thermal behavior is reversible and the intensity of the third harmonic signal thus faithfully reflects the phase change, although some hysteresis is observed due to the supercooling of the polymer sample prior to crystallization (see Figure 38). In all of the polysilanes examined, the values measured for $\chi^{(3)}$ varied inversely with thickness for spin-coated samples. It was suggested that this phenomenon may be due to partial polymer orientation induced by spin coating, a possibility supported by IR dichroic studies on films of varying thickness.[275] If true, this suggests that larger and orientationally dependent values for $\chi^{(3)}$ should be attainable for more highly oriented samples.

Two reports on the nonlinear photochemical decomposition of polysilane derivatives have appeared. In

TABLE 17. Third-Order Nonlinear Susceptibility Values ($\chi^{(3)}$) for Poly(di-n-hexylsilane) and Poly(methylphenylsilane) in Comparison with a Number of π-Conjugated Organic Polymers

polymer	fundamental	$\chi^{(3)}$, esu	technique
single crystal (R = CH$_2$OTs)	1.89 μm	9.85×10^{-10}	4-wave mixing
cast film (R = (CH$_2$)$_4$O$_2$CNHCH$_2$CO$_2$C$_4$H$_9$)	585 nm	4×10^{-10} (red)	4-wave mixing
	605 nm	2.5×10^{-11} (yellow)	
LB film	1.06 μm	3×10^{-11} (red)	Maker fringes
polymerized LB film (R^1 = (CH$_2$)$_{15}$CH$_3$, R^2 = (CH$_2$)$_8$CO$_2$Cd)	1.64 μm	~1.3×10^{-12} (red)	Maker fringes
		~1.3×10^{-12} (blue)	
film (biaxial)	585 nm	9×10^{-12}	4-wave mixing
	604 nm		
film (amorphous)	1.85 μm	7.8×10^{-12}	Maker fringes
[(C$_6$H$_{13}$)$_2$Si]$_n$	film (unoriented), 23 °C	1.1×10^{-11}	Maker fringes
[(C$_6$H$_{13}$)$_2$Ge]$_n$	film (unoriented), 23 °C	6.5×10^{-12}	Maker fringes
(PhSiMe)$_n$	film (amorphous), 23 °C	1.5×10^{-12}	Maker fringes

Note: the last three rows have fundamental wavelength 1.06 μm, 1.06 μm, 1.06 μm respectively.

Figure 38. Third harmonic signal versus temperature for a 120-nm-thick poly(di-n-hexylsilane) film at a constant angle of incidence and with a 1064-nm fundamental wavelength. The temperature offset between heating and cooling transitions is due to supercooling.

1985 Marinero[276] described the multiphoton decomposition of poly(cyclohexylmethylsilane) using either 532- or 620-nm light. For power levels in excess of 2.5 GW/cm^2, decreases in the polymer absorption maximum at 320 nm were noted, but no significant blue shift was observed. Film thickness measurements indicated that ablative volatilization was responsible for the changes in the optical density. Analysis of the film thickness loss as a function of incident intensity revealed an I^n dependence, where $n = 2.6$–3.3.

Schellenberg et al.[277] have also described the nonlinear photodecomposition of poly(di-n-hexylsilane) upon exposure to intense pulsed laser light at 532 or 560 nm. Both wavelengths caused significant bleaching of the absorption of the crystalline phase at 375 nm, but ablation was not observed. Instead, the progressive blue shifting of the absorption maximum suggested that significant chain scission and polymer molecular weight reduction were occurring. Plots of the changes in op-

tical density vs I^2 were linear, suggesting that the photodecomposition was a two-photon process. While linear bleaching using a 0.3-mW HeCd laser at 325 nm was independent of laser polarization, for the visible pulsed laser exposures bleaching was observed only in a direction parallel to the polarization of the laser light. The anisotropic change in absorption had an associated change in the refractive index, and this induced birefringence can be large enough ($\Delta n \sim 2.6 \times 10^{-2}$ at $\lambda = 632.8$ nm) to allow fabrication of channel waveguides by photoexposure. The factors contributing to the photoinduced birefringence and the role played by the polymer structure are unknown at this time.

Measurements of the third-order susceptibilities for a number of polysilanes by degenerate four wave mixing techniques have also been reported. McGraw and co-workers[278] have reported a $\chi^{(3)}$ value for 2.9×10^{-12} esu for an atactic, amorphous film of poly(methyloctyl-silane) and have resolved its nuclear (38%) and electronic (68%) contributions. This particular polymer has a very low glass transition temperature ($<$–50 °C). Yang et al.[279] have recently described the measurement and temporal behavior of $\chi^{(3)}$ for poly(methylphenyl-silane) both in solution and as films using picosecond Kerr gate and degenerate four wave mixing techniques. The picosecond response time of the third-order signal is consistent with an electronic effect and the $\chi^{(3)}$ value measured was comparable to previous measurements. A much slower component is attributed to a refractive index grating created from the radiation pressure.

In summary, although the study of the NLO properties of polysilane derivatives is in its infancy, the substantial nonlinearities, favorable spectral characteristics, and the capacity for high-resolution lithographic imaging suggest that future studies will be fruitful.

XIII. Concluding Remarks

From auspicious beginnings the field of organosilicon chemistry has grown into a major area of study with numerous industrial applications. Similarly, the tremendous expansion in the study of high molecular weight, soluble substituted silane polymers has evolved from initial reports of poorly characterized, intractable materials prepared in the 1920s. This growth in interest has not been linear with time, and it was really the discovery of the unusual electronic properties of soluble oligomeric silanes that fueled the current theoretical and experimental studies on the high polymers.

The unusual characteristics of the silane oligomers initially caused speculation regarding the stability and properties of high molecular weight linear polymers, but serious research efforts were inhibited by the belief that the intractability observed for early derivatives was intrinsic to the class. Finally, about 10 years ago, the synthesis of the first soluble high molecular weight polysilane derivatives in combination with the discovery of the first commercial application caused the explosive growth in this area that is still evident. Initial primitive theoretical studies have been supplemented by more sophisticated techniques, resulting in a better understanding of the nature of the electronic ground and excited states of polysilane derivatives. These studies, in concert with spectroscopic work, have led to the conclusion that in many regards the electronic properties of the polysilanes, in spite of the σ-bonded nature of the backbone, more closely resemble those of π-conjugated polymers than their saturated carbon backbone analogues. The electronic properties such as ionization potentials, polarizability, absorption and emission characteristics, etc. depend not only on the degree of polymerization but also on the conformation of the polymer backbone. This latter feature was originally unanticipated for a σ bond system and has been rationalized in terms of long-range, geometry-dependent orbital interactions.

The unusual electronic properties have spurred the synthesis and characterization of a large number of soluble homo- and copolymers. In spite of the synthetic activity, it is somewhat ironic that the original technique employed in the 1920s for the preparation of the first polysilane derivatives, i.e., Wurtz–Fittig type coupling, is still the principal procedure used today in spite of its obvious drawbacks and deficiencies. New synthetic procedures, particularly those offering some promise of stereocontrol and functional group tolerance, remain an important priority in this field.

The generally excellent thermal and mechanical properties of these materials, coupled with their unusual electronic characteristics and photolability, have led to many potentially interesting applications. The first of these to be exploited commercially was the use of polysilanes as thermal ceramic precursors. This was soon followed by applications that exploited the photolability of polysilane derivatives for the photoinitiation of vinyl polymerization and in many imaging applications. The curious electronic properties of the polysilanes have also attracted attention in areas such as photoconduction and charge conduction and, most recently, as new materials with interesting nonlinear optical characteristics. In this last area, it is anticipated that their capacity for high-resolution imaging coupled with the unusual optical properties is a unique combination with much utility.

In summary, it appears that high molecular weight soluble substituted silane polymers constitute a class of radiation-sensitive polymers that are both scientifically interesting and show considerable application potential. Although the class of materials is quite old, they have been recently rediscovered and modern techniques have been applied for characterization. As a result of these efforts, it seems likely that the future will bring new breakthroughs in understanding and utility.

References

(1) Gilman, H.; Atwell, W. H.; Schweke, G. L. *Chem. Ind. (London)* **1964**, 1063.
(2) Gilman, H.; Atwell, W. H.; Schweke, G. L. *J. Organomet. Chem.* **1964**, 2, 369.
(3) Pitt, C. G. In *Homoatomic Rings, Chains and Macromolecules of Main-Group Elements*; Rheingold, A. L., Ed.; Elsevier: New York, 1977; Chaper 8 and references cited therein.
(4) Hengge, E. *Top. Curr. Chem.* **1974**, 51.
(5) Hengge, E. *J. Organomet. Chem. Lib.* **1979**, 9, 261.
(6) West, R. In *Comprehensive Organometallic Chemistry*; Abel, E., Ed.; Pergamon Press: Oxford, England, 1982; Chapter 9.4, p 365.
(7) West, R. *Pure Appl. Chem.* **1982**, 54, 1041.
(8) Kumada, M.; Tamao, K. *Adv. Organomet. Chem.* **1968**, 6, 19.
(9) Raabe, G.; Michl, J. *Chem. Rev.* **1985**, 85, 419. In *Chemistry of Organic Silicon Compounds*; Patai, S., Rappoport, Z., Eds.; Wiley: New York, 1989; p 1015.
(10) Ishikawa, M.; Kumada, M. *Adv. Organomet. Chem.* **1986**, 19, 51.
(11) Ishikawa, M.; Kumada, M. *Rev. Silicon, Germanium, Tin, Lead Compd.* **1979**, 4, 7.
(12) Miller, R. D.; Sooriyakumaran, R. *J. Polym. Sci., Polym. Chem. Ed.* **1987**, 25, 111.
(13) Trefonas, P., III; West, R. *J. Polym. Sci., Polym. Chem. Ed.* **1985**, 23, 2099.
(14) Kipping, F. S. *J. Chem. Soc.* **1921**, 119, 830.
(15) Kipping, F. S. *J. Chem. Soc.* **1924**, 125, 2291.
(16) Burkhard, C. *J. Am. Chem. Soc.* **1949**, 71, 963.
(17) Burkhard, C. U.S. Patent 2,554,976, 1951.
(18) Clark, H. U.S. Patent 2,606,879, 1952.
(19) Clark, H. U.S. Patent 2,563,005, 1951.
(20) Hiyashi, J.; Omori, M.; Yajima, S. U.S. Patent 4,159,259, 1979.
(21) Yajima, S.; Hayashi, J.; Omori, M. *Chem. Lett.* **1975**, 931.
(22) Yajima, S.; Okamura, K.; Hayashi, J.; Omori, M. *J. Am. Ceram. Soc.* **1976**, 59, 324.
(23) Yajima, S. *Ceram. Bull.* **1983**, 62, 993.
(24) Yajima, S.; Hasegawa, Y.; Hayashi, J.; Iimura, M. *J. Mater. Sci.* **1978**, 13, 2569.
(25) Hasegawa, Y.; Iimura, M.; Yajima, S. *J. Mater. Sci.* **1980**, 15, 720.
(26) Hasegawa, Y.; Okamura, K. *J. Mater. Sci.* **1983**, 18, 3633.
(27) Hasegawa, Y.; Okamura, K. *J. Mater. Sci.* **1985**, 20, 321.
(28) Wesson, J. P.; Williams, T. C. *J. Polym. Sci., Polym. Chem. Ed.* **1979**, 17, 2833.

(29) Wesson, J. P.; Williams, T. C. *J. Polym. Sci., Polym. Chem. Ed.* **1980**, *18*, 959.

(30) Wesson, J. P.; Williams, T. C. *J. Polym. Sci., Polym. Chem. Ed.* **1981**, *19*, 65.

(31) West, R.; David, L. D.; Djurovich, P. I.; Stearley, K. L.; Srinivasan, K. S. V.; Yu, H. *J. Am. Chem. Soc.* **1981**, *103*, 7352.

(32) David, L.; West, R. U.S. Patent 4,324,901, 1982.

(33) West, R. U.S. Patent 4,260,780, 1981.

(34) Trujillo, R. E. *J. Organomet. Chem.* **1980**, *198*, C27.

(35) West, R. *J. Organomet. Chem.* **1986**, *300*, 327.

(36) Trefonas, P. T. In *Polysilanes and Polycarbosilanes*. In *Encyclopedia of Polymer Science and Engineering*; Wiley: New York, 1988; Vol. 13, p 162.

(37) West, R.; Maxka, J. In *Inorganic and Organometallic Polymers*; ACS Symposium Series 360; Zeldin, M., Wynne, K. J., Allcock, H. R., Eds.; American Chemical Society: Washington, DC, 1988; Chapter 2.

(38) David, L. *Chem. Br.* **1987**, *23*(6), 553.

(39) West, R. In *Chemistry of Organic Silicon Compounds*; Patai, S., Rappoport, Z., Eds.; Wiley: New York, 1989; p 1207.

(40) Miller, R. D. *Polym. News* **1988**, *12*, 326.

(41) Worsfold, D. J. In *Inorganic and Organometallic Polymers*; ACS Symposium Series 360; Zeldin, M., Wynne, K. J., Allcock, H. R., Eds.; American Chemical Society: Washington, DC, 1988; Chapter 9.

(42) Grough, L. F. Ph.D. Thesis, University of Wisconsin, 1980.

(43) Bianconi, P. A.; Weidman, T. D. *J. Am. Chem. Soc.* **1988**, *110*, 2342.

(44) Trefonas, P., III; Djurovich, P. I.; Zhang, X.-H.; West, R.; Miller, R. D.; Hofer, D. *J. Polym. Sci., Polym. Lett. Ed.* **1983**, *21*, 819.

(45) Hengge, E.; Reuter, H. *Naturwissenshaften* **1962**, *42*, 574.

(46) Miller, R. D.; Hofer, D.; McKean, D. R.; Willson, C. G.; West, R.; Trefonas, P. T., III. In *Materials for Microlithography*; ACS Symposium Series 266; Thompson, L. F., Willson, C. G., Frechet, J. M. J., Eds.; American Chemical Society: Washington, DC, 1984; Chapter 14.

(47) Miller, R. D.; Hofer, D.; Rabolt, J. F.; Sooriyakumaran, R.; Willson, C. G.; Fickes, G. N.; Guillet, J. E. In *Polymers for High Technology: Electronics and Photonics*; ACS Symposium Series 346; Bowden, M. J., Turner, S. R., Eds.; American Chemical Society: Washington, DC, 1987; Chapter 15.

(48) Miller, R. D.; Rabolt, J. F.; Sooriyakumaran, R.; Fleming, W.; Fickes, G. N.; Farmer, B. L.; Kuzmany, H. In *Inorganic and Organometallic Polymers*; ACS Symposium Series 360; American Chemical Society: Washington, DC, 1988; Chapter 4.

(49) Harrah, L. A.; Zeigler, J. M. *Macromolecules* **1987**, *20*, 601.

(50) Zeigler, J. M.; Harrah, L. A.; Johnson, A. W. *Proc. SPIE* **1985**, *539*, 166.

(51) Zeigler, J. M. *Polym. Prepr.* **1986**, *27*, 109.

(52) Miller, R. D.; Sooriyakumaran, R. *Macromolecules* **1988**, *21*, 3120.

(53) Miller, R. D.; Sooriyakumaran, R. *J. Polym. Sci., Polym. Lett. Ed.* **1987**, *25*, 321.

(54) Stüger, H.; West, R. *Macromolecules* **1985**, *18*, 2349.

(55) Horguchi, R.; Onishi, Y.; Hayase, S. *Macromolecules* **1988**, *21*, 304.

(56) Nagai, Y.; Matsumoto, H. Jpn. Tokkyo Koho JP 63 41,534 [88 41,531]; *Chem. Abstr.* **1988**, *109*, 191128z.

(57) Harrah, L. A.; Zeigler, J. *Macromolecules* **1987**, *20*, 2037.

(58) (a) Watanabe, H.; Akutsu, Y.; Shinohara, A.; Shinohara, S.; Yamaguchi, Y.; Ohta, A.; Onozuka, M.; Nagai, Y. *Chem. Lett.* **1988**, 1883. (b) Rosilio, C.; Rosilio, A.; Serre, B. *Microelectron. Eng.* **1988**, *8*, 55.

(59) Miller, R. D.; Fickes, G. N., unpublished results.

(60) West, R., private communication.

(61) Bovey, F. A.; Kwei, T. K. In *Macromolecules: An Introduction to Polymer Science*; Bovey, F. A., Winslow, F. H., Eds.; Academic Press: New York, 1979; Chapter 3.

(62) Schilling, F. C.; Bovey, F. A.; Zeigler, J. M. *Macromolecules* **1986**, *19*, 2309.

(63) Wolff, A. R.; Maxka, J.; West, R. *J. Polym. Sci., Polym. Chem. Ed.* **1988**, *26*, 713.

(64) Wolff, A. R.; Nozue, I.; Maxka, J.; West, R. *J. Polym. Sci., Polym. Chem. Ed.* **1988**, *26*, 701.

(65) Todesco, R. V.; Basheer, R. *J. Polym. Sci., Polym. Chem. Ed.* **1986**, *24*, 1943.

(66) Todesco, R. V.; Kamat, P. V. *Macromolecules* **1986**, *19*, 196.

(67) Zhang, X.-H.; West, R. *J. Polym. Sci., Polym. Chem. Ed.* **1984**, *22*, 159.

(68) Zhang, X.-H.; West, R. *J. Polym. Sci., Polym. Chem. Ed.* **1984**, *22*, 225.

(69) Zhang, X.-H.; West, R. *J. Polym. Sci., Polym. Lett. Ed.* **1985**, *23*, 479.

(70) Swan, S. P.; Tsai, Y.-G.; Huang, H.-Y. *Polym. Prepr.* **1987**, *28*, 260.

(71) Swan, S. P.; Tsai, Y.-G.; Huang, H.-Y. In *Inorganic and Organometallic Polymers*; ACS Symposium Series 360; Zeldin, M., Wynne, K. J., Allcock, H. R., Eds.; American Chemical Society: Washington, DC, 1988; Chapter 9.

(72) Pannell, K. H.; Rozell, J. M.; Zeigler, J. M. *Macromolecules* **1988**, *21*, 276.

(73) Rosilio, C.; Rosilio, A.; Serre, B. *Microelectron. Eng.* **1987**, *6*, 399.

(74) Reference deleted.

(75) Fujino, M.; Matsumoto, N.; Ban, H.; Sukegawa, K. *J. Polym. Sci., Polym. Lett. Ed.* **1988**, *26*, 109.

(76) Zeigler, J. M.; Harrah, L. A.; Johnson, A. W. *Polym. Prepr.* **1987**, *28*, 424.

(77) Gauthier, S.; Worsfold, D. J. *Abstr. XXI Organosilicon Symp.* **1988**, 35.

(78) Heitz, W. *Macromol. Chem. Macromol. Symp.* **1986**, *4*, 35.

(79) Aitken, C. T.; Harrod, J. F.; Samuel, E. *J. Organomet. Chem.* **1985**, *279*, C11.

(80) Aitken, C. T.; Harrod, J. F.; Samuel, E. *J. Am. Chem. Soc.* **1986**, *108*, 4059.

(81) Aitken, C. T.; Harrod, J. F.; Samuel, E. *Can. J. Chem.* **1986**, *64*, 1677.

(82) Harrod, J. F. In *Inorganic and Organometallic Polymers*; ACS Symposium Series 360; Zeldin, M., Wynne, K. J., Allcock, H. R., Eds.; American Chemical Society: Washington, DC, 1988; Chapter 7.

(83) Matyjaszewski, K.; Chen, Y. L.; Kim, H. K. In *Inorganic and Organometallic Polymers*; ACS Symposium Series 360; Zeldin, M., Wynne, K. J., Allcock, H. R., Eds.; American Chemical Society: Washington, DC, 1988; Chapter 6.

(84) Kim, H. K.; Matyjaszewski, K. *J. Am. Chem. Soc.* **1988**, *110*, 3321.

(85) Yoshino, K.; Sugimoto, R. Jpn. Kokai Tokkyo Koho 62 241,936 [87 241,926]; *Chem. Abstr.* **1988**, *108*, 187474w.

(86) Diaz, A. F.; Miller, R. D. *J. Electrochem. Soc.* **1985**, *132*, 834.

(87) Ban, H.; Sukegawa, K.; Tagawa, S. *Macromolecules* **1987**, *20*, 1775.

(88) Yenca, F.; Chen, Y. L.; Matyjaszewski, K. *Polym. Prepr.* **1987**, *28*, 222.

(89) Hrkach, J.; Ruehl, K.; Matyjaszewski, K. *Polym. Prepr.* **1988**, *29*, 112.

(90) Trefonas, P., III; West, R. *J. Polym. Sci., Polym. Lett. Ed.* **1985**, *23*, 469.

(91) Hengge, E.; Litscher, G. *Angew. Chem., Int. Ed. Engl.* **1976**, *15*, 370.

(92) Hengge, E.; Litscher, G. *Monatsh. Chem.* **1978**, *109*, 1217.

(93) Walsh, R. *Acc. Chem. Res.* **1981**, *14*, 246.

(94) Cotts, P. M.; Miller, R. D.; Trefonas, P., III; West, R.; Fickes, G. N. *Macromolecules* **1987**, *20*, 1047.

(95) Sawan, S.; Tsai, Y.-G.; Huang, H.-Y. *Polym. Prepr.* **1988**, *29*, 252.

(96) Hummel, J. P.; Stackhouse, J.; Mislow, K. *Tetrahedron* **1977**, *33*, 1925.

(97) Damewood, J. R., Jr.; West, R. *Macromolecules* **1985**, *18*, 159.

(98) Welsh, W. J.; DeBolt, L.; Mark, J. E. *Macromolecules* **1986**, *19*, 2978.

(99) Hönig, H.; Hassler, K. *Monatsh. Chem.* **1982**, *113*, 129.

(100) Dewar, M. J. S.; Lo, D. H.; Ramsden, C. A. *J. Am. Chem. Soc.* **1975**, *97*, 1311.

(101) Verwoerd, W. S. *J. Comput. Chem.* **1982**, *3*, 445.

(102) Bigelow, R. W.; McGrane, K. M. *J. Polym. Sci., Polym. Phys. Ed.* **1986**, *24*, 1233.

(103) Takeda, K.; Matsumoto, N.; Fukuchi, M. *Phys. Rev. B* **1984**, *30*, 5871.

(104) Mintmire, J. W.; Oritz, J. V. *Macromolecules* **1988**, *21*, 1189.

(105) Nelson, J. T.; Pietro, W. J. *J. Phys. Chem.* **1988**, *92*, 1365.

(106) Teramae, H.; Yamabe, T.; Imamura, A. *Theor. Chim. Acta* **1983**, *64*, 1.

(107) Ensslin, W.; Bergmann, H.; Elbel, S. *J. Chem. Soc., Faraday Trans. 2* **1975**, *71*, 913.

(108) Pfeiffer, M.; Spangenberg, H. J. *Z. Phys. Chem.* **1966**, *232*, 47. Cox, A. P.; Varma, R. *J. Chem. Phys.* **1967**, *46*, 2007.

(109) McCrary, V. R.; Sette, F.; Chen, C. T.; Lovinger, A. J.; Robin, M. B.; Stöhr, J.; Zeigler, J. M. *J. Chem. Phys.* **1988**, *88*, 5925.

(110) Kuzmany, H.; Rabolt, J. F.; Farmer, B. L.; Miller, R. D. *J. Chem. Phys.* **1986**, *85*, 7413.

(111) Lovinger, A. J.; Schilling, F. C.; Bovey, F. A.; Zeigler, J. M. *Macromolecules* **1986**, *19*, 2657.

(112) Ernst, C. A.; Allred, A. L.; Ratner, M. A. *J. Organomet. Chem.* **1979**, *178*, 119.

(113) Damewood, J. R., Jr. *Macromolecules* **1985**, *18*, 1793.

(114) Farmer, B. L.; Rabolt, J. F.; Miller, R. D. *Macromolecules* **1987**, *20*, 1167.

(115) Schilling, F. C.; Bovey, F. A.; Lovinger, A. J.; Zeigler, J. M. *Bull. Am. Phys. Soc.* **1988**, *33*(3), 657.

(116) Miller, R. D.; Farmer, B. L.; Fleming, W.; Sooriyakumaran, R.; Rabolt, J. F. *J. Am. Chem. Soc.* **1987**, *109*, 2509.

(117) Sundararajan, P. R. *Macromolecules* **1988**, *21*, 1256.

(118) Welsh, W. J.; Damewood, J. R., Jr.; West, R. *Macromolecules* **1989**, *22*, 2947.

(119) Trefonas, P.; West, R.; Miller, R. D.; Hofer, D. *J. Polym. Sci., Polym. Lett. Ed.* **1983**, *21*, 823.

(120) Johnson, G. E.; McGrane, K. M. In *Photophysics of Polymers*; ACS Symposium Series 358; Hoyle, C. E., Torkelson,

J. M., Eds.; American Chemical Society: Washington, DC, 1987; p 499.

(121) Frierson, M. R.; Imam, M. R.; Zalkow, V. B.; Allinger, N. L. J. Org. Chem. **1988**, 53, 5248.

(122) Bock, H.; Ensslin, W. Angew. Chem., Int. Ed. Engl. **1971**, 10, 404.

(123) Bock, H.; Ensslin, W.; Fehér, F.; Freund, R. J. Am. Chem. Soc. **1976**, 98, 668.

(124) Dyachkov, P. N.; Ioslovich, N. V.; Levin, A. A. Theor. Chim. Acta **1975**, 40, 237.

(125) Shorygin, P. P.; Petukhov, V. A.; Nefedov, O. M.; Kolesnikov, S. P.; Shiryaev, V. I. Teor. Eksp. Khim., Akad. Nauk Ukr. SSR **1966**, 2, 190; Chem. Abstr. **1966**, 65, 14660f.

(126) Herman, A.; Dreczewski, B.; Wojnowski, W. Chem. Phys. **1985**, 98, 475.

(127) Allred, A. L.; Ernst, C. A.; Ratner, M. A. In Homoatomic Rings, Chains and Macromolecules of Main-Group Elements; Rheingold, A. L., Ed.; Elsevier: New York, 1977; p 307.

(128) Boberski, W. G.; Allred, A. L. J. Organomet. Chem. **1975**, 88, 65.

(129) Pitt, C. G.; Bursey, M. M.; Rogerson, P. F. J. Am. Chem. Soc. **1970**, 92, 519.

(130) Herman, A.; Dreczewski, B.; Wojnowski, W. J. Organomet. Chem. **1983**, 251, 7.

(131) Reference deleted.

(132) Bigelow, R. W. Chem. Phys. Lett. **1986**, 126, 63.

(133) Bigelow, R. W. Organometallics **1986**, 5, 1502.

(134) Klingensmith, K. A.; Downing, J. W.; Miller, R. D.; Michl, J. J. Am. Chem. Soc. **1986**, 108, 7438.

(135) Reference deleted.

(136) Halevi, E. A.; Winkelhofer, G.; Meisl, M.; Janoschek, R. J. Organomet. Chem. **1985**, 294, 151.

(137) Reference deleted.

(138) Reference deleted.

(139) Michl, J.; Balaji, V. In Computational Advances in Organic Chemistry; Ogretir, C., Csizanadia, I. G., Eds.; NATO-ASI Series C; Kluwer Academic Publishers: Dordrecht, Holland, in press.

(140) Takeda, K.; Fujino, M.; Seki, K.; Inokuchi, H. Phys. Rev. B **1987**, 36, 8129.

(141) Takeda, K.; Teramae, H.; Matsumoto, N. J. Am. Chem. Soc. **1986**, 108, 8186.

(142) Seki, K.; Mori, T.; Inokuchi, H.; Murano, K. Bull. Chem. Soc. Jpn. **1988**, 61, 351.

(143) Tanaka, K.; Kobayashi, H.; Koike, T.; Yamabe, T.; Osawa, Y.; Niwa, S.; Yasuda, N. Synth. Met. **1988**, 25, 289.

(144) Sandorfy, C. Can. J. Chem. **1955**, 33, 1337.

(145) Reference deleted.

(146) (a) Loubriel, G.; Zeigler, J. Phys. Rev. B **1986**, 33, 4203. (b) Gilman, H.; Chapman, D. R. J. Organomet. Chem. **1966**, 5, 392.

(147) Pitt, C. G.; Carey, R. N.; Toren, E. C., Jr. J. Am. Chem. Soc. **1972**, 94, 3806.

(148) Pitt, C. G.; Bock, H. J. Chem. Soc., Chem. Commun. **1972**, 28.

(149) Cotts, P. M.; Miller, R. D.; Sooriyakumaran, R. Bull. Am. Phys. Soc. **1988**, 33(3), 656.

(150) Michl, J.; Downing, J. W.; Karatsu, T.; Klingensmith, K. A.; Wallraff, G. M.; Miller, R. D. In Inorganic and Organometallic Polymers; ACS Symposium Series 360; Zeldin, M., Wynne, K., Allcock, H., Eds.; American Chemical Society: Washington, DC, 1988; Chapter 5, p 61.

(151) Michl, J.; Downing, J. W.; Karatsu, T.; McKinley, A. J.; Poggi, G.; Wallraff, G. M.; Sooriyakumaran, R.; Miller, R. D. Pure Appl. Chem. **1988**, 60, 959.

(152) Harrah, L. A.; Zeigler, J. M. In Photophysics of Polymers; Hoyle, C. E., Torkelson, J. M., Eds.; ACS Symposium Series 358; American Chemical Society: Washington, DC, 1987; p 482.

(153) Harada, Y.; Murrell, J. N.; Sheena, H. H. Chem. Phys. Lett. **1968**, 1, 595.

(154) Pitt, C. G.; Jones, L. L.; Ramsey, B. G. J. Am. Chem. Soc. **1967**, 89, 5471.

(155) Ramsey, B. G. In Electronic Transitions in Organometalloids; Academic Press: New York, 1969; p 113.

(156) Herman, A. Chem. Phys. **1988**, 122, 53.

(157) Robin, M. B. In Higher Excited States of Polyatomic Molecules; Academic Press: New York, 1974; Vol. 1, p 305.

(158) Pitt, C. G. J. Am. Chem. Soc. **1969**, 91, 6613.

(159) Michl, J.; Thulstrup, E. W. Tetrahedron **1976**, 32, 205.

(160) Lippert, E.; Rettig, W.; Bonačic-Koutecky, V.; Heisel, F.; Miehe, A. Adv. Chem. Phys. **1987**, 68, 173.

(161) Sakurai, H. In Silicon Chemistry; Corey, J. Y., Corey, E. R., Gaspar, P. P., Eds.; Ellis Horwood Publishers: Chichester, 1988; Chapter 16.

(162) Surjan, P. R.; Poirier, R. A.; Kuzmany, H. In Electronic Properties of Conjugated Polymers; Springer Ser. Solid-State Sci. **1987**, 76, 314.

(163) Balaji, V., Michl, J., unpublished results.

(164) Berkovitch-Yellin, Z.; Ellis, D. E.; Ratner, M. A. Chem. Phys. **1981**, 62, 21.

(165) Reference 3, p 205.

(166) Takeda, K.; Matsumoto, N. J. Phys. C: Solid State Phys. **1985**, 18, 6121.

(167) Kim, Y. R.; Lee, M.; Thorne, J. R. G.; Hochstrasser, R. M.; Zeigler, J. M. Chem. Phys. Lett. **1988**, 145, 75.

(168) Thorne, J. R. G.; Hochstrasser, R. M.; Zeigler, J. M. J. Phys. Chem. **1988**, 92, 4275.

(169) Michl, J.; Karatsu, T.; Wallraff, G. M.; Klingensmith, K. A.; Miller, R. D., unpublished results.

(170) Trefonas, P., III; Damewood, J. R., Jr.; West, R.; Miller, R. D. Organometallics **1985**, 4, 1318.

(171) Harrah, L. A.; Zeigler, J. M. J. Polym. Sci., Polym. Lett. Ed. **1985**, 23, 209.

(172) Rawiso, M.; Aime, J. P.; Fave, J. L.; Schott, M.; Müller, M. A.; Schmidt, M.; Baumgartl, H.; Wegner, G. J. Phys. Fr. **1988**, 49, 861 and references cited therein.

(173) Schweitzer, K. S. Chem. Phys. Lett. **1986**, 125, 118.

(174) Schweitzer, K. S. J. Chem. Phys. **1986**, 85, 1156.

(175) Schweitzer, K. S. J. Chem. Phys. **1986**, 85, 1176.

(176) Schweitzer, K. S. Polym. Prepr. **1986**, 27(2), 354.

(177) Miller, R. D.; Hofer, D.; Rabolt, J.; Fickes, G. N. J. Am. Chem. Soc. **1985**, 107, 2172.

(178) Rabolt, J. F.; Hofer, D.; Miller, R. D.; Fickes, G. N. Macromolecules **1986**, 19, 611.

(179) Reference deleted.

(180) Reference deleted.

(181) Gobbi, G. C.; Fleming, W. W.; Sooriyakumaran, R.; Miller, R. D. J. Am. Chem. Soc. **1986**, 108, 5624.

(182) Schilling, F. C.; Bovey, F. A.; Lovinger, A. J.; Zeigler, J. M. Macromolecules **1986**, 19, 2660.

(183) Weber, P.; Guillon, D.; Skoulios, A.; Miller, R. D. J. Phys. Fr. **1989**, 50, 793.

(184) Wells, A. F. In Structural Inorganic Chemistry, 3rd ed.; Oxford University Press: Oxford, England, 1962.

(185) Poggi, G.; Downing, J. W.; Michl, J., unpublished results.

(186) Miller, R. D.; Sooriyakumaran, R.; Fickes, G. N., unpublished results.

(187) Farmer, B. L.; Miller, R. D.; Rabolt, J. F.; Fleming, W. W.; Fickes, G. N. Bull. Am. Phys. Soc. **1988**, 33(3), 657.

(188) Hallmark, V. M.; Sooriyakumaran, R.; Miller, R. D.; Rabolt, J. F. J. Chem. Phys. **1989**, 90, 2486.

(189) Ovchinnikov, Y. E.; Shklover, V. E.; Dementev, V. V.; Frunze, T. M.; Struchkov, Y. T. Abstr., 8th Int. Symp. Organosilicon Chem. **1987**, 227.

(190) Kagawa, T.; Fujino, M.; Takeda, K.; Matsumoto, N. Solid State Commun. **1986**, 57, 635.

(191) Harrah, L. A.; Zeigler, J. M. J. Polym. Sci., Polym. Lett. Ed. **1987**, 25, 205.

(192) Trommsdorff, H. P.; Zeigler, J. M.; Hochstrasser, R. M. J. Chem. Phys. **1988**, 89, 4440.

(193) Ban, H.; Sukegawa, K. J. Appl. Polym. Sci. **1987**, 33, 2787.

(194) Willson, C. G. In Introduction to Microlithography: Theory, Materials, and Processing; ACS Symposium Series 219; Thompson, L. F., Willson, C. G., Bowden, M. J., Eds.; American Chemical Society: Washington, DC, 1983; Chapter 6.

(195) Miller, R. D.; Guillet, J. E.; Moore, J. Polym. Prepr. **1988**, 29(1), 552.

(196) Taylor, G. N.; Hellman, M. Y.; Wolf, T.; Zeigler, J. M. Proc. SPIE **1988**, 920, 274.

(197) Ban, H.; Sukegawa, K. J. Polym. Sci., Polym. Chem. Ed. **1988**, 26, 521.

(198) Johnson, G. E.; McGrane, K. M. Polym. Prepr. **1986**, 27, 352.

(199) Horn, K. A.; Whitenack, A. A. J. Phys. Chem. **1988**, 92, 3875.

(200) Nakadaira, Y.; Komatsu, N.; Sakurai, H. Chem. Lett. **1985**, 1781.

(201) Wilt, J. W. In Reactive Intermediates; Abramovitch, R. A., Ed.; Plenum Press: New York, 1983; Chapter 3.

(202) Dohmaru, T. In Chemical Kinetics of Small Organic Radicals; Alfazzi, Z. B., Ed.; CRC Press: Boca Raton, FL, 1988; Vol. III, Chapter 16.

(203) Boudjouk, P.; Roberts, J. R.; Golino, C. M.; Sommer, L. H. J. Am. Chem. Soc. **1972**, 94, 7926.

(204) Hawari, J. A.; Griller, D.; Weber, W. P.; Gaspar, P. P. J. Organomet. Chem. **1987**, 326, 335.

(205) Gaspar, P. P.; Holter, D.; Koveczny, C.; Corey, J. Y. Acc. Chem. Res. **1987**, 20, 329 and references cited therein.

(206) Ishikawa, M.; Tokaoka, T.; Kumada, M. J. Organomet. Chem. **1972**, 42, 333.

(207) Nate, K.; Ishikawa, M.; Imamura, N.; Murakami, Y. J. Polym. Sci., Polym. Chem. Ed. **1986**, 24, 1551.

(208) Ishikawa, M.; Nate, K. In Inorganic and Organometallic Polymers; ACS Symposium Series 360; Zeldin, M., Wynne, K. J., Allcock, H. R., Eds.; American Chemical Society: Washington, DC, 1988; Chapter 16.

(209) Ishikawa, M.; Hongzhi, N.; Matsusaki, K.; Nate, K.; Inoue, T.; Yokono, H. J. Polym. Sci., Polym. Lett. Ed. **1984**, 22, 669.

(210) Nate, K.; Ishikawa, M.; Ni, H.; Watanabe, H.; Saheki, Y. *Organometallics* **1987**, *6*, 1673.

(211) Trefonas, P., III; West, R.; Miller, R. D. *J. Am. Chem. Soc.* **1985**, *107*, 2737.

(212) Karatsu, T.; Miller, R. D.; Sooriyakumaran, R.; Michl, J. *J. Am. Chem. Soc.* **1989**, *111*, 1140.

(213) Turro, N. J.; Ramamurthy, V.; Cherry, W.; Farneth, W. *Chem. Rev.* **1978**, *78*, 125.

(214) Miller, R. D. In *Advances in Chemistry*; Zeigler, J. M., Fearon, F. G., Eds.; American Chemical Society: Washington, DC, in press.

(215) McKinley, A. J.; Karatsu, T.; Wallraff, G. M.; Miller, R. D.; Sooriyakumaran, R.; Michl, J. *Organometallics* **1988**, *7*, 2567.

(216) Sawrey, B. A.; O'Neal, H.; Ring, M. A.; Coffey, D. *Int. J. Chem. Kinet.* **1984**, *16*, 801. Rickborn, S. F.; Ring, M. A.; O'Neal, H. E. *Int. J. Chem. Kinet.* **1984**, *16*, 1371.

(217) Davidson, I. M. T.; Howard, A. V. *J. Chem. Soc., Faraday Trans. 1* **1975**, *71*, 69. Chen, Y. S.; Cohen, B. H.; Gaspar, P. P. *J. Organomet. Chem.* **1980**, *195*, C1.

(218) Sakurai, H.; Sakaba, H.; Nakadaira, Y. *J. Am. Chem. Soc.* **1982**, *104*, 6156. Sakurai, H.; Nakadaira, Y.; Sakaba, H. *Organometallics* **1983**, *2*, 1484.

(219) Ramsey, B. G. *J. Organomet. Chem.* **1974**, *67*, C67.

(220) Sakurai, H.; Kobayashi, Y.; Nakadaira, Y. *J. Am. Chem. Soc.* **1974**, *96*, 2656.

(221) Sakurai, H. *J. Organomet. Chem.* **1980**, *200*, 261.

(222) (a) Davidson, I. M. T.; Howard, A. V. *J. Chem. Soc., Faraday Trans. 1* **1975**, *71*, 69. Davidson, I. M. T.; Matthews, J. I. *J. Chem. Soc., Faraday Trans. 1* **1976**, *72*, 1403. Davidson, I. M. T.; Hughes, K. J.; Ijadi-Maghsoodi, S. *Organometallics* **1987**, *6*, 639. (b) Pedley, J. B.; Naylor, R. D.; Kirby, S. P. *Thermochemical Data of Organic Compounds*; Chapman and Hall: London, 1986; p 278. Benson, S. W. *Thermochemical Kinetics*; Wiley: New York, 1976; p 77.

(223) Hinze, J.; Jaffe, H. H. *J. Am. Chem. Soc.* **1962**, *84*, 540. The atomic electron affinities were updated from: Mead, R. D.; Stevens, A. E.; Lineberger, W. C. In *Gas Phase Ion Chemistry*; Bowers, M. T., Ed.; Academic Press: Orlando, 1984; Vol. 3, p242.

(224) Shuna, K.; Kumada, M. *J. Org. Chem.* **1958**, *23*, 139.

(225) Hasegawa, Y.; Okamura, K. *J. Mater. Sci.* **1986**, *21*, 321.

(226) Kumar, K.; Litt, M. H. *J. Polym. Sci., Polym. Lett. Ed.* **1988**, *26*, 25.

(227) Mazdyasni, K. S.; West, R.; David, L. D. *J. Am. Ceram. Soc.* **1978**, *61*, 504.

(228) Niihara, K.; Yamamoto, T.; Arima, J.; Takemoto, R.; Suganama, K.; Watanabe, N.; Nishikawa, T.; Okumura, M. *J. Polym. Sci., Polym. Chem. Ed.*, in press.

(229) West, R. In *Ultrastructure Processing of Ceramics, Glasses, and Composites*; Hensch, L. L., Ulrich, D. R., Eds.; Wiley: New York, 1984; Part 3, Chapter 19.

(230) Sinclair, R. In *Ultrastructure Processing of Ceramics, Glasses and Composites*; Hench, L. L., Ulrich, D. R., Eds.; Wiley: New York, 1984; Chapter 21.

(231) West, R.; Wolff, A. R.; Peterson, D. J. *J. Radiat. Curing* **1986**, *13*, 35.

(232) Wolff, A.; West, R. *Appl. Organomet. Chem.* **1987**, *1*, 7.

(233) Naarman, H.; Theophilou, N.; Geral, L.; Sledz, J.; Schien, F. German Patent DE3634281, 1988; *Chem. Abstr.* **1988**, *109*, 120989u.

(234) Usuki, A.; Murase, M. Jpn Kokai Tokkyo Koho JP 62 59,632 [87 59,632]; *Chem. Abstr.* **1987**, *107*, 218592u.

(235) Du, Z.; Wen, K.; Lin, J. *Shandong Daxue Xuebao, Ziran, Kexueban* **1987**, *22*, 115; *Chem. Abstr.* **1988**, *108*, 56695w.

(236) Kepler, R. G.; Zeigler, J. M.; Harrah, L. A.; Kurtz, S. R. *Phys. Rev. B* **1987**, *35*, 2818.

(237) Fujino, M. *Chem. Phys. Lett.* **1987**, *136*, 451.

(238) Stolka, M.; Yuh, H.-J.; McGrane, K.; Pai, D. M. *J. Polym. Sci., Polym. Chem. Ed.* **1987**, *25*, 823.

(239) Abkowitz, M.; Knier, F. E.; Yuh, H.-J.; Weagley, R. J.; Stolka, M. *Solid State Commun.* **1987**, *62*, 547.

(240) Abkowitz, M.; Stolka, M. *Philos. Mag. Lett.* **1988**, *58*, 239.

(241) Samuel, L. M.; Sanda, P. N.; Miller, R. D. *Chem. Phys. Lett.* **1989**, *159*, 227.

(242) Rice, M. J.; Phillpot, S. R. *Phys. Rev. Lett.* **1987**, *58*, 937.

(243) Miller, R. D.; MacDonald, S. A. *J. Imaging Sci.* **1987**, *31*, 43.

(244) Miller, R. D.; Hofer, D.; Fickes, G. N.; Willson, C. G.; Ma-

rinero, E. E.; Trefonas, P., III; West, R. *Polym. Eng. Sci.* **1986**, *26*, 1129.

(245) Reichmanis, E.; Smolinsky, G.; Wilkins, C. W., Jr. *Solid State Technol.* **1985**, *28*(8), 130.

(246) Lin, B. In *Introduction to Microlithography: Theory, Materials, and Processing*; ACS Symposium Series 219; Thompson, L. F., Willson, C. G., Bowden, M. J., Eds.; American Chemical Society: Washington, DC, 1983; Chapter 6.

(247) Moreau, W. M. In *Semiconductor Lithography: Principles, Practices and Materials*; Plenum Press: New York, 1988; Chapter 13.

(248) Moreau, W. M. In *Semiconductor Lithography: Principles, Practices and Materials*; Plenum Press: New York, 1988; Chapter 12.

(249) Hiraoka, H.; Hofer, D. C.; Miller, R. D.; Pederson, L. A.; Willson, C. G. U.S. Patent 4,464,460, 1984.

(250) Srinivasan, R. *Science* **1986**, *234*, 559 and references cited therein.

(251) Miller, R. D. In *Silicon Chemistry*; Corey, J. Y., Corey, E. R., Gaspar, P. P., Eds.; Ellis Horwood Ltd.: Chichester, England, 1988; Chapter 35.

(252) Hofer, D. C.; Miller, R. D.; Willson, C. G. *Proc. SPIE* **1984**, *469*, 16.

(253) Moreau, W. M. In *Semiconductor Lithography: Principles, Practices and Materials*; Plenum Press: New York, 1988; Chapter 2.

(254) Miller, R. D.; Willson, C. G.; Wallraff, G. M.; Clecak, N.; Sooriyakumaran, R.; Michl, J.; Karatsu, T.; McKinley, A. J.; Klingensmith, K. A.; Downing, J. *Polym. Eng. Sci.* **1989**, *29*, 882.

(255) Miller, R. D.; Wallraff, G.; Clecak, N.; Sooriyakumaran, R.; Michl, J.; Karatsu, T.; McKinley, A. J.; Klingensmith, K. A.; Downing, J. *Polym. Mater. Sci. Eng.* **1989**, *60*, 49.

(256) Hofer, D. C.; Jain, K.; Miller, R. D. *IBM Tech. Disclos. Bull.* **1984**, *26*, 5683.

(257) Marinero, E. E.; Miller, R. D. *Appl. Phys. Lett.* **1987**, *50*, 1041.

(258) Hansen, S. G.; Robitaille, T. E. *J. Appl. Phys.* **1987**, *62*, 1394.

(259) Magnera, T. F.; Balaji, V.; Michl, J. In *Silicon Chemistry*; Corey, J. Y., Corey, E. R., Gaspar, P. P., Eds.; Ellis Horwood Ltd.: Chichester, England, 1988; Chapter 45.

(260) Magnera, T. F.; Balaji, V.; Michl, J.; Miller, R. D.; Sooriyakumaran, R. *Macromolecules* **1989**, *22*, 1624.

(261) Reference deleted.

(262) Reference deleted.

(263) Reference deleted.

(264) Griffing, B. F.; West, P. R. *Polym. Eng. Sci.* **1983**, *23*, 947.

(265) West, P. R.; Griffing, B. F. *Proc. SPIE* **1983**, *394*, 33.

(266) Hofer, D. C.; Miller, R. D.; Willson, C. G.; Neureuther, A. R. *Proc. SPIE* **1984**, *469*, 108.

(267) Miller, R. D.; Fickes, G. N. *J. Polym. Sci., Polym. Chem. Ed.*, in press.

(268) Schnabel, W. In *Aspects of Degradation and Stabilization of Polymers*; Jellinik, H. H. G., Ed.; Elsevier: Amsterdam, 1978; Chapter 4.

(269) Ban, H.; Sukegawa, K.; Tagawa, S. *Macromolecules* **1988**, *21*, 45.

(270) Irie, S.; Oka, K.; Irie, M. *Macromolecules* **1988**, *21*, 110.

(271) Williams, D. J., Ed. *Nonlinear Optical Properties of Organic and Polymeric Materials*; ACS Symposium Series 233; American Chemical Society: Washington, DC, 1983.

(272) Williams, D. J. *Angew. Chem., Int. Ed. Engl.* **1984**, *23*, 640.

(273) Kajzar, F.; Messier, J.; Rosilio, C. *J. Appl. Phys.* **1986**, *60*, 3040.

(274) Baumert, J. C.; Bjorklund, G. C.; Jundt, D. H.; Jurich, M. C.; Looser, H.; Miller, R. D.; Rabolt, J.; Sooriyakumaran, R.; Swalen, J. D.; Twieg, R. J. *Appl. Phys. Lett.* **1988**, *53*, 1147.

(275) Miller, R. D.; Sooriyakumaran, R.; Rabolt, J. F. *Bull. Am. Phys. Soc.* **1987**, *32*, 886.

(276) Marinero, E. E. *Chem. Phys. Lett.* **1985**, *115*, 501.

(277) Schellenberg, F. M.; Byer, R. L.; Zavislan, J.; Miller, R. D. In *Nonlinear Optics of Organics and Semiconductors*; Kyobayashi, T., Ed.; Springer-Verlag: New York, 1989; p 192.

(278) McGraw, D. J.; Siegman, A. E.; Wallraff, G. M.; Miller, R. D. *Appl. Phys. Lett.*, in press.

(279) Yang, L.; Wang, Q. Z.; Ho, P. P.; Dorsenville, R.; Alfano, R. R.; Zou, W. K.; Yang, N. L. *Appl. Phys. Lett.* **1988**, *53*, 1245.